

UC Davis

UC Davis Electronic Theses and Dissertations

Title

Aerosolization and Thermal Degradation Chemistry of Electronic Cigarettes

Permalink

<https://escholarship.org/uc/item/1c55k6gr>

Author

Li, Yichen

Publication Date

2021

Peer reviewed|Thesis/dissertation

Aerosolization and Thermal Degradation Chemistry of Electronic Cigarettes

By

YICHEN LI

DISSERTATION

Submitted in partial satisfaction of the requirements for the degree of

DOCTOR OF PHILOSOPHY

in

Agricultural and Environmental Chemistry

in the

OFFICE OF GRADUATE STUDIES

of the

UNIVERSITY OF CALIFORNIA, DAVIS

Approved:

Tran B. Nguyen, Chair

Kent E. Pinkerton

Peter G. Green

Committee in Charge

2021

Aerosolization and Thermal Degradation Chemistry of Electronic Cigarettes

Abstract

by

Yichen Li

Doctor of Philosophy in Agricultural and Environmental Chemistry

University of California, Davis

Electronic cigarettes (e-cigarettes) are battery-operated devices for nicotine delivery that operate by vaping or aerosolizing an “e-liquid” that contains propylene glycol (PG), vegetable glycerin (VG), nicotine, and different flavoring chemicals. E-cigarettes have been regarded as a “less-harm” alternative to combustible tobacco cigarettes, and their worldwide market share has been increasing exponentially in recent years. In the e-cigarette device vessel, the e-liquid is heated by an atomizer (metal coil) to create an e-cigarette aerosol mixture, which includes both gas and particle phases. Both nicotine-based and cannabinoid-based e-liquids are common in e-cigarette use. Due to their relative novelty, e-cigarettes have not been subject to significant regulatory action until the outbreak of e-cigarette or vaping use-associated lung injury (EVALI) starting from 2019 that killed more than 60 people. In the EVALI outbreak, cannabis vapes (mainly from extracted tetrahydrocannabinol oil) that were adulterated with vitamin E acetate (VEA) in the black market are thought, but not yet confirmed, to be causal agents. After the EVALI outbreak, e-cigarette flavors were banned in closed-tank systems.

During the heat-induced aerosolization process of e-liquid, many thermal degradation products have been identified and characterized (e.g., formaldehyde, acetaldehyde, acetone) that are produced from the thermal degradation of PG and VG, as well as flavorant mixtures. Previous

research studies indicate that the production of thermal degradation products depends on puff regimen, coil temperature, e-liquid composition, and possibly other factors. However, knowledge gaps still exist regarding the large variety of thermal degradation products that remain unidentified or unquantified, and the intrinsic relationship between actual coil temperature and e-liquid composition to the thermal degradation of e-liquid. In addition, the thermal degradation mechanism of VEA and THC is still unknown.

In this work, high performance liquid chromatography (HPLC) coupled with electrospray ionization (ESI) high resolution mass spectrometry (HRMS) are used for the chemical analysis of thermal degradation carbonyl compounds and organic acids. Both carbonyls and acids are derivatized with 2,4-dinitrophenylhydrazine (2,4-DNPH) prior to mass spectrometry analysis. A novel theoretical chemistry model was developed to predict the analytical sensitivities of carbonyl(acid)-DNPH derivatives in ESI negative mode for the analyte compounds for which corresponding DNPH derivatives standards are unavailable. This characterization method enabled an untargeted analysis and the most comprehensive picture, to date, of the carbonyls and acids that are generated from both PG/VG and VEA/THC vaping systems. Over 40 thermal degradation carbonyls and acids were characterized from the thermal degradation of PG, VG, VEA and THC, while nearly 20 cannabinoids and derivatives were also identified by the same methods. PG, VG, and VEA were analyzed by gas chromatography to enable mass closure for the aerosolization process.

Moreover, this work systematically studies how changing the vaping parameters, including coil temperature, e-liquid composition and puff regimen, alters the production of aerosol mass and

carbonyl degradation products. The thermal degradation mechanism of PG and VG is proposed from the results, including differences between heat-induced dehydration and oxidant-induced decomposition. The thermal degradation chemistry of THC and VEA is also studied, and the corresponding mechanisms proposed. In summary, this work provides important chemical-specific information that may be helpful for the fundamental understanding of chemistry in e-cigarettes and for guiding regulatory action. Corresponding toxicology and in vivo studies are needed to further evaluate the health risk of e-cigarette use.

Dedicated to
my family Jianchun Li, Zhongli Xie and Xiaoping Liu
for their endless love and support

Acknowledgement

First and foremost, enormous gratitude and sincere appreciation are due to my Ph.D supervisors, Prof. Tran B. Nguyen and Prof. Kent E. Pinkerton, who have been unstinting in their consistent guidance, continuous support and constructive critique during the past years. I really appreciate that Prof. Nguyen provided me a position as a graduate student researcher and shared her knowledge with me about instrument operation, academic writing, and most importantly, the way of thinking as a Ph.D researcher. Her enthusiasm and creative ideas about research lighted up my interest in the field of e-cigarette chemistry and inspired me to contribute to the field with my knowledge and work. I also want to thank Prof. Pinkerton for his insightful advice about the direction of the project as well as his warm support and care through my whole Ph.D career. I believe that without his guidance and support, I would never have succeeded in receiving the Ph.D degree.

I also want to give my deep appreciation to Dr. Peter G. Green, Prof. Cort Anastasio, Prof. Matt J. Hengel and Prof. Dean J. Tantillo for the support and advice they have given in their specialized field in analytical chemistry, atmosphere chemistry, and computational chemistry, which kept me toward the right direction of completing the project. The advice and questions they brought up in my qualifying examination about the project also helped me build a more comprehensive knowledge system. Moreover, I want to give my special thanks to Dr. Peter G. Green as my dissertation committee member to help me improve the quality of my dissertation.

Moreover, I also want to thank to all my colleagues in Prof. Nguyen's as well as in Prof. Pinkerton's group. All of them have generously given their time to me and support my research in their way. In particular I am grateful to undergraduate students Amanda E. Burns, Lillian N. Tran, and Karizza A. Abellar who helped me conduct parts of the necessary experiments; to the visiting scientist and postdoc in our group Dr. Kelvin H. Bates and Dr. James D. Cope, who have helped me a lot in the technical solutions about instrument operation, maintenance and organic synthesis; to my lab mate Guy J.P. Burke, who had discussed a lot with me from science to life; to the Ph.D students in Prof. Pinkerton's lab Morgan E. Poindexter and Xiaohan Li for their support in discussing experiment details as well as the suggestions in the revision of manuscripts; to our collaborator Dr. Amy K. Madl, who had given me much useful suggestion during the revision of manuscripts.

Finally, I would express my deepest gratitude to my family, who has given me enormous support and love during my hardest time and believe in me no matter what choice that I choose for my life. Also I want to thanks my friends who play high quality tennis and basketball games in the past years with me, which really helped me reduce pressure and keep health in research life.

Table of contents

Abstract.....	ii
Dedication.....	v
Acknowledgement.....	vi
List of Figures.....	xi
List of Schemes.....	xiii
List of Tables.....	xiv
Chapter 1. Introduction.....	1
1.1 The overview of e-cigarettes.....	1
1.1.1 The principle of e-cigarettes.....	1
1.1.2 The invention and evolution of e-cigarette.....	1
1.1.3 Prevalence of e-cigarette use.....	3
1.2 The composition of e-liquid.....	4
1.2.1 Regular e-liquid.....	4
1.2.2 Cannabis e-liquid.....	8
1.3 The thermal degradation products of e-cigarettes.....	10
1.3.1 The thermal degradation of regular e-liquid compositions	10
1.3.2 The thermal degradation of cannabis e-liquid compositions	13
1.4 Current analytical technology for the characterization of thermal degradation products.....	17
Chapter 2. Application of High-Resolution Mass Spectrometry and a Theoretical Model to the Quantification of Multifunctional Carbonyls and Organic Acids in e-Cigarette Aerosol.....	20
Abstract.....	20
2.1 Introduction.....	21
2.2 Experimental.....	24
2.2.1 E-cigarette aerosol sample generation and extraction.....	25
2.2.2 Identification by high-resolution mass spectrometry and tandem mass spectrometry....	26
2.2.3 Separation by high performance liquid chromatography coupled with high resolution	

mass spectrometry (HPLC-HRMS).....	27
2.2.4 Theoretical calculations by Gaussian.....	28
2.3 Result and discussion.....	30
2.3.1 Chemical structures of multifunctional carbonyls and acids.....	32
2.3.2 Quantification of DNPH hydrazones of multifunctional carbonyls and acids.....	35
Chapter 3. Impact of e-Liquid Composition, Coil Temperature, and Puff Topography on the Aerosol Chemistry of Electronic Cigarettes.....	45
Abstract.....	45
3.1 Introduction.....	46
3.2 Experimental.....	49
3.2.1 E-cigarette sample generation and extraction.....	49
3.2.2 Particle-phase PG, VG, and nicotine characterized by GC-MS.....	54
3.2.3 Carbonyls and organic acids characterized by high performance liquid chromatography- high resolution mass spectrometry (HPLC-HRMS).....	54
3.2.4 Volatile/semivolatile PG and VG characterized by chemical ionization triple quadrupole mass spectrometer (CIMS).....	55
3.3 Result and discussion.....	57
3.3.1 Coil temperature.....	57
3.3.2 E-liquid composition.....	64
3.3.3 Puff Duration.....	69
3.3.4. Mass Balance Closure and Volatility.....	70
3.3.5. Health Impacts.....	72
3.4 Conclusion.....	75
Chapter 4. Vaping aerosols from Vitamin E Acetate and Tetrahydrocannabinol oil: chemistry and composition.....	77
Abstract.....	77
4.1 Introduction.....	78
4.2 Experimental.....	80
4.2.1 Vaping aerosol generation and extraction.....	80

4.2.2 Thermal degradation carbonyls, acids, and cannabinoids characterized by HPLC- HRMS.....	83
4.3 Result and discussion.....	85
Chapter 5. Conclusion.....	99
References.....	102

List of Figures

Figure 2.1 The concentration of main thermal degradation products in e-cigarette aerosol in this work.....	20
Figure 2.2 Sample collection, extraction and analysis set up. Legend: A) TE-2B smoking machine, B) adjustable settings for puffing duration and frequency, C) holder for e-cigarette cartridges, D) outflow from device, D) DNPH impregnated silica cartridges, F) extraction protocol into autosampler vials.....	24
Figure 2.3 Linear dynamic range (5, 10, 20, 50, 200 puffs) of different carbonyl compounds (thermal degradation products of PG and VG, and flavoring chemicals).....	25
Figure 2.4 Concentration standard curves of 13 carbonyl-DNPH mixture standards, $R^2=0.99$ for all standard curves. Analyte names in legend are listed for the carbonyls, in descending order of sensitivity.....	28
Figure 2.5. Electrostatic potential map (ESP) of a) formaldehyde, acetaldehyde, acrolein and hydroxyacetone b) the correspond negative ion. c) deprotonation reaction in Electrospray Ionization (ESI) negative mode.....	29
Figure 2.6 (a) Total ion chromatogram (TIC) of the e-cigarette aerosol sample extracts and single ion chromatograms (SIC) for four select deprotonation ions of carbonyl-DNPH hydrazones (b) Corresponding integrated mass spectrum of the TIC and individual mass spectra of four SIC....	31
Figure 2.7 Correlation between the observed ESI sensitivities of standard carbonyl-DNPH hydrazones and calculated ΔG_d (gas phase, $R^2 =0.63$). The data point of valeraldehyde was excluded because it was considered as an outlier by Cook's Distance ($D_i=0.84$).....	36
Figure 2.8 Correlation between the sensitivity of carbonyl-DNPH standards and the calculated ΔG_d (solution phase).....	37
Figure 3.1 The estimated composition of e-liquid and corresponding e-cigarette aerosol at vaping temperature of 373 °F including both gas phase and particle phase.....	45
Figure 3.2 Device and sampling set up. The total aerosol and the particle fraction of total aerosol (captured by a 0.2-um pore hydrophilic-surface PTFE filter) were analyzed independently. The difference is termed the volatile/semi-volatile fraction in the gas phase.....	49
Figure 3.3 The temperature and power readings during the vaping process, as monitored by device software compared to coil temperature measured by thermocouple.....	50
Figure 3.4 Particle size and distribution of e-cigarette aerosol, as sampled via direct puffing into a 100 mL glass bulb (black) and sampling the same mixture through a HEPA filter (orange). The HEPA filter particle removal efficiency is estimated to be > 99.8%.....	53
Figure 3.5 The relationship between the production of particle mass and a) measured coil temperatures, or b) temperatures set by the Evolv software for four different coils using e-liquid with a 30:70 PG:VG ratio by volume and 3 mg/mL nicotine.....	57
Figure 3.6 The production of representative carbonyl compounds and various coil temperatures.....	58
Figure 3.7 The absolute concentrations of representative carbonyl compounds and nicotine observed in aerosols from vaping e-liquid at various PG:VG ratios at a coil temperature of 375 °F (191 °C).....	65

Figure 3.8 The production yield percent of representative carbonyl compounds and nicotine, as normalized by total aerosol mass, from vaping e-liquid at various PG:VG ratios at a coil temperature of 375 °F (191 °C).....66

Figure 3.9 Particle mass (blue filled squares) and representative carbonyl compounds produced during vaping with various puff durations, at a 375 °F (191 °C) coil temperature and 30:70 PG/VG e-liquid ratio by volume. A non-linear best fit relationship for particle mass is shown.....69

Figure 3.10 Distribution of total mass loss from the e-liquid as nonvolatile (NV) particles captured by a filter or volatile/semivolatile (V/SV) compounds at different PG:VG ratios and a measured coil temperature of 375 °F (191 °C), 3 s puff duration and 3 mg/ml nicotine concentration. For the 30:70 PG:VG ratio sample (insert), the V/SV fraction was measured by CIMS to be primarily PG, and the nonvolatile (NV) fraction was measured by GC-MS to be primarily VG. The measured V/SV mass closed the balance of mass determined from gravimetric analysis.....70

Figure 3.11 CIMS mass spectrum for the e-cigarette aerosol, after the background signal in the lab air has been subtracted. The spectra shows that the major content is PG (detected as PG•CF₃O-, m/z 161) and VG (detected as VG•CF₃O-, m/z 177). The relative sensitivity of VG is higher than PG, which is not accounted for in this plot. After all dilution corrections and sensitivity calibrations, the concentrations of PG (22.5 ± 8 mg/puff) and VG (4 ± 2 mg/puff) are obtained. Hydroxycarbonyls such as hydroxyacetone are well-observed by CIMS, but had negligible signal.....71

Figure 3.12 Simplified model of mass loss during e-cigarette vaping. The VG percent (black open triangles) in the e-liquid, PG percent (black open circles) in the e-liquid, and aerosolized mass (blue filled circles) all change during vaping. The model starts with 1000 mg e-liquid at 30:70 PG:VG volume ratio (26:74 mass ratio), and losing mass per puff as reported in Table 2 as a function of e-liquid PG content ($f(\text{PG}\%) = 16.92e(0.0231x\text{PG})$) that is remaining in the e-liquid, and assuming an 8:1 mass loss ratio for PG:VG as measured by total mass loss for 100% PG compared to 100% VG e-liquid.....72

Figure 4.1 The setup of vaping device (mod) and collection system. Particles fraction of vaping aerosol will be collected by micro-glass fiber. Carbonyls, acids and cannabinoids in aerosol will be collected on 2,4-DNPH cartridge for the HPLC-HRMS analysis.....81

Figure 4.2 Stacked single ion chromatogram (SIC) of the main thermal degradation products and aerosolized components from the vaping aerosol of a) VEA, b) VEA/extracted THC oil = 1:1, c) extracted THC oil at 455 ± 10°F (235 °C).....85

Figure 4.3 The normalized mass of thermal degradation carbonyl compounds by particle mass collected on Cambridge Filter Pad by vaping VEA, extracted THC oil and their mixture at 455 ± 10°F (235 °C).....96

List of Schemes

Scheme 1.1 The chemical structure of PG, VG, nicotine, and representative flavor compounds and acid additives.....	6
Scheme 1.2 The chemical structure of CBD, THC and other potential cutting agents.....	8
Scheme 1.3 a) The structure of thermal degradation products that has been identified from PG and VG; b) The structure and potential transform pathway of tobacco-specific nitrosamines.....	11
Scheme 1.4 The structure of potential thermal degradation products from different common used diluents of cannabis e-liquid identified by the NIST database of GC-MS spectrum.....	14
Scheme 1.5 The structure of potential thermal degradation products from THC and representative terpenoids including myrcene, limonene and linalool.....	16
Scheme 2.1 Reactions between carbonyls or acids and 2,4-DNPH to form carbonyl-DNPH hydrazone and acid-DNPH adducts.....	23
Scheme 2.2 Representative reaction pathways for the formation of carbonyl compounds and acids in e-cigarette aerosol by thermal degradation of (a) VG and (b) PG. Select flavoring chemicals are shown in (c). Compound in boxes have been quantified in this work. Legend key: 1) formaldehyde, 2) acetaldehyde, 3) acrolein, 4) acetone, 5) propionaldehyde, 6) formic acid, 7) acetic acid, 8) dihydroxyacetone, 9) glyceraldehyde, 10) hydroxyacetone, 11) lactaldehyde, 12) glycolaldehyde, 13) glyoxal, 14) methylglyoxal, 15) diacetyl, 16) 2,3-pentanedione, 17) acetoin, 18) levulinic acid, 19) vanillin.....	30
Scheme 2.3 Proposed MS ⁿ fragmentation mechanism for the deprotonation ion [M-H] ⁻ of acetaldehyde-DNPH.....	33
Scheme 2.4 Proposed MS ⁿ fragmentation mechanism for the deprotonation ion [M-H] ⁻ of dihydroxyacetone-DNPH.....	34
Scheme 2.5 Proposed MS ⁿ fragmentation mechanism for the deprotonation ion [M-H] ⁻ of glyceraldehyde-DNPH.....	35
Scheme 3.1 Proposed mechanism of PG and VG degradation in the e-cigarette device from (a) heat induced dehydration and (b) radical reaction pathways, with further oxidation and bond cleavage to form final products. Legend key: 1) acetone, 2) propionaldehyde, 3) hydroxyacetone, 4) formaldehyde, 5) acetaldehyde, 6) 1-hydroxypropanal, 7) acrolein, 8) methylglyoxal, 9) lactaldehyde, 10) glyceraldehyde, 11) glyoxal, 12) dihydroxyacetone, 13) glycolaldehyde.....	39
Scheme 4.1 Proposed oxidation and thermal degradation pathway of VEA. The corresponding peaks in Table 1 was labeled after the chemical formulas. The thermal degradation products C ₁₇ H ₂₂ O ₄ , C ₂₂ H ₃₂ O ₄ , C ₂₃ H ₃₄ O ₄ , C ₂₅ H ₃₈ O ₄ was identified but not labeled in Figure 4.2 due to the relative small peak intensity.....	89
Scheme 4.2 Proposed radical reaction mechanism for the thermal degradation of VEA. The corresponding peaks in Table 1 was labeled after the chemical formulas. The formation of most abundant peaks (peak 18 - C ₁₂ H ₁₄ O ₄ , 23 - C ₈ H ₁₆ O, 31 - C ₁₁ H ₂₂ O) from benzylic radical and tertiary radical were shown (cleavage bonds f, i, l in Scheme 4.1).....	90
Scheme 4.3 Proposed oxidation and thermal degradation pathway of CBG and THC. The corresponding peaks of carbonyls in Table 1 was labeled after the chemical formulas. The thermal degradation carbonyl products C ₈ H ₁₄ O, C ₈ H ₁₄ O ₂ , C ₅ H ₈ O ₂ , C ₁₃ H ₁₈ O ₃ was identified but not	

labeled in Figure 4.2 due to the relative small peak intensity. The peaks of cannabinoids cannot be labeled due to the existence of isomers.93

Scheme 4.4 Proposed radical reaction mechanism for the thermal degradation of CBG.....94

Scheme 4.5 Proposed radical reaction mechanism for the thermal degradation of THC.....94

List of Tables

Table 2.1 Comparison between the concentrations calculated by different methods.....37

Table 2.2 Carbonyls/acids characterized by HPLC-HRMS. Each experiment was performed triplicate, and the data are expressed as the average (\pm SD), errors are 1σ including delivering aerosol, DNPH derivatization, and ESI sensitivity calculation. The concentrations of five simple carbonyls were calculated by concentration calibrations using authentic standards, while the concentrations of the rest of the compounds were calculated using calculated ESI sensitivities. Concentrations in $\mu\text{g}/\text{m}^3$ were calculated by the total mass of the compounds divided by the total volume of air flowing through the smoking machine during sampling. Due to potential sampling losses, reported concentration values represent a lower limit.....38

Table 3.1 Experimental conditions for e-cigarette aerosol sample generation. Coil temperatures were measured by a thermocouple and controlled to within a standard deviation of 5 °F (3 °C), variable temperatures correspond to 157, 191, 216, 246, 266 °C.....52

Table 3.2 Total mass of e-cigarette aerosol and particle phase composition from e-liquids of different PG/VG ratios and temperatures.....64

Table 4.1 Calibrated m/z, correspond ion and molecular formula, proposed thermal degradation products from VEA and THC.....86

Table 4.2 Particle mass collected on Cambridge Filter Pad by vaping VEA, VEA/extracted THC oil, and extracted THC oil. Low temperature range is 315 ± 10 °F (157 °C), medium temperature range is 455 ± 10 °F (235 °C), high temperature range is 545 ± 10 °F (285 °C). N.D. = not detected, the high temperature data for THC is unavailable.....95

Chapter 1. Introduction

1.1 The overview of e-cigarettes

1.1.1 The principle of e-cigarettes

Electronic cigarettes (e-cigarettes), sometimes referred as “e-cigs”, “e-hookahs,” “vape pens,” and “electronic nicotine delivery systems (ENDS)”, are rechargeable electronic nicotine delivery devices that are alternatives to smoking tobacco cigarettes.¹⁻⁴ E-cigarettes consist of four parts: an atomizer (metal coil), a battery, an e-liquid reservoir (cartridge or tank) and an electronic control system.⁵⁻⁶ The atomizer heats and aerosolizes the e-liquid during the “vaping” process when the user takes a puff or presses the button; this generates a nicotine-containing e-cigarette aerosol (commonly referred as “vapor”) that will be inhaled by the user for the purpose of nicotine intake. Unlike traditional tobacco products, there is no combustion in the use of e-cigarettes, which eliminates the intake of tar and other harmful and potential harmful chemicals (HPHCs) generated through cigarette or cigar smoking. In addition, the tar generated through conventional smoking which is extremely toxic to human and damages the smoker's lungs through biochemical and mechanical process over a long time period⁷⁻⁹ can also be eliminated through e-cigarette use. To date, e-cigarettes have been widely regarded as a “less harm” alternative to traditional cigarettes that can be used to help smoking cessation.¹⁰⁻¹¹ However, the controversy of e-cigarette use has been increasing in recent years, since the beneficial link between e-cigarettes and smoking cessation is debated and emerging health issues had been found, related to the use of different kinds of e-cigarettes.^{11,12} It is noteworthy that thermal degradation products have been characterized due to the vaping process, some of which are known to have negative human health effects.^{2, 13-14}

1.1.2 The invention and evolution of e-cigarette

The development of a nicotine aerosol generation device started in 1963,¹⁵ while the modern e-cigarette was invented by a Chinese pharmacist Han Li, who thought of vaporizing nicotine-containing propylene glycol using a high frequency ultrasound-emitting element, causing a smoke-like vapor.¹⁶ E-cigarettes was first introduced to Chinese market starting from 2004,¹⁷ then entered the European and the US market in 2006 and 2007.¹⁸ The later design of the e-cigarette has changed from the earlier ultrasonic vaporization method to a battery-operated heating element.

E-cigarette device design has evolved significantly since its introduction. The first-generation e-cigarettes use fixed and low voltage batteries, with a physical appearance similar to combustible cigarettes and are often referred to as “cig-a-like”.¹⁹ There exist two versions of the first-generation e-cigarette on the market, one is a two-part design, in which the replaceable atomizer and e-liquid reservoir are in one part, while the battery is separated in another part. The second style combines the atomizing unit, e-liquid reservoir and battery into one part. The first-generation product is still widely sold on the market. The second-generation e-cigarette typically has a larger variable voltage battery with a device referred to as a “clearomizer”.²⁰ It has a removable atomizing unit with a filament, separated into a e-liquid reservoir and battery. The e-liquid tank of the second-generation device has a larger volume reservoir compared to first generation systems, and can be refilled with different e-liquids. The third-generation e-cigarette, known as the “Mod”, has modified batteries that is able to vary the device power, voltage and, thus, temperature.²¹ It has a removable atomizing unit and larger e-liquid tank compared to the original clearomizers.²² The Sub-Ohm tank with low resistance coils in atomizers is highly customized, as it is designed to create a large cloud (aerosol) with a strong delivery of nicotine and other additives. Stainless steel, nickel and titanium are typical materials used for the coil in third-generation devices, as these

materials enable linear temperature changes with the adjustment of device power output.⁵ The fourth-generation e-cigarette is referred to as “Pod-Mods”, and contains a prefilled or refillable “pod” cartridge with a modifiable (mod) system.²³ The compatible prefilled pod cartridges usually contain nicotine with PG/VG, THC or CBD as oils, and flavoring compounds.

In addition to e-cigarettes, an inhalation device called a “vaporizer” is also available on the market; it applies non-combustion heat to aerosolize dry herbs or oil to release the active substance (e.g., THC or CBD) in these materials without combustion.²⁴ Moreover, “dabbing” or “dibbing” is a specific term that describes the action or practice of inhaling small quantities of a concentrated and vaporized drug, typically cannabis oil or resin. It usually simulates the aerosolization process by placing the extracted THC oil concentrates on a hot surface.^{25,26}

1.1.3 Prevalence of e-cigarette use

Since its first commercial introduction to the United States, sales in the e-cigarette industry has increased to \$3.5 billion by 2015.²⁷ The e-cigarette industry has greatly impacted the use of new tobacco products among youth. The prevalence of e-cigarette use (defined as 1 day use in the last 30 days) among high school students increased from 1.5% in 2011 to 16% in 2015, which surpasses the prevalence of conventional cigarette use among high school students.²⁸ According to a report by the Centers for Disease Control and Prevention (CDC) in 2020, 19.6% of high school students (3.02 million) and 4.7% of middle school students (550,000) reported current e-cigarette use.²⁹ Among current e-cigarette users, 38.9% of high school students and 20.0% of middle school students have used e-cigarettes on 20 or more of the past 30 days; 22.5% of high school users and 9.4% of middle school users reported daily use. Among all current e-cigarette users, 82.9% used

flavored e-cigarettes.²⁹ Investigators conducting toxicology and human health studies of acute and chronic use of e-cigarettes are struggling to keep pace with e-cigarettes' popularity and product changes. The study of the health effects of these products is complicated by the fact that there are hundreds (and perhaps thousands) of e-cigarette devices and thousands of commercially-available e-liquids available to consumers. Further, the new generations of e-cigarettes have increased the flexibility of use for consumers by allowing any e-liquid to be added to the tank and a large range of variable power settings, which can increase the temperature of the device, as well as the output of vapor/aerosol and delivery of nicotine.

1.2 The composition of e-liquid

1.2.1 Regular e-liquid

E-liquid is the solvent-based liquid that converts to an aerosol by the atomizer during the heating process. The composition of typical regular e-liquid for nicotine delivery usually include propylene glycol (PG), vegetable glycerin (VG), water, nicotine, and flavoring additives.^{30, 31} PG and VG are typically used as solvents in order to produce an aerosol that simulates cigarette smoke. PG (IUPAC name propane-1,2-diol) is a transparent and viscous liquid at room temperature with a sweet taste.³² It has very low volatility with a boiling point of 188 °C.³³ The use of PG is generally regarded as safe (GRAS) for oral consumption, and it is usually used as a humectant and preservative in food, tobacco and the personal care industry. Moreover, PG is also used in the pharmaceutical industry as a solvent for drug delivery. Although it is widely used, the toxicology at a high concentration is increasingly recognized and recently reported.³⁴⁻³⁶ VG (glycerol, IUPAC name propane-1,2,3-triol) is a colorless and odorless viscous liquid with a boiling point of 290 °C.³⁷⁻³⁸ It also has low volatility and a sweet taste, serving as a humectant, solvent, and sweetener in food, pharmaceutical and personal care applications. Both PG and VG have multiple hydroxyl groups,

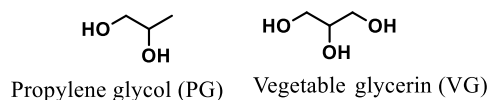
which results in the strong intermolecular force in the e-liquid and e-cigarette aerosol by forming multiple hydrogen bonds.³⁹ Vaporization of PG and VG requires a relatively high temperature, although PG and VG start decomposing within the temperature range of e-cigarette use.⁴⁰⁻⁴¹ The ratio of PG and VG in e-liquid varies in different products based on whether flavor (higher level of PG) or more aerosol mass or “cloud” (higher level of VG) is desired, while the most common two ratios are 50% PG/50% VG and 70% VG/30% PG. E-liquids containing more PG delivered more nicotine to these e-cigarette users.⁴² The chemical structure of PG and VG are shown in **Scheme 1.1a**.

Nicotine is a chiral alkaloid produced in the nightshade family of plants, which has been widely used as recreational or anxiolytic compounds.⁴³ Nicotine is a highly addictive compound that acts as receptor agonist for nicotinic acetylcholine receptors; its binding strength is better than the neurotransmitter acetylcholine.^{44,45} Therefore, nicotine is the equivalent to an increase in the amount of neurotransmitters, which results in increased secretion of dopamine from the reward center of the human brain. The average amount of absorbed nicotine per cigarette is about 2 mg, while the nicotine content of commercially available e-liquids varies from low to high (commonly 0.3–5% by volume).⁴⁶⁻⁴⁹ The chemical structure of nicotine is shown in **Scheme 1.1b**.

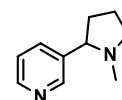
Beside PG, VG and nicotine, most e-liquids contain flavor chemicals that have been certified as safe for ingestion in the food industry. The use of flavor compounds to create various flavor combinations (e.g., different fruits, candy or vanilla)⁵⁰ is attractive to consumers. There are various chemical families of flavorants used on the market, including aldehyde (e.g., vanillin, ethyl vanillin, benzaldehyde, tolualdehyde, piperonal, cinnamaldehyde),^{51 52} ketone (e.g., diacetyl, maltol, ethyl maltol, menthone),⁵³ alcohol (e.g., benzyl alcohol, menthol),⁵⁴ monoterpene (e.g., limonene, linalool)⁵⁵ and ester (e.g., ethyl butyrate, ethyl acetate, ethyl isovalerate).⁵⁶ An

important category is aldehyde, which has been recognized as “primary irritants” of the mucosal tissue of the respiratory tract.⁵⁷ Behar et al.⁵⁸ has identified that the most commonly used flavoring chemicals are menthone, p-anisaldehyde, menthol, cinnaldehyde, vanillin, and ethyl maltol, which has been found in 41 – 80% of commercial e-liquids. The transfer of these flavoring chemicals from e-liquid to e-cigarette aerosol is very efficient (mean transfer = 98%), while it has also been found that the refilled fluids that have lower concentrations of flavoring chemicals exhibit lower cytotoxicity, suggesting the toxicity of the e-cigarette aerosol is related to the concentration of the

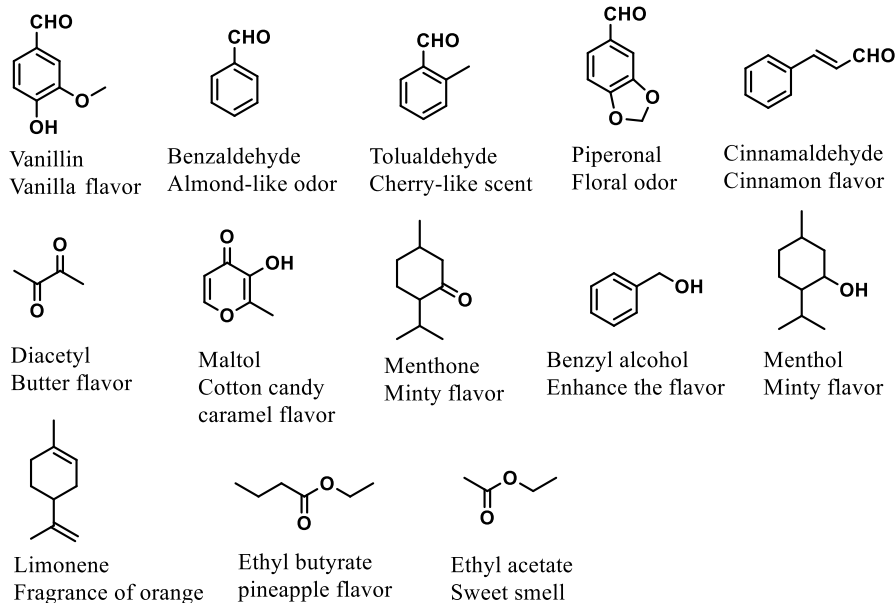
a) Solvent of e-liquid



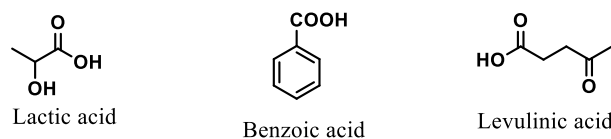
b) Nicotine



c) Representative flavor compounds



d) Representative organic acids



Scheme 1.1 The chemical structures of PG, VG, nicotine, and representative flavor compounds and acid additives.

flavoring chemicals.⁵⁸ However, with the significant increase in the array of different e-liquid products, it is difficult to comprehensively characterize all flavor compounds on the market. Previous research found flavor chemicals to be 1-4% of the total e-liquid volume,⁵⁷ although the concentration of some specific flavor chemicals were sufficiently high enough to possibly be of concern for inhalation toxicology. Some specific flavoring chemicals like diacetyl has been found (recognized) to cause adverse health effects to e-cigarette users, even if they are safe to digest.⁵⁹ Diacetyl is a chemical used as artificial flavor in candy, popcorn and other food items, while also used in e-liquids to provide a butter flavor. However, the inhalation of diacetyl may be associated with permanent lung damage like “popcorn lung” and trigger breathing problems, as well as wheezing or other forms of respiratory disease.⁵³ Moreover, Khlystov et al. ⁶⁰ found that the addition of flavoring chemicals significantly increased the emission level of small aldehydes due to the degradation of flavoring molecules. The chemical structures of a number of representative flavoring compounds are shown in **Scheme 1.1c**.

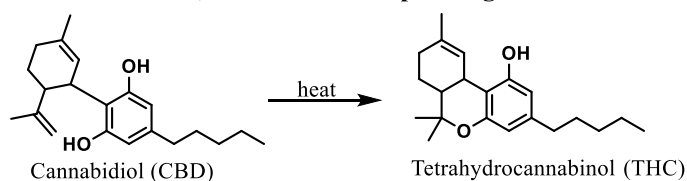
Organic acids additives have also recently been found in e-liquids. Organic acids are used to protonate nicotine to form nicotine salts, which are found naturally in tobacco leaves and are widely used as an alternative to free-base nicotine in e-cigarettes.⁶¹ Nicotine salts are thought to amplify the delivery of nicotine to the user without changing the concentration of added free base nicotine which could cause throat irritation.⁶² The speed of e-cigarette nicotine salts uptake in humans is similar to the speed of nicotine uptake in combustible cigarettes. Research on nicotine salts is limited, and the health risk of persistent inhalation of nicotine salts is unknown at this time. There exist more than 20 nicotine salts available on the market, and the most commonly used weak acid in the formation nicotine salts includes lactic acid, benzoic acid and levulinic acid.⁶³ The

chemical structures of representative acids that are used for nicotine salts are shown in **Scheme 1.1d**.

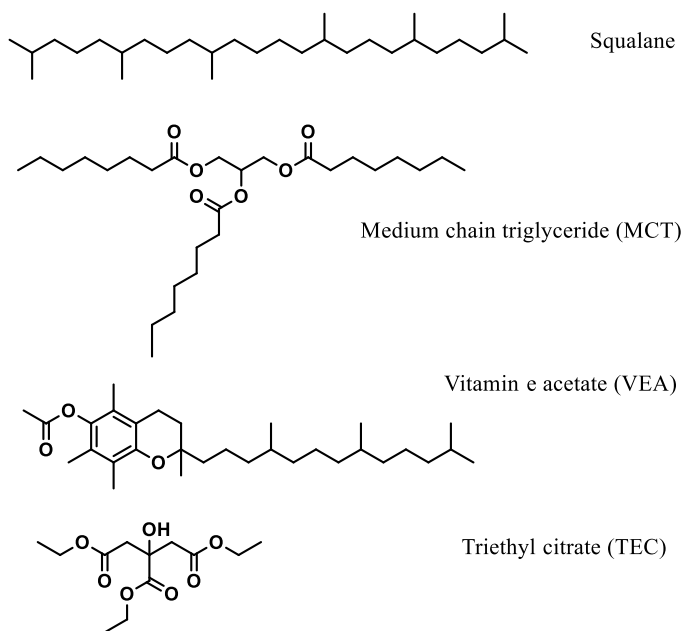
1.2.2 Cannabis e-liquid

The active ingredient in cannabis e-liquid is tetrahydrocannabinol (THC). Delta-9-tetrahydrocannabinol (Δ^9 -THC) is the critical component for inducing a psychoactive effect, and is the more popular isomer on the market; however, delta-8 is gaining popularity. THC is found in marijuana, also called weed, herb and some other terms, which is the mixture of dried flowers of *cannabis sativa*.⁶⁴ Cannabis concentrate refers to the product of distilling down the most desired

a) Structure of CBD, THC and corresponding transform route



b) Structure of commonly used cutting agents



Scheme 1.2 The chemical structures of CBD, THC and other potential cutting agents.

parts of the plants.^{65,66} It usually contains all the cannabinoids and terpenes that already exist in

cannabis flowers, but without the undesired part of the plants. THC concentrate is an oil-like extract that contains a high dosage of THC and terpenes from marijuana. Cannabinoids and terpenes are responsible for the psycho-activity, aroma and flavors desired by many e-cigarette users. THC can be absorbed into the bloodstream and transmitted to the brain following smoking or inhaling the aerosol formed by the e-cigarette device, with binding to the endocannabinoid receptors located in the different parts of brain that are responsible for basic function, such as thinking, movement and pleasure.^{67, 68}

Hemp is also used for oil extraction; it has more cannabidiol (CBD) content than THC.⁶⁹ CBD is one of 113 identified cannabinoids; it does not have the same psychoactivity as THC, and more research is needed to determine its biological effects. The use CBD in e-cigarettes is widespread and CBD in e-cigarettes can act as the precursor to THC. It has been found that 25 – 52% of CBD can transform into other cannabinoids (e.g., THC, cannabinol and cannabichromene); THC is the main pyrolysis product of CBD under typical e-cigarette operational temperature ranges (250 - 400 °C) under both oxidative and inert conditions.⁶⁷ THC-containing products are generally sold as prefilled cartridge or in dropper bottles for refill. The structures of CBD, THC and corresponding transformation routes are shown in **Scheme 1.2a**.

Beside the psychoactive ingredient, THC cartridges sold on the black market usually contain cutting agents to dilute the THC concentrates; these cutting agents generally have similar viscosity to the THC concentrates to make the mixture appear pure. Since THC is hydrophobic, i.e., not dissolved in water, the typical cutting agents include squalane oil, medium chain triglyceride (MCT) oil, vitamin E acetate (VEA), and triethyl citrate (TEC).⁷⁰ The safety of these agents has

not been fully accessed for vaping inhalation. The structures of these common cutting agents are shown in **Scheme 1.2b**.

1.3 The thermal degradation products of e-cigarettes

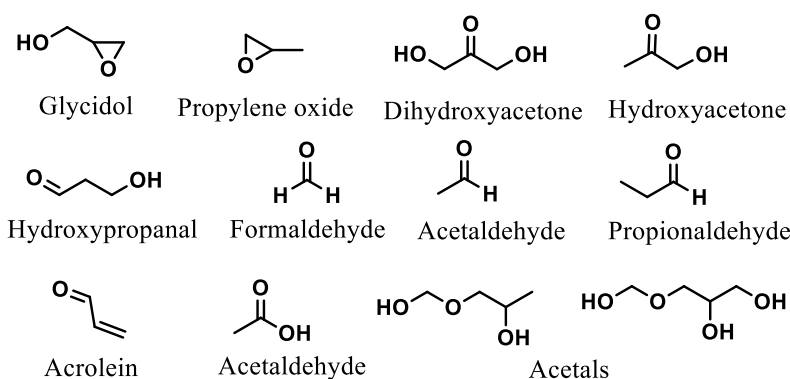
1.3.1 The thermal degradation products of typical e-liquid compositions

Since PG and VG are the main components in the conventional vaping e-liquid, the thermal degradation of PG and VG is important to the fundamental understanding of vaping chemistry. There is a long history of study for PG and VG chemistry. VG was successfully prepared by Scheele in 1779. It has been stated that thermal degradation might happen during the distillation process of VG, where acrolein was identified as the thermal degradation products of VG in 19th century.⁷¹ Subsequently, the American organic chemist John Ulric Nef provided an understanding of the dissociation reaction in the glycol-glycerin series.⁷² In the experiments of Nef, the VG sample was heated to 450 °C and carbon monoxide and hydrogen were identified in the collected gas. Furthermore, hydroxyacetone, formaldehyde, acetaldehyde, acrolein and a series of acetals were found in the fractionated residues. Nef proposed that glycidol is formed at a relative low temperature, but at an elevated temperature, the glycidol will go through a tautomerization process to form hydroxyacetone or hydroxypropanal. Acrolein can be formed by the dehydration of hydroxypropanal, while hydroxyacetone is further decomposed into acetaldehyde and formaldehyde at the temperature studied by Nef. Hemiacetal and cyclic acetals can be formed by reaction of the thermal degradation carbonyl compounds with excess glycerol.⁷³ For the thermal degradation of PG, Nef identified propionaldehyde in the fractionated residue. However, there was no acetone found in volatile fraction, which suggested that the propylene oxide may not form as an intermediate during the thermal degradation, or propionaldehyde is the main product from

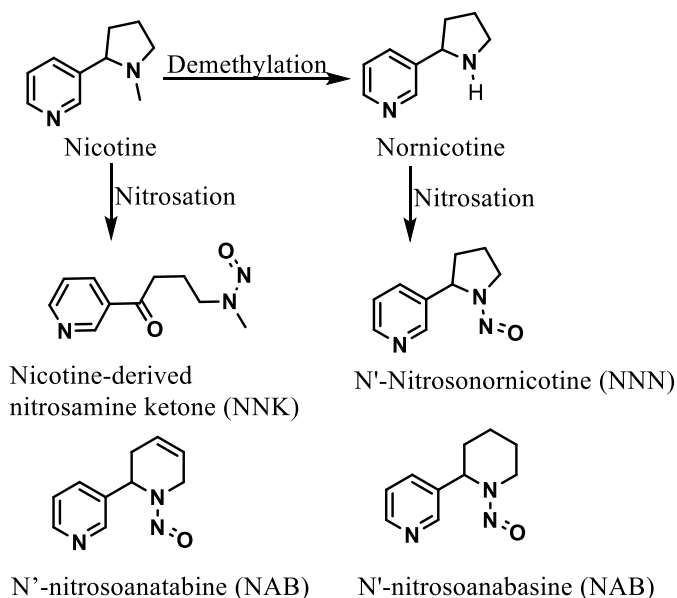
tautomerization. Generally, Nef provided the fundamental knowledge for the current understanding of PG and VG chemistry.⁷⁴

More research about the thermal degradation of PG and VG has been done recently. For example, Laino et al.⁷⁵ showed that the thermal degradation of VG can form formaldehyde,

a) Thermal degradation products from PG and VG



b) The structure of tobacco-specific nitrosamines



Scheme 1.3 a) The structures of thermal degradation products that has been identified from PG and VG; b) The structure and potential transform pathway of tobacco-specific nitrosamines.

acetaldehyde, and acrolein via the formation of glycidol, while PG can generate propionaldehyde and acetone via the intermediate formation of propylene oxide.⁷⁶ Diaz et al.⁷⁷ suggested PG could also participate in a heat-induced radical-mediated degradation pathway, proposed to be initiated by O₂ insertion to C-H bonds to generate the OH radical that further propagates the radical chain, forming at least five products. The radical-mediated pathway of VG has also been proposed by other researchers, and at least seven thermal degradation products have been observed in the process.⁷⁸⁻⁸⁰ Some multifunctional degradation products (e.g., glycolaldehyde, with hydroxyl and aldehyde groups) can further react to form simple carbonyls,^{81,82} and accretion reactions between carbon-centered radicals or stable products (e.g., hemiacetal formation) can further complicate the chemistry of e-cigarette aerosols.⁸³⁻⁸⁴ The fragmentation of aliphatic alcohols tend to produce compounds that have a carbonyl (ketone or aldehyde) moiety;^{85,86} however, because PG and VG are polyols, their degradation will also result in carbonyls functionalized with hydroxyl groups in addition to the simple types. Organic acid formation may also occur to a certain degree, possibly as a carbonyl oxidation process. The structures of potential thermal degradation products of PG and VG are shown in **Scheme 1.3a**.

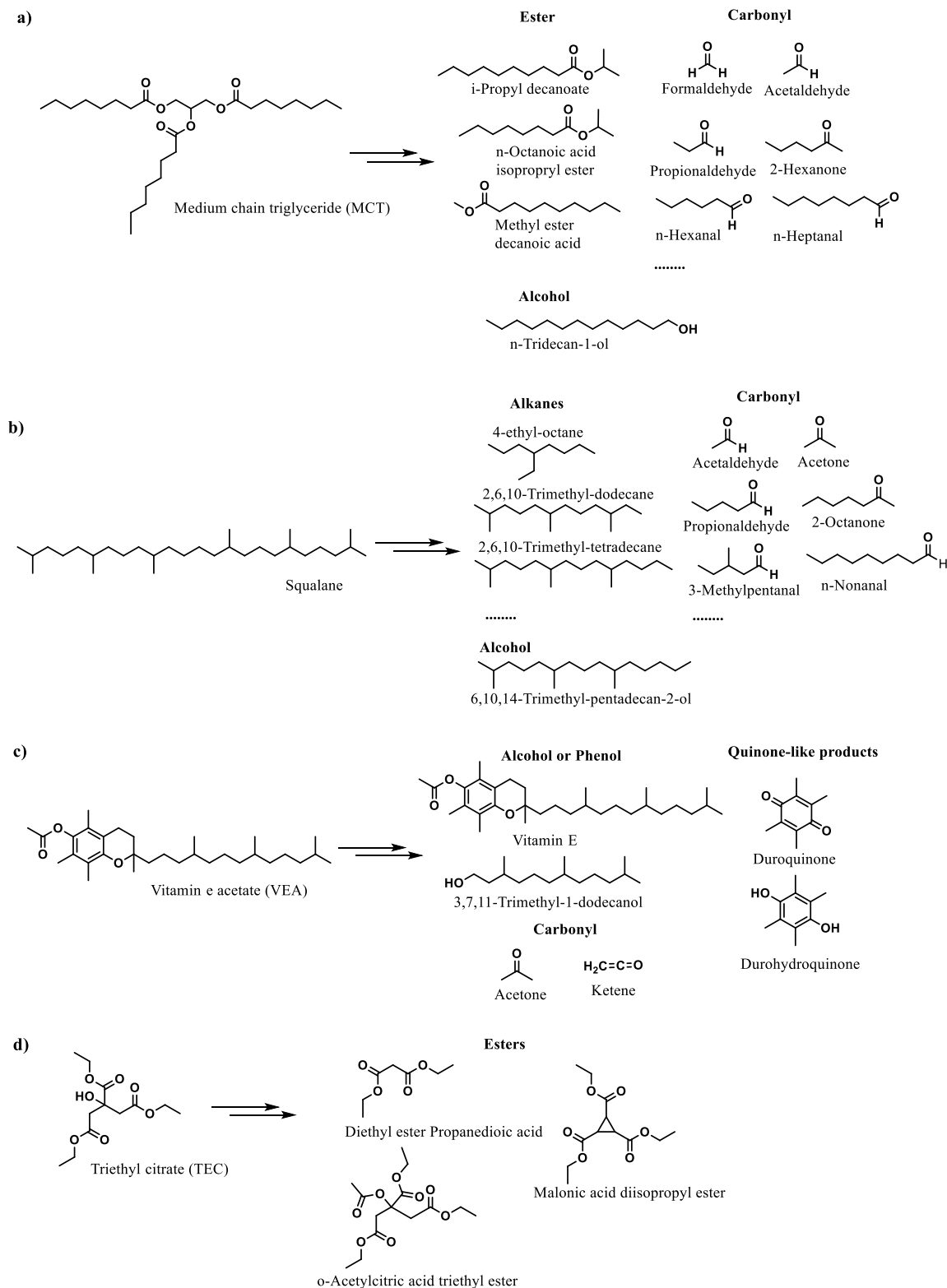
Nicotine may also go through a thermal degradation pathway to form potentially harmful constituents, such as N'-Nitrosornicotine (NNN) and the related tobacco constituent 4-(methylnitrosamino)-1-(3-pyridyl)-1-butanone (NNK). NNN and NNK have been regarded as important carcinogenic tobacco-specific nitrosamines (TSNAs), since they are known to induce carcinogenesis through DNA adduction and mutation, as well as to improve tumor growth through receptor-mediated effects.⁸⁷ They are present in both the smoke of cigarettes and e-cigarette aerosols, as well as the saliva of tobacco and e-cigarette users. NNN can be formed endogenously

from nornicotine, which is a tobacco constituent and nicotine metabolite. Bustamante et al.⁸⁸ has quantified NNN in the saliva of e-cigarette users, ranging from nonquantifiable to 14.6 pg/mL, while the NNN level in saliva of smokers range from nonquantifiable to 739 pg/mL. Although the total exposure of NNN in e-cigarette users is significantly lower than smokers, the NNN can still be formed through the use of e-cigarettes. Moreover, Farsalinos et al.⁸⁹ found that NNK will not be formed within the temperature range of e-cigarette operation. However, other research has found that 2.8 ng NNK can be delivered per 15 puffs,⁹⁰ and is found in 89% of e-liquids from Korea.⁹¹ Moreover, N'-nitrosoanatabine (NAT) and N'-nitrosoanabasine (NAB) are also detected in e-liquids. They are classified in the Category 3 carcinogens, although the metabolic pathway of NAB has not yet been identified.⁸⁷ The structures of NNN, NNK, NAT and NAB and transformation pathways are shown in **Scheme 1.3b**.

1.3.2 The thermal degradation of cannabis e-liquid compositions

Compared to regular e-liquids, there is only very limited research data available for the thermal degradation of cannabis e-liquids, as marijuana (and specifically THC) are still federally classified as a Category 1 controlled substance by the US Drug Enforcement Administration (DEA) and access to cannabis samples and analysis in research is greatly restricted. Research on e-liquid diluents or CBD-related vapes do not require a DEA license.

Jiang et al.⁷⁰ tested seven commonly used e-liquid diluents in an e-cigarette device with a THC-infused cartridge including PG, VG, medium-chain triglyceride (MCT) oil, squalane (SQL) oil, vitamin E, VEA, and triethyl citrate (TEC). The GC-MS spectra of unvaped e-liquids were compared to the vaping emissions to investigate the thermal degradation products during the



Scheme 1.4 The structures of potential thermal degradation products from different common used diluents of cannabis e-liquid identified by the NIST database of GC-MS spectrum.

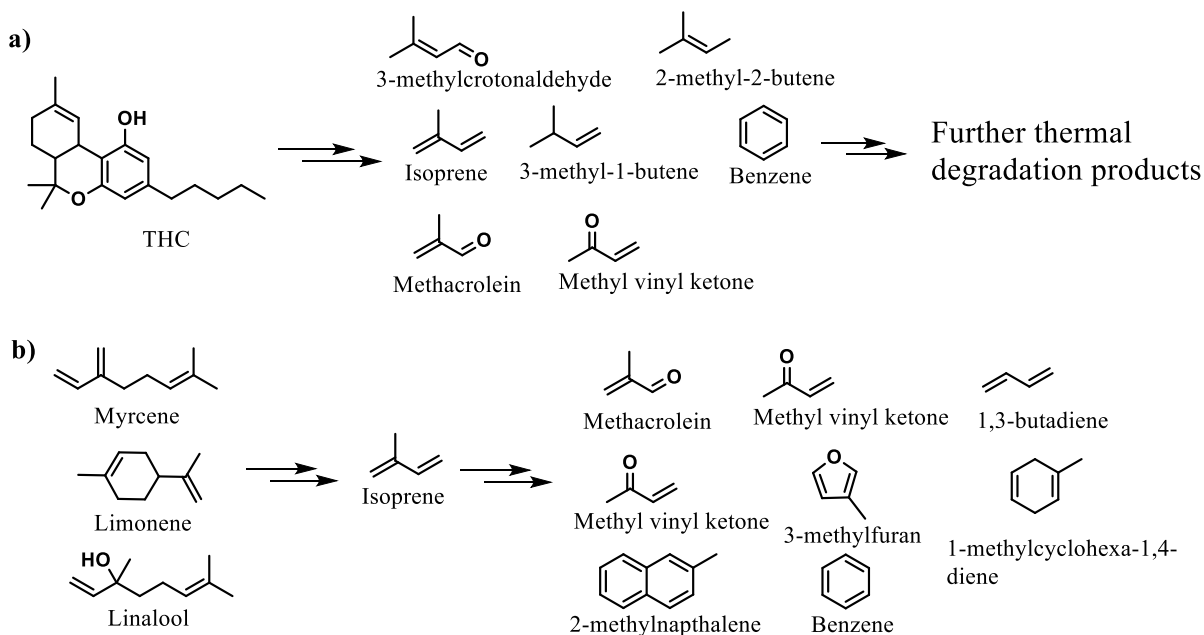
vaping process. Generally, significant changes were observed in the GC-MS spectrum with vaping

emission condensates compared to unvaped e-liquids, suggesting that the chemical composition of vaping products are very different from the original diluent. The thermal degradation products include carbonyls, alkyl alcohols, esters, carbonxylic acid, and alkanes. Specifically, the main thermal degradation products of MCT oil includes an ester that has the same molecular backbone and precursors in MCT oil, as well as carbonyl compounds generated from the chain breaking. The thermal degradation products of squalane include different alkanes and carbonyls from chain breaking. Alcohols were also identified as oxidation products, presumably through OH chemistry. Acetone, 3,7,11-Trimethyl-1-dodecanol and duroquinone have been found in the e-liquids containing vitamin E and VEA. Durohydroquinone was also identified from the thermal degradation of VEA. Multiple esters were identified from the thermal degradation of triethyl citrate. Moreover, Riordan-Short et al.⁹² found the decomposition of VEA could occur within the temperature range of e-cigarette use (180 - 300 °C), even though its boiling point is approximately 485 °C. Most of thermal degradation products are aldehydes and ketones that may come from the oxidation of the aliphatic side-chain of VEA. Ketene ($\text{H}_2\text{C}=\text{C}=\text{O}$), a toxic gas, has also been identified as a potential thermal degradation product of VEA.⁹³ The structures of potential thermal degradation products of different diluents are shown in **Scheme 1.4**.

The legalization of recreational cannabis use in several states, including California, have significantly increased the popularity of various consumption methods for cannabis extract in e-cigarettes (e.g., dabbing, cartridge vaporizers, top-loading vaporizers). The chemistry of the extracted THC or CBD oil related to dabbing or vaping is very limited due to the aforementioned research restrictions. Moreover, since the extracted cannabis oil is a complex mixture, the source of harmful or potentially harmful constituents (HPHCs) in the vaping aerosol of extracted THC or

CBD oil is not clear. These constituents may come from cannabinoids, terpenes, extraction solvents (such as butane) or other components that originate from either plants or chemical processing. Meehan-Atrach et al.²⁶ identified the thermal degradation products of THC to include methacrolein, benzene, and methyl vinyl ketone when using cartridge vaporizer and dabbing. Moreover, four relatively abundant thermal degradation products including isoprene, 2-methyl-2-butene, 3-methylcrotonaldehyde, and 3-methyl-1-butene have been shown to be derived from the common radical intermediate of THC, as THC contains a monoterpene moiety and has been shown to emit similar volatile products to terpenes during the vaping process.⁹⁴ Research has also been performed on the pyrolysis of CBD and olivetol derivatives with intact pentyl chains.⁹⁵

Terpenes and terpenoids are also present in cannabis extracts since they already exist in cannabis plants. Terpenes and terpenoids are also used as flavoring compounds in both cannabis and conventional vapes. Myrcene is the most abundant terpene in cannabis, followed by limonene,



Scheme 1.5 The structures of potential thermal degradation products from THC and representative terpenoids including myrcene, limonene and linalool.

linalool, pinene, caryophyllene, and humulene, in addition to 68 other terpenes found in trace amounts.⁹⁶ Monoterpenes, sesquiterpenes alcohols and triterpenes are of particular concern because of their relatively high presence and the potential formation of low molecular weight oxidized thermal degradation products.⁹⁷ Tang et al.⁹⁷ heated the mixture of 12 terpenoids that usually present in the cannabis extract and identified multiple degradation byproducts, including isoprene, 2,5-dihydroxytoluene, 6-MHO, benzene and some carbonyl products (e.g., formaldehyde, acetaldehyde, acrolein, methacrolein). Meehan-Atrash et al.⁹⁸ also identified isoprene, methacrolein, benzene, methyl vinyl ketone and other potential thermal degradation products from myrcene, limonene and linalool. The structures of potential thermal degradation products of THC and representative terpenoids are shown in **Scheme 1.5**.

1.4 Current analytical technology for the characterization of thermal degradation products

Many sample collection and analytical methods have been applied for the detection and quantification of components in both the original e-liquid and the e-cigarette aerosol. The collection methods include filter pad collection (e.g., glass fiber filter, quartz filter, PTFE filter), adsorbent cartridges (XAD sorbent tubes, silica cartridges impregnated with derivatization agents), and gas collection bags. Gas chromatography (GC) and liquid chromatography (LC) coupled with different detectors including mass spectrometry, UV-Vis, and others (e.g., GC-MS, GC-FID, GC-NPD, HPLC-UV, HPLC-HRMS, HPLC-MS/MS) are usually applied for the characterization of components in e-cigarette aerosol.² Besides chromatography, nuclear magnetic resonance (NMR) has also been applied to the characterization of e-cigarette thermal degradation products. Jensen et al.⁷⁴ have published a library of ¹H NMR spectra for many thermal degradation products in e-cigarette aerosol that are derived from PG and VG. These technologies are also applied for the

characterization of including volatile organic compounds (e.g., acrylamide, benzene, propylene oxide), carbonyls (e.g., formaldehyde, acetaldehyde), nicotine and tobacco specific nitrosamines (e.g., NNN, NNK), polycyclic aromatic hydrocarbons (PAHs, e.g., acenaphthene, chrysene, fluorene), heavy metals (e.g., aluminum, chromium, copper, cobalt), and flavoring compounds.²

VOCs are normally detected by GC-FID, GC-MS and related instruments. Lee et al.⁹⁹ detected VOCs including ethanol, acetonitrile, isopropyl alcohol, benzene and toluene using the GC method from National Institute for Occupational Safety and Health (NIOSH) that employ evacuated canisters lined with fused silica for sample collection.¹⁰⁰ Carbonyl compounds are usually derivatized by 2,4 - dinitrophenylhydrazine (2,4 – DNPH) in solution or on silica gel cartridges impregnated by 2,4 – DNPH, followed by analysis on HPLC-UV or HPLC-MS. Nicotine, TSNAs, and PAHs are usually captured on filter pads and analyzed by GC-MS. Trace metals are usually captured on quartz filters and analyzed by ICP-MS.

The e-cigarette aerosol includes a liquid-like particle phase and a gas phase. Most e-cigarette emissions are semivolatile, which can partition to both the gas and particle phases depending on different environmental conditions and chemical properties (e.g., boiling point, vapor pressure, hydrogen bonds). Pankow et al.⁵⁵ predicted that the phase distribution of various components in e-cigarette aerosol are related to the mass concentration of particles ($\mu\text{g}/\text{m}^3$), the composition of particles, the vapor pressure of the chemical, and the ambient temperature. For example, formaldehyde can be found mainly in the gas phase even at the highest level of total particulate level of e-cigarette aerosol, while formaldehyde hemiacetals partition into the particle phase, even at the lowest total particulate matter levels.

Although simple thermal degradation products such as formaldehyde, acetaldehyde, and acrolein are commonly quantified in the literature, the reported levels of specific components significantly vary in different publications. This might be due to the diversity and complexity of e-cigarette products, as devices from different brands and design generations vary in power settings, coil type (e.g., coil material and surface area) and puff topography (e.g., puff volume). Another potential reason is that there is no standard sampling and analytical methods for the target analytes in e-cigarettes aerosols. For example, Eddingsaas et al.¹⁰¹ found that the use of limited collection methods (e.g., only filter pad collection or impinger collection, as opposed to a broader suite) will not identify all aerosol components. This suggests a more comprehensive approach, using a combination of techniques, is needed for the collection of e-cigarette aerosols. Moreover, thousands of e-liquid formulations with different PG:VG ratios and different flavoring compounds introduce further challenges to a unified understanding of the e-cigarette chemistry in the literature. This suggests a need to isolate key e-liquid ingredients to study their fundamental chemistry, instead of sampling from commercial e-liquid blends that are proprietary in composition, in order to have a more predictive understanding of thermal degradation in e-cigarette vessels.

Chapter 2. Application of high-resolution mass spectrometry and a theoretical model to the quantification of multifunctional carbonyls and organic acids in e-cigarette aerosol

Abstract

E-cigarette aerosol (particle and gas) is a complex mixture of chemicals, of which the profile is highly dependent on device operating parameters and e-liquid flavor formulation. The thermal degradation of the e-liquid solvents propylene glycol and glycerol often generate multifunctional carbonyls that are challenging to quantify due to unavailability of standards. We developed a theoretical method to calculate the relative electrospray ionization sensitivities of hydrazones of organic acids and carbonyls with 2,4-dinitrophenylhydrazine (DNPH) based on their gas phase basicities ($\Delta G_{\text{deprotonation}}$). This method enabled quantification by liquid chromatography high-resolution mass spectrometry (HPLC-HRMS) in the absence of chemical standards. Accurate mass and tandem multistage mass spectrometry (MS^n) were used for structure identification of vaping products. We quantified five simple carbonyls, six hydroxycarbonyls, four dicarbonyls, three acids, and one phenolic carbonyl in the e-cigarette aerosol with Classic Tobacco flavor. Our results

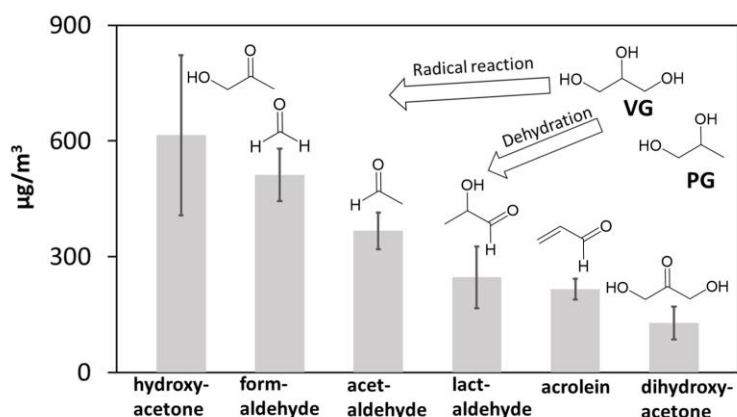


Figure 2.1 The concentration of main thermal degradation products in e-cigarette aerosol in this work.

suggest that hydroxycarbonyls, such as hydroxyacetone, lactaldehyde, and dihydroxyacetone can be significant components in e-cigarette aerosol, but have received less attention in the literature and have poorly-understood health effects. The data support the radical-mediated e-liquid thermal degradation scheme that has been previously proposed and emphasize the need for more research on the chemistry and toxicology of complex product formation in e-cigarette aerosol.

2.1 Introduction

Since its introduction to the United States in 2007, the electronic (e-) cigarette market has expanded significantly.^{102, 28} The prevalence of e-cigarette use was 3.2% for adults and 7.6% for young adults (aged 18-24) in 2018.¹⁰³ The prevalence of e-cigarette use among high school students increased from 1.5% in 2011 to 27.5% in 2019, eclipsing conventional cigarettes among youth.^{104,105} With the growing population of e-cigarette users, the evidence that e-cigarette use is related to higher frequency of cigarette smoking,¹⁰⁶ and the lack of historical governmental regulation, there is a significant need to fill existing data gaps on chemistry, toxicology, and clinical/behavioral patterns to inform on e-cigarette consumer safety and risk.¹⁰⁷⁻¹⁰⁹ E-cigarettes have been suggested as a reduced harm alternative to traditional tobacco-based products due to the reduced presence of well-studied toxicants formed during tobacco combustion.¹¹⁰ However, the use of e-cigarette may have its own risk, such as electronic cigarette or vaping-associated lung injury (EVALI),¹¹¹⁻¹¹³ respiratory function impairment, inhalation of carcinogenic carbonyls, and changes in gene expression.^{114,115} Furthermore, as e-cigarette emissions are not completely inhaled, there is potential for bystander or secondary exposure to non-users from the exhaled aerosol to the environment.¹¹⁶ Recent works^{117,118} have provided insights into how e-cigarette components and emissions affect indoor air quality and exposure pathways.¹¹⁹⁻¹²³ Yet to date, there remain major

gaps in our knowledge of a complete chemical profile generated from the vaping process, as well as detailed mechanisms producing those chemicals. Moreover, the astonishing variety of e-cigarette products and innumerable flavors available on the market, combined with the fast pace of product alterations due to the steady increase in e-cigarette popularity, present significant challenges in e-cigarette research and the estimation of user risk.¹²⁴

The thermal degradation of propylene glycol (PG) and vegetable glycerin (VG), the primary components of e-liquid,¹²⁵⁻¹²⁷ can generate complex chemical products through a series of reactions. Laino et al.⁷⁵ showed that the thermal degradation of VG can form formaldehyde, acetaldehyde, acrolein by dehydration via the formation of glycidol, while PG can generate propionaldehyde and acetone via the intermediate formation of propylene oxide.^{76,72} Diaz et al.⁷⁷ suggested PG could also participate in a heat-induced radical-mediated degradation pathway, initiated by O₂ insertion to C-H bonds to generate the OH radical that further propagate the radical chain, forming at least five degradation products. The radical-mediated pathway of VG has also been proposed by other researchers, and at least seven thermal degradation products have been observed in the process.⁷⁸⁻⁸⁰ Some degradation products (e.g., glycolaldehyde) can react further to form simple carbonyls,^{81,82} and accretion reactions between carbon-centered radicals or stable products (e.g., hemiacetal formation)^{83,84} can further complicate the chemistry of e-cigarette aerosols.

The fragmentation of aliphatic alcohols tend to produce compounds that have a carbonyl (ketone or aldehyde) moiety,^{85,86}

However, since PG and VG are polyols, their degradation will also result in carbonyls functionalized with hydroxyl groups in addition to the simple types.

Organic acid formation may also occur to an extent, possibly as a carbonyl oxidation

process. Some thermal degradation products have well-documented toxicity to humans (e.g., formaldehyde, acetaldehyde, acrolein),¹²⁸⁻¹³⁰ while others have suspected toxicity (e.g.,

dihydroxyacetone, glyoxal, formic acid). In addition to thermal degradation products,¹³¹⁻¹³³ hundreds of flavoring ingredients may be added to e-liquids and vaporized in e-cigarette aerosol,

which can potentially lead to adverse health impacts.^{53,57} Jensen et al.³⁴ identified the largest variety of thermal degradation products to date from aerosolized e-liquid using Nuclear Magnetic

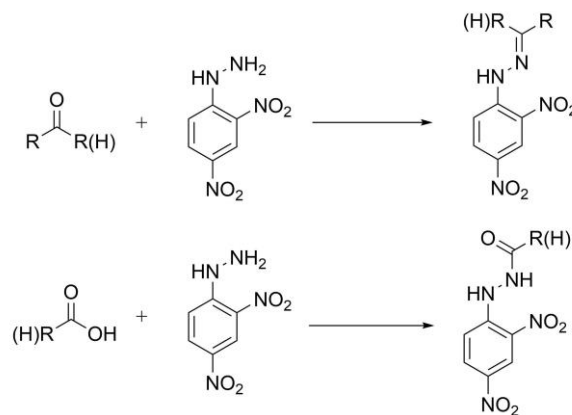
Resonance (NMR); however, the data are not quantitative in that work. Since most compounds in e-cigarettes have a carbonyl moiety, quantification is conventionally done by derivatizing with

2,4-dinitrophenylhydrazine (2,4-DNPH) to produce hydrazone adducts (**Scheme 2.1**),¹³⁴⁻¹³⁶ followed by analysis with liquid-chromatography (LC) or gas chromatography (GC) using

authentic carbonyl-DNPH standards for calibration of chromatographic peak areas.^{14, 60, 137-141}

Even so, authentic carbonyl-DNPH standards are not available for many complex products.

Synthesis of carbonyl-DNPH standards may be done;¹⁴² however, the process to synthesize, purify, and purity-check is laborious, requires specialty equipment, and requires reasonable synthetic



Scheme 2.1 Reactions between carbonyls or acids and 2,4-DNPH to form carbonyl-DNPH hydrazone and acid-DNPH adduct.

chemistry skills. Synthesis of DNPH hydrazones of multi-carbonyls require additional purification steps to isolate the mono- and multi-hydrazones. In addition, some carbonyls (e.g., certain ketoaldehydes and others) are not commercially available as starting material, requiring their own separate synthesis. Thus, an approach to quantify without chemical standards is an attractive alternative.

Furthermore, spectroscopic chromatography methods that rely on retention time and UV-visible absorbance spectra may be limited by co-elution or indistinctive spectra, even when utilizing authentic chemical standards. The coupling between chromatography and high-resolution mass spectrometry (HRMS) is a powerful tool for chemical identification,¹⁴³ as it removes the co-elution limitation by enabling molecular formula assignments from exact mass. The goals of this work are twofold: (1) use high mass resolving power coupled to chromatography to better identify DNPH hydrazones of functionalized and simple carbonyls and acids, and (2) develop a method to quantify e-cigarette chemical products for which analytical standard are unavailable.

2.2 Experimental

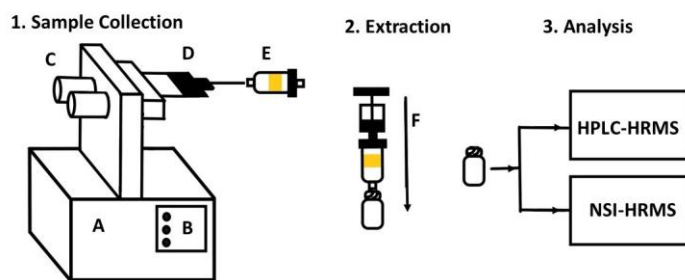


Figure 2.2 Sample collection, extraction and analysis set up. Legend: A) TE-2B smoking machine, B) adjustable settings for puffing duration and frequency, C) holder for e-cigarette cartridges, D) outflow from device, D) DNPH impregnated silica cartridges, F) extraction protocol into autosampler vials.

2.2.1 E-cigarette aerosol sample generation and extraction

First-generation disposable e-cigarettes from blu[®] (Imperial Brands Inc., Bristol, United Kingdom.), a popular e-cigarette brand,¹⁴⁴ with “Classic Tobacco” e-liquid cartridges were used for this study. The blu[®] e-cigarettes are comprised of a rechargeable battery with a capacity of 140 mAh, an atomizer with coil resistance of 3.5 ohm, and a disposable, non-refillable e-liquid cartridge with proprietary ingredients. Batteries were charged after every 20 min of usage and the e-liquid cartridge was replaced after 400 puffs. A TE-2B smoking machine (Fig. 2.2, Teague Enterprises Inc., Woodland, CA) was used to generate e-cigarette aerosol for the analysis. The apparatus puffed two e-cigarettes, in alternating turns, at a frequency of 8 puffs/min (4 puffs for each e-cigarette) for a 2 second puff duration. The average flow rate was 2.3 L/min and the puff volume was 77 mL, quantified by a primary flow calibrator (A.P. Buck Inc., Orlando, FL). E-cigarette aerosol samples were collected through (1) 2,4-dinitrophenylhydrazine (2,4-DNPH) cartridges (Supelco Inc., 350 mg DNPH, Bellefonte, PA) for carbonyls/acids and (2) 47 mm Polytetrafluoroethylene filters (Millipore Sigma, 0.2 μm pore, Burlington, MA) for nicotine. A

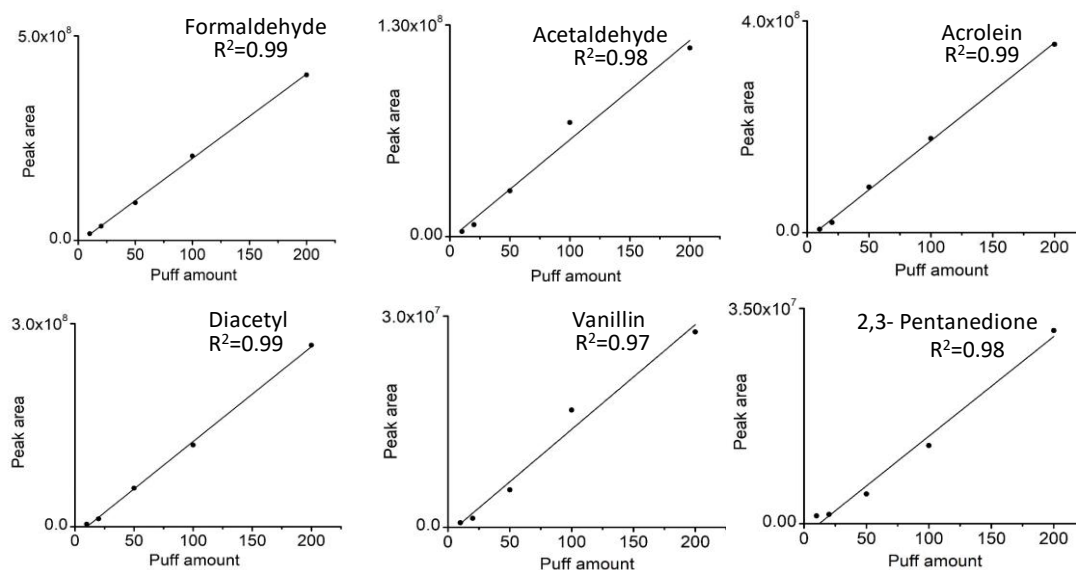


Figure 2.3 Linear dynamic range (5, 10, 20, 50, 200 puffs) of different carbonyl compounds (thermal degradation products of PG and VG, and flavoring chemicals).

total of 200 puffs were collected for each analysis, which is within the linear dynamic range of the analysis ($R^2 = 0.97 - 0.99$ from 5 – 200 puffs, **Fig. 2.3**). The emission profile was stable, within the uncertainty of the analysis, for the first and second 200-puff collection of each cartridge. After collection, DNPH cartridges were extracted with 2 mL acetonitrile (Fisher Scientific Inc., LC-MS grade, Hampton, NH) into 1.5 mL autosampler vials (approximately 0.5 mL remains in the cartridge). Consecutive extractions of DNPH cartridges for 40-, 80-, and 200-puff samples confirmed that >97% of both DNPH and its hydrazones were extracted after the first 2 mL volume. The samples were diluted using LC-MS acetonitrile to the desired concentrations for direct-infusion HRMS and MSⁿ analyses (**Section 2.2.2**). Extracts were used for HPLC-HRMS analyses (**Section 2.2.3**) without dilution. All samples were promptly analyzed after preparation; sample collection and analyses were performed in triplicate.

2.2.2 Identification by high-resolution mass spectrometry and tandem mass spectrometry

Diluted carbonyl-DNPH extracts were analyzed for molecular composition using a linear-trap-quadrupole Orbitrap (LTQ-Orbitrap) mass spectrometer (Thermo Corp., Waltham, MA) at a mass resolving power of $\sim 60,000$ $m/\Delta m$ at m/z 400. The extracts were directly infused into a capillary nano-electrospray ion source (ESI, 50 μm fused-silica capillary tip, 4 kV spray voltage, 275°C capillary temperature, 5 $\mu\text{L min}^{-1}$ flow) and the spectra taken in the negative ion mode. An external mass calibration was performed using the ESI-L tuning mix (Agilent Inc., Santa Clara, CA) immediately prior to the MS analysis, such that the mass accuracy was adjusted to be approximately 1 ppm for standard compounds. Molecular assignments were performed using the MIDAS v.3.21 molecular formula calculator (Florida State Univ.). Insights into molecular structure were obtained using collision induced dissociation (CID) multistage tandem mass

spectrometry (MS^n , stages 2 – 4) in the LTQ-Orbitrap. CID energy was tuned for each mass, such that the precursor ion has 10 – 20% normalized abundance. Thermo Xcalibur software was used for data processing.

2.2.3 Separation by high performance liquid chromatography coupled with high resolution mass spectrometry (HPLC-HRMS)

DNPH hydrazones were quantified by HPLC coupled to the same LTQ-Orbitrap in **2.2** with an electrospray ionization (ESI) source, operating in the negative ion mode at a mass range of m/z 150 – 500 to cover the mass range of carbonyl-DNPH and dicarbonyl-(DNPH)₂ adducts observed in this work. Separation by HPLC was performed using a C₁₈ column end-capped with dimethyl-n-octadecyl silane (Poroshell EC-C₁₈, 2.1 x 100 mm, 2.7 μ m, 120 Å pores, Agilent Technologies, Inc., Santa Clara, CA) and a mobile phase of LC-MS grade water with 0.1% formic acid (A) and acetonitrile (B). The analytes were eluted over the course of 37 minutes at 0.27 mL/min with the following gradient program: 40% B (3.33 min), 50% B (14.6 min), 60% B (20 min), 100% B (32 min), 40% B (37 min). After separation by chromatography, single ion chromatography (SIC) for the accurate m/z of DNPH adducts that were identified by the methods in **2.2.2** was used for quantification. A carbonyl-DNPH standard solution (M-1004-10X, Accustandard, Inc., New Haven, CT), comprised of 13 carbonyl-DNPH analytes was used to obtain the concentration standard curves for calculating the concentration of formaldehyde, acetaldehyde, acetone, acrolein and propionaldehyde in e-cigarette aerosol (**Fig. 2.4**). From application of the standard curves and propagating the remaining errors of the analysis (e.g., uncertainties in peak area determination, standard concentration uncertainties, and syringe volume uncertainties), the $\pm 1\sigma$ uncertainty for calibrated compounds is 10%-20%. The concentration of the remaining carbonyls and organic

acids are calculated by their SIC peak areas and the calculated sensitivities to the ESI negative ion mode in 2.2.4. The concentration of nicotine was also measured by the same method using the positive ion mode.

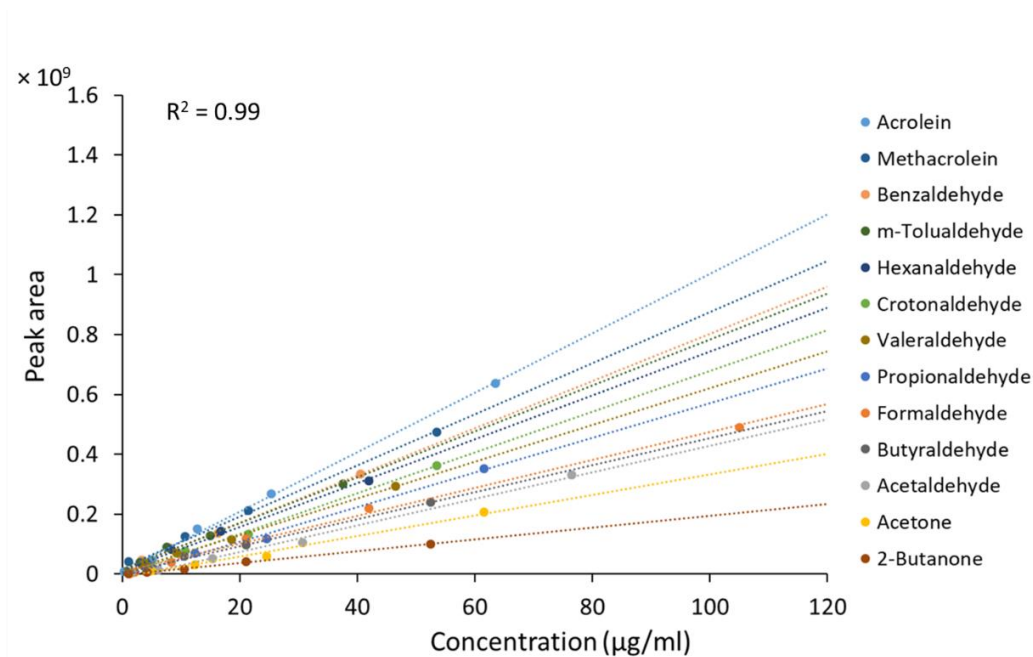


Figure 2.4 Concentration standard curves of 13 carbonyl-DNPH mixture standards, $R^2=0.99$ for all standard curves. Analyte names in legend are listed for the carbonyls, in descending order of sensitivity.

2.2.4 Theoretical calculations by Gaussian

The chemical structures of the DNPH hydrazones affect their deprotonation efficiency in the ESI negative ion mode, and thus, their calibration sensitivity in HPLC-HRMS. The Gibbs free energy change of the deprotonation reaction (ΔG_d) of carbonyl-DNPH compounds that occurs in the ESI negative ion mode was calculated by Gaussian 09 (Gaussian Inc., USA) in both the gas phase and solution phase. The structural geometry optimization and frequency calculation was performed by density functional theory (DFT) using the M06-2X functional and 6-31g+(d,p) basis

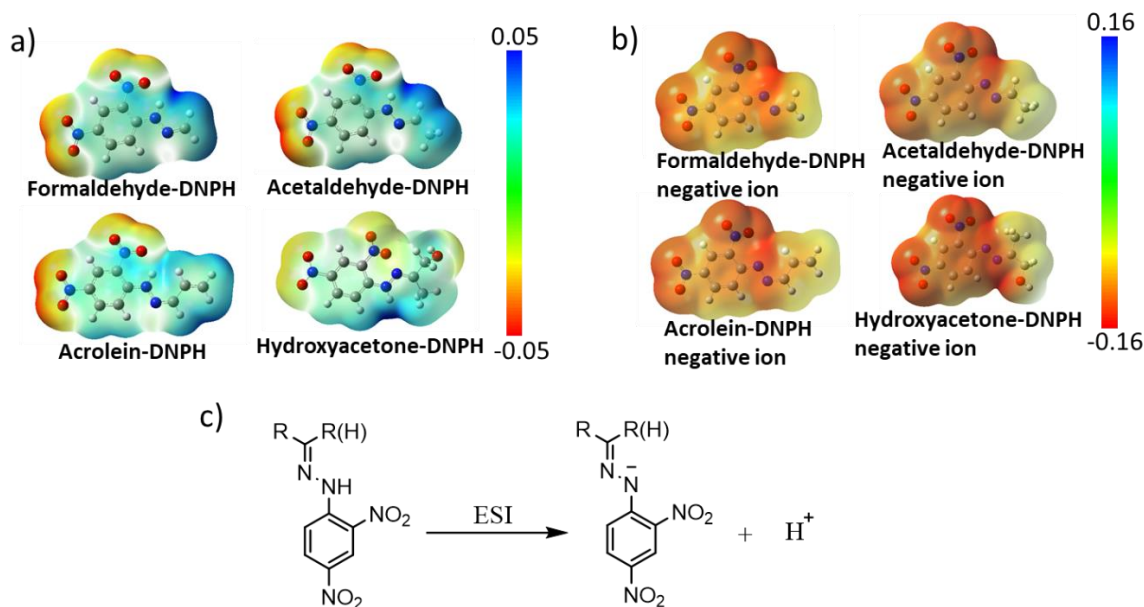
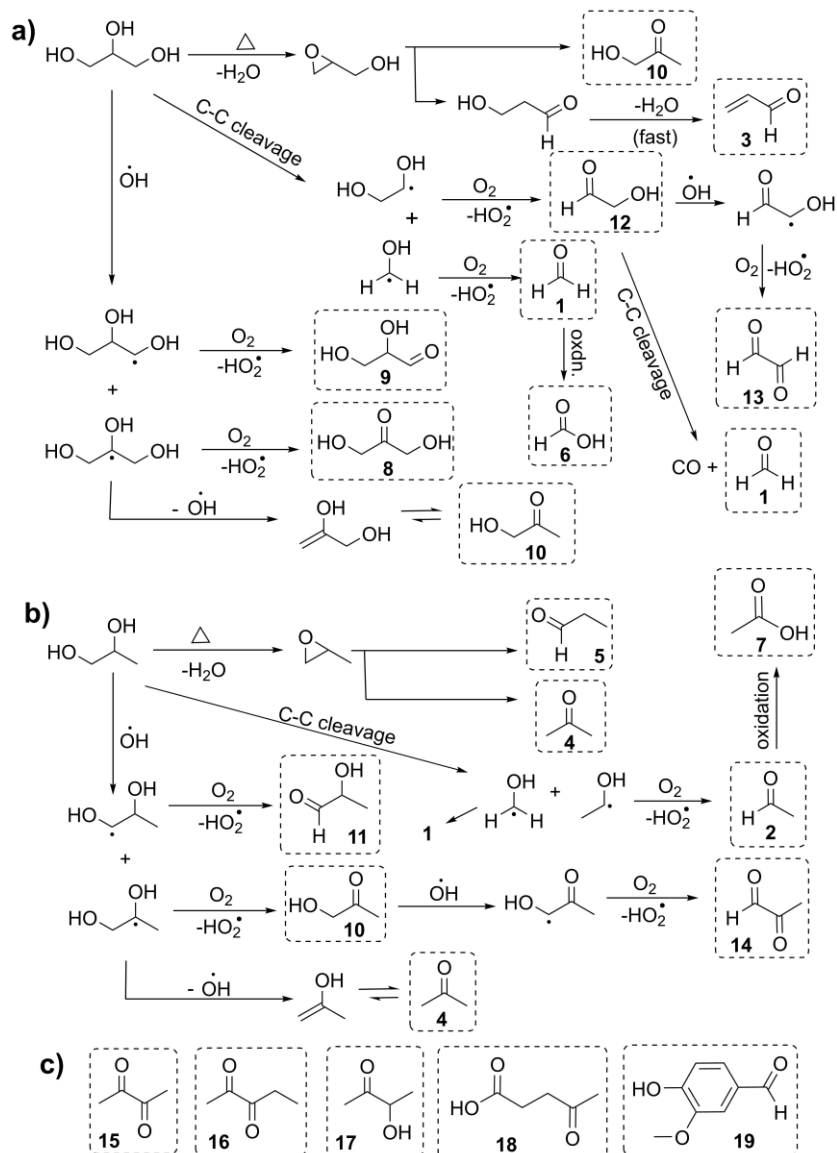


Figure 2.5 Electrostatic potential map (ESP) of **a)** formaldehyde, acetaldehyde, acrolein and hydroxyacetone **b)** the correspond negative ion. **c)** deprotonation reaction in Electrospray Ionization (ESI) negative mode.

set, which has been recommended for the study of main-group thermochemistry in recent years.¹⁴⁵⁻¹⁴⁷ First, the ΔG_d values for the 13 carbonyl-DNPH compounds in the analytical standard mixture were calculated to obtain a relationship to their measured ESI sensitivities. The relationship between the ΔG_d and ESI sensitivities was then extended to calculate the relative theoretical ESI sensitivities for the DNPH hydrazones for which commercial standards are not available. Calculated sensitivities were then used to estimate the concentrations of carbonyl-DNPH hydrazones in e-cigarette aerosol extractions with the method described in 2.2.3. The mass concentrations of different carbonyls/acids in air ($\mu\text{g}/\text{m}^3$) were calculated by the total mass concentration of the specific carbonyls/acids in the HPLC-HRMS analysis divided by the total volume of air that flowed through the DNPH cartridge during the vaping collection process.

2.3 Results and Discussion



Scheme 2.2 Representative reaction pathways for the formation of carbonyl compounds and acids in *e*-cigarette aerosol by thermal degradation of (a) VG and (b) PG.²⁹⁻³⁶ Select flavoring chemicals are shown in (c). Compound in boxes have been quantified in this work. Legend key: 1) formaldehyde, 2) acetaldehyde, 3) acrolein, 4) acetone, 5) propionaldehyde, 6) formic acid, 7) acetic acid, 8) dihydroxyacetone, 9) glyceraldehyde, 10) hydroxyacetone, 11) lactaldehyde, 12) glycolaldehyde, 13) glyoxal, 14) methylglyoxal, 15) diacetyl, 16) 2,3-pentanedione, 17) acetoin, 18) levulinic acid, 19) vanillin.

The method reported in this work offers unambiguous identification and a large quantification range for functionalized carbonyl compounds and organic acids. This is useful for studying *e*-

cigarette thermal degradation chemistry, as well as other environmental chemistry topics (e.g., gas-phase chemistry, aqueous oxidation reactions, etc.). A total of nineteen DNPH hydrazones in the e-cigarette aerosol sample were observed (**Scheme 2.2**): five simple carbonyls, six hydroxycarbonyls, four dicarbonyls, three acids, and one phenolic carbonyl. Hydroxycarbonyls comprised 3 of the top 6 most abundant compounds. Uchiyama et al., recently found that some compounds are emitted purely as gas-phase species (e.g., acetaldehyde, acrolein), some as purely particulates (e.g., glyoxal, nicotine), and some as both (e.g., formaldehyde). Both the concentration and phase information is useful for estimation of exposure risk.

Much of the chemical identification for DNPH hydrazones ($C_cH_nO_nN_n$) can be directly derived from the exact mass of the detected $[M-H]^-$ ions alone. As the formation of DNPH hydrazones replaces only one atom (O with N, **Scheme 2.2**), it is straightforward to deduce the original molecular formula of the carbonyl or acid from the hydrazone formula. The chemical structures were confirmed as in **2.3.1**. All analytes are baseline separated in the chromatographic spectrum

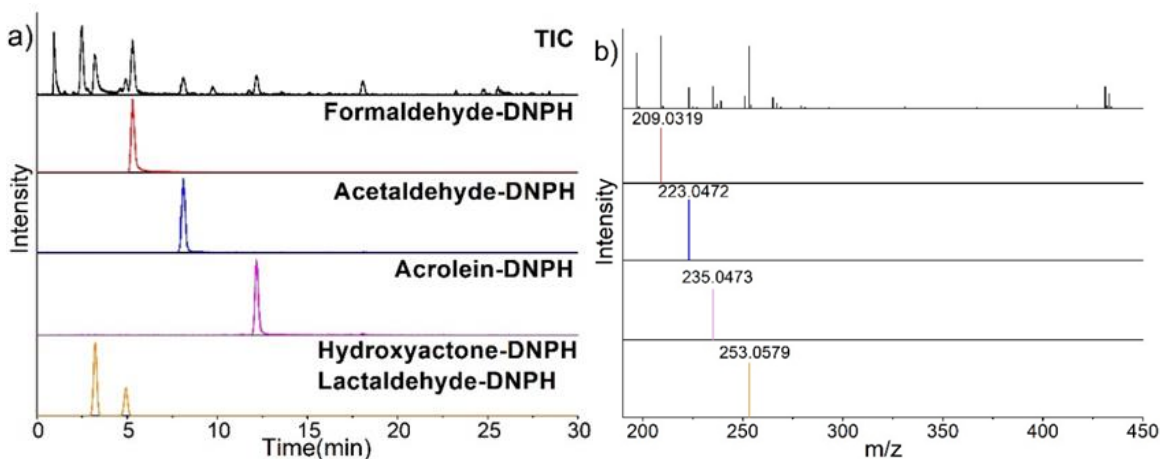


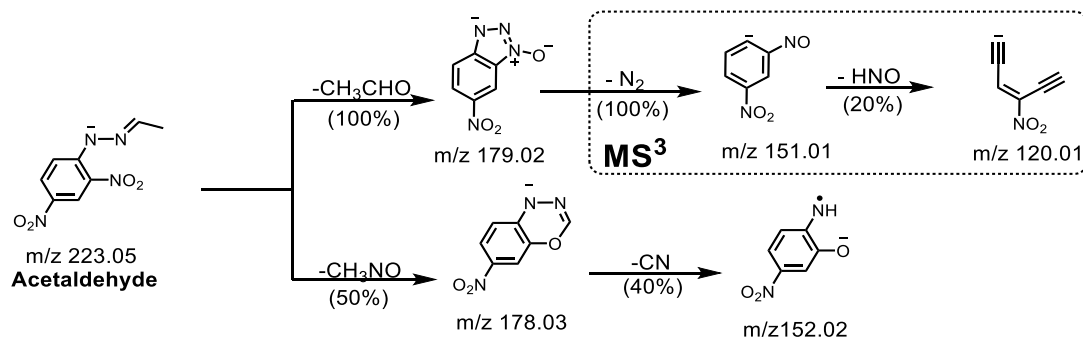
Figure 2.6 (a) Total ion chromatogram (TIC) of the e-cigarette aerosol sample extracts and single ion chromatograms (SIC) for four select deprotonation ions of carbonyl-DNPH hydrazones (b) Corresponding integrated mass spectrum of the TIC and individual mass spectra of four SIC.

using accurate mass single-ion-chromatography (SIC). **Figure 2.6a** shows the total ion chromatography (TIC) and SIC of select carbonyl-DNPH compounds, **Figure 2.6b** shows the corresponding integrated mass spectrum of TIC and each SIC. From the TIC, it is clear that e-cigarette aerosol is a complex system which contains a large number of carbonyls/acids. Co-elution is common in the TIC (e.g., lactaldehyde-DNPH co-eluted with formaldehyde-DNPH); however, the SIC isolates the chromatographic peaks of the desired m/z, avoiding co-elution and misidentification. We also found that acetone-DNPH co-eluted with vanillin-DNPH in the chromatography. This will have led to an overestimation of the abundance of acetone using a chromatography method without HRMS, as vanillin-DNPH is not commercially available.

2.3.1 Chemical structures of multifunctional carbonyls and acids

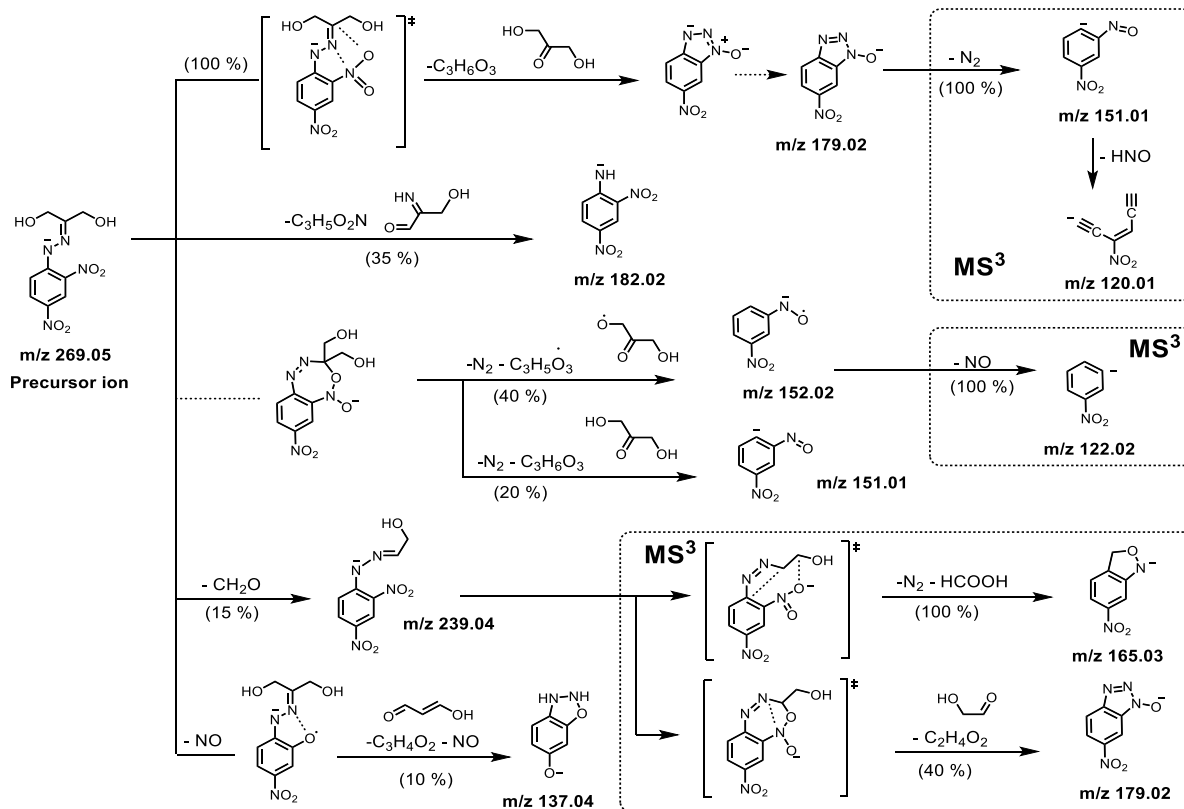
Beyond molecular formulas, it is advantageous to confirm the exact bonding sites of carbonyls and other moieties to give insight to chemical mechanisms and aid in theoretical calculations of reaction energies, as these calculations are sensitive to structures. The chemical structure of DNPH adducts was identified by their neutral and radical losses in tandem multistage mass spectrometry (MS^n) using collision induced dissociation (CID),^{148,149} which often helps to elucidate the exact carbon location of the moiety-of-interest for small molecules. For example, alcohols adjacent to a beta carbon with an abstractable hydrogen (e.g., glucose) can lose H_2O by H-shift rearrangement,¹⁵⁰ while those bonded to aromatic (e.g. phenol) or other non-abstractable sites do not show this loss in the negative ion mode. For nitroaromatics such as DNPH, the electron-withdrawing groups of NO_2 exerts a strong stabilizing effect on anion radicals, and facilitates NO_2 -mediated rearrangements (often leading to loss of NO or an O-migration).^{151, 152}

For small ions like acetaldehyde-DNPH, there is no other reasonable carbonyl structure that exists for the molecular formula, and MS^n confirms this structure with expected fragmentation of CH_3NO and CH_3CHO (**Scheme 2.3**). However, there are some ambiguous formulas such as $C_3H_6O_3$, which



Scheme 2.3 Proposed MS^n fragmentation mechanism for the deprotonation ion $[M-H]^-$ of acetaldehyde-DNPH

may belong to structural isomers dihydroxyacetone and glyceraldehyde. Both of these hydroxycarbonyls are proposed to exist in e-cigarette aerosol after NMR analysis, but are impossible to distinguish with chromatography as they have the same UV-absorption and m/z .³⁴ With MS^n fragmentation, we found that dihydroxyacetone (**Scheme 2.4**) is the main product. Even though several fragmentation pathways for these isomers are similar (e.g., $269.05 \rightarrow 179.02$ (C_3H_6O loss) and $269.05 \rightarrow 239.04$ (NO loss)), the H_2O loss and $C_2H_4O_2$ loss that is expected for glyceraldehyde-DNPH were observed to be negligible in the mass spectrum (**Scheme 2.5**). The preferred formation of dihydroxyacetone over glyceraldehyde supports the radical-mediated oxidation pathways suggested by Diaz et al.,⁷⁷ as radical abstraction of the H in VG should lead preferentially to a secondary alkyl radical compared to the primary radical (**Scheme 2.2**, leading

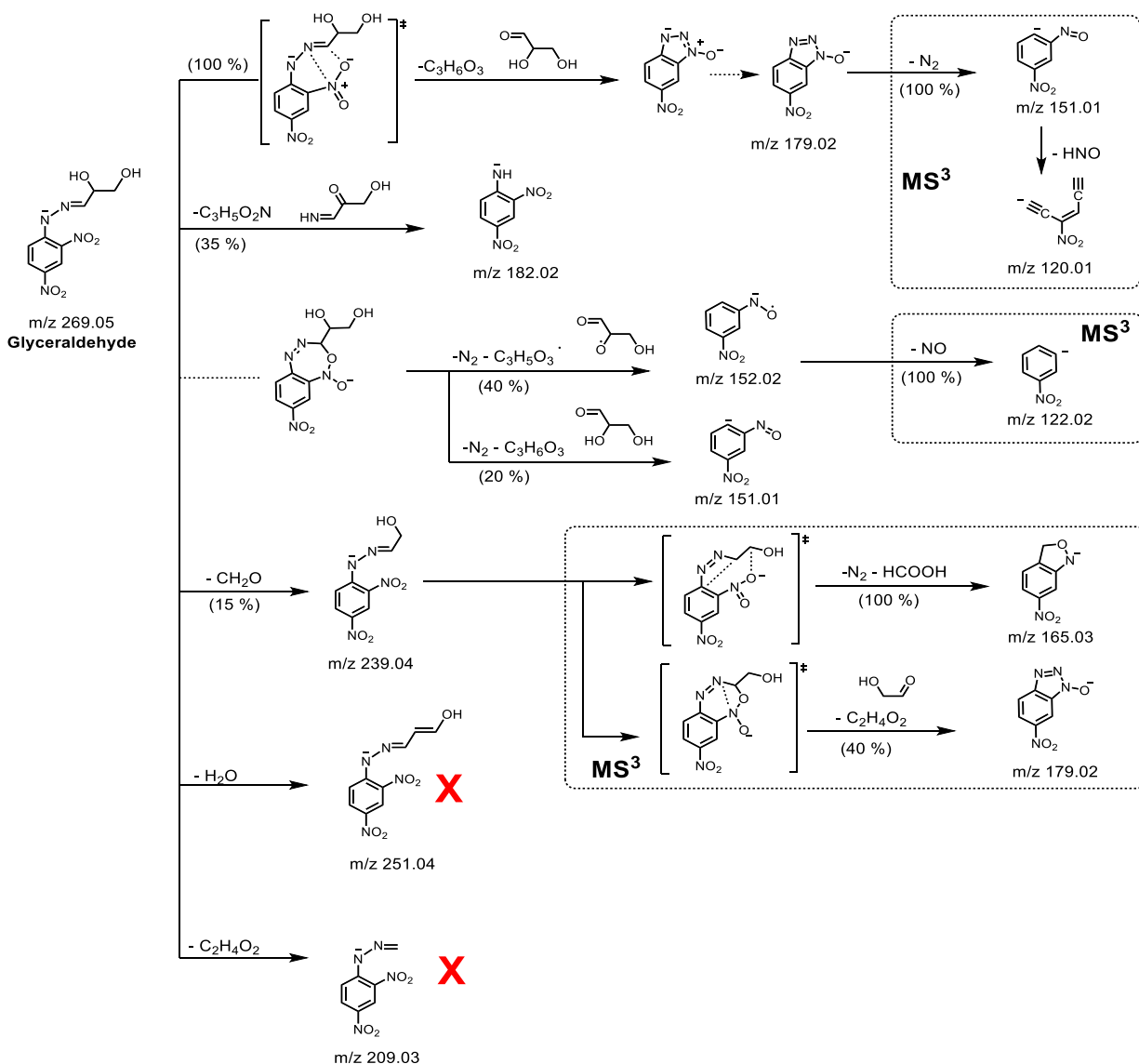


Scheme 2.4 Proposed MS^n fragmentation mechanism for the deprotonation ion $[\text{M}-\text{H}]^-$ of dihydroxyacetone-DNPH.

to **8** and **9**, respectively). The initiating radicals are suggested to be reactive oxygen species such as hydroxyl radical,⁷⁸ and as such, the degradation products can be described by processes that occur in atmospheric chemistry.¹⁵³ Some of the products identified here can be expected from the thermal degradation of PG and VG (e.g., formaldehyde, acetaldehyde, acetone, hydroxyacetone, glycolaldehyde, dihydroxyacetone, etc.),⁷⁴ which is in agreement with the proposed mechanism, while others are likely to be flavoring additives (e.g., 2,3-pentanedione, vanillin, acetoin. etc.).⁵³

A shared product ion after fragmentation of the DNPH hydrazones is $\text{C}_6\text{H}_3\text{N}_4\text{O}_3^-$ (m/z 179.02), which is the modified DNPH after the O-rearrangement loss of the original carbonyl/acid. Other similar loss pathways are those of the DNPH itself, including loss of HONO, NO_2 , and NO (after

NO₂ rearrangement to ONO). There are also distinctive fragmentation pathways for each ion, which are summarized in **Table 2.2**.



Scheme 2.5 Proposed MSⁿ fragmentation mechanism for the deprotonation ion [M-H]⁻ of glyceraldehyde-DNPH

2.3.2 Quantification of DNPH hydrazones of multifunctional carbonyls and acids

While the process of ionization in ESI is complex, it has been demonstrated that there are key factors influencing the ionization efficiency (IE) of different compounds.^{145, 154-157} For example, for the same family of compounds, there is a relationship between negative ion electrospray

ionization (ESI) response and pK_a^{158} of the dissociation equilibrium $\text{HA} \rightleftharpoons \text{A}^- + \text{H}^+$, which is directly related to basicity. We calculate the basicity (as defined for A^-) in terms of $\Delta G_{\text{deprotonation}}$ (ΔG_d),^{159,160} because the deprotonated $[\text{M-H}]^-$ ion is usually detected in the ESI negative mode. Our calculations of the electrostatic potential maps of carbonyl-DNPH hydrazones show that they have a primary acidic proton (**Fig. 2.5**); thus, they are excellent candidates for which gas phase basicity (ΔG_d) can be used to parameterize ionization efficiency in the ESI negative mode. We emphasize that the theoretical chemistry results in this work only provide a relative indication of sensitivity, not absolute calibration factors, and only for the same family of compounds that are protonated or deprotonated. The relative theoretical sensitivities are then anchored by absolute ESI calibrations for the carbonyl-DNPH compounds where standards are commercially available.

Figure 2.7 shows the relationship between the measured negative ion mode ESI sensitivities of 13 carbonyl-DNPH standards and their calculated ΔG_d ($R^2 = 0.63$). Valeraldehyde was excluded because it was considered an outlier by Cook's Distance ($D_i = 0.84$).¹⁶¹ The deviation from the linear trend line is $\pm 31\%$, which, when propagated with the peak integration uncertainty in the HPLC-HRMS analysis, result in an average 1σ uncertainty

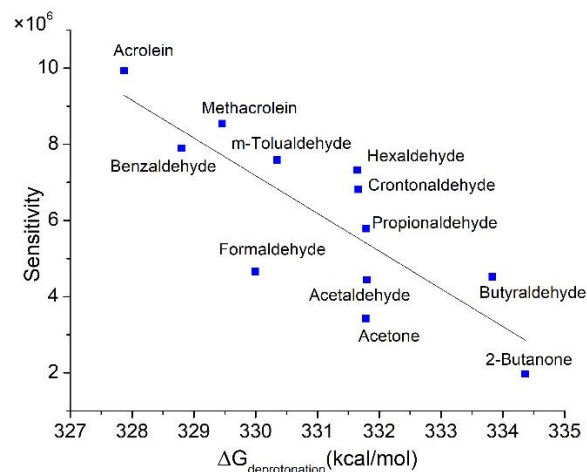


Figure 2.7 Correlation between the observed ESI sensitivities of standard carbonyl-DNPH hydrazones and calculated ΔG_d (gas phase, $R^2 = 0.63$). The data point of valeraldehyde was excluded because it was considered an outlier by Cook's Distance ($D_i = 0.84$).

of 31-50% for all compounds lacking in commercial standards. ΔG_d were also calculated in the

acetonitrile solution phase, which also gave reasonable correlations to ESI sensitivity (Fig. 2.8). Although we opted to use gas-phase ΔG_d due to the stronger correlation, both theoretical models yielded results that are different by 1 – 24% (Table 2.1). Wheeler et al.¹⁶² found that integration grid or molecular orientation may influence the DFT-based energy calculation at certain theory level for specific molecular systems.

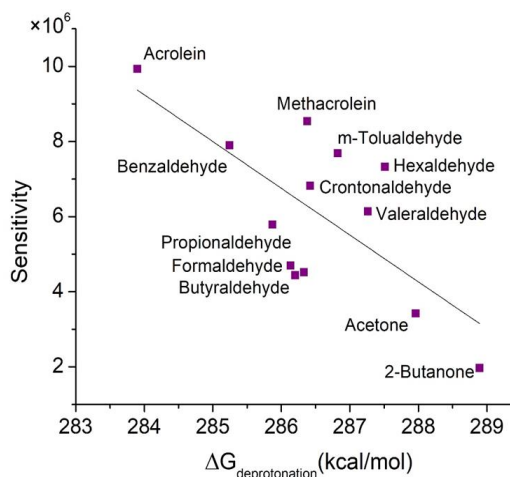


Figure 2.8 Correlation between the sensitivity of carbonyl-DNPH standards and the calculated ΔG_d (solution phase)

In this work, three random orientations for formaldehyde-DNPH, acetaldehyde-DNPH and acetone-DNPH hydrazones were chosen to test the sensitivity of the calculation to the DFT initiation factors; we found that the values of ΔG_d are identical after geometry optimization and free energy calculation. Table 2.1 also shows that concentrations calculated using authentic standards are different than those of theoretical models by 10 - 53% (a combination of uncertainties in both methods). The uncertainty in concentrations calculated by the theoretical model for compounds lacking in commercial standards (31 - 50%) remains considerable, and may be targeted

Table 2.1. Comparison between the concentrations calculated by different methods

	Conc. by standard curves (μg/ml)	Conc. by gas phase model (μg/ml)	Difference between gas phase model and standard curves	Conc. by solvent phase model (μg/ml)	Difference between solvent phase model and standard curves	Difference between solvent phase model and gas phase model
Formaldehyde-DNPH	103±12	68.5±23	33%	74.7±34	28%	-9%
Acetaldehyde-DNPH	53.8±6.8	41.5±14	23%	34.4±15.7	36%	17%
Acetone-DNPH	10.4±2.1	4.9±1.6	53%	6.1±2.8	41%	24%
Acrolein-DNPH	26.2±3.4	29.1±9.9	-11%	28.9±13.2	-10%	0.6%
Propionaldehyde-DNPH	5.7±1.3	4.6±1.6	19%	3.6±1.7	37%	22%

for improvement in future studies. While this uncertainty range is larger than the uncertainty when using analytical standards (~ 10 - 20 %), it is an improvement to the alternatives of (a) not having quantitative data for complex carbonyls and acids, or (b) using “proxy” chemical standards to estimate concentration, which may have highly different analytical sensitivities for similar molecular formulas (e.g., the DNPH derivative of C₃H₄O is 350% more sensitive than that of C₃H₆O in electrospray ionization) and, thus, introduce uncertainties of over 100%.

The trend of ΔG_d and ESI sensitivity (**Fig. 2.7**) arises from the intrinsic relationship between deprotonation efficiency and the ability of the aromatic product ion to stabilize the negative charge initially formed on the N atom (**Fig. 2.5**).^{145, 158} Acrolein is the most sensitive compound in ESI negative mode because it has conjugated double bonds, i.e., additional pi orbitals for the negative charge to be delocalized.¹⁶³ Also, ketones have lower sensitivities than aldehydes because the electron donating group (methyl group and ethyl group) on both sides of the C=N bond slightly destabilizes the negative ions.¹⁶⁴ A limitation of this model occurs for compounds that have similar ΔG_d . In this situation, other factors like molecular volume (MV) and polarity (log P) may also play an important role for these compounds.¹⁵⁷ Despite the limitations, this method is applicable to the compounds found in e-cigarette aerosol and enables the first estimation of concentrations for complex carbonyls that have not yet been quantified with acceptable uncertainty. Furthermore, this computational technique offers an advantage compared to the time expenditure, costs, and chemical usage of synthesizing standards.

Table 2.2 Carbonyls/acids characterized by HPLC-HRMS. Each experiment was performed triplicate, and the data are expressed as the average ($\pm SD$), errors are 1σ including delivering aerosol, DNPH derivatization, and ESI sensitivity calculation. The concentrations of five simple carbonyls were calculated by concentration calibrations using authentic standards, while the concentrations of the rest of the compounds were calculated using calculated ESI sensitivities. Concentrations in $\mu\text{g}/\text{m}^3$ were calculated by the total mass of the compounds divided by the total

volume of air flowing through the smoking machine during sampling. Due to potential sampling losses, reported concentration values represent a lower limit.

Number in Scheme 2	Carbonyls/Acids	Observed m/z of DNPH hydrazones	Specific fragmentation pathway of DNPH hydrazones/ adducts	Mass per 10 puff (μg)	Concentration ($\mu\text{g}/\text{m}^3$)
1	Formaldehyde	209.032	209.03 \rightarrow 167.01(-CH ₂ N ₂) 209.03 \rightarrow 179.02(-CH ₂ O)	1.5 \pm 0.2	512 \pm 68
2	Acetaldehyde	223.047	223.05 \rightarrow 179.02(-CH ₃ CHO) 223.05 \rightarrow 178.03(-CH ₃ NO)	1.1 \pm 0.13	367 \pm 47
3	Acetone	237.063	237.06 \rightarrow 179.02(-C ₃ H ₆ O) 237.06 \rightarrow 163.03((-C ₃ H ₆ O ₂)	0.24 \pm 0.05	88 \pm 18
4	Acrolein	235.047	235.05 \rightarrow 163.03(-C ₃ H ₄ O ₂) 235.05 \rightarrow 167.01(-C ₃ H ₄ N ₂)	0.61 \pm 0.08	216 \pm 27
5	Propionaldehyde	237.063	237.06 \rightarrow 179.02(-C ₃ H ₆ O) 237.06 \rightarrow 209.03(-C ₂ H ₄)	0.14 \pm 0.03	48 \pm 11
6	Formic acid	225.027	225.03 \rightarrow 182.02(-HOCN)	0.04 \pm 0.02	13 \pm 7
7	Acetic acid	239.042	239.04 \rightarrow 209.04(-NO) 239.04 \rightarrow 179.02(-C ₂ H ₄ O ₂)	0.07 \pm 0.03	23 \pm 9
8	Dihydroxyacetone	269.053	269.05 \rightarrow 179.02(-C ₃ H ₆ O ₃) 269.05 \rightarrow 182.02(-C ₃ H ₅ O ₂ N)	0.37 \pm 0.12	128 \pm 43
9	Glyceraldehyde	269.053	269.05 \rightarrow 179.02(-C ₃ H ₆ O ₃) 269.05 \rightarrow 182.02(-C ₃ H ₅ O ₂ N) 269.05 \rightarrow 251.04(-H ₂ O)	0.05 \pm 0.02	19 \pm 8
10	Hydroxyacetone	253.058 433.085	253.06 \rightarrow 182.02(-C ₃ H ₅ ON) 253.06 \rightarrow 177.03(-N ₂ , -CH ₄ O ₂)	1.8 \pm 0.6	615 \pm 208
11	Lactaldehyde	253.058 433.085	253.06 \rightarrow 182.02(-C ₃ H ₅ ON)	0.71 \pm 0.23	247 \pm 80
12	Glycoaldehyde	239.042	239.04 \rightarrow 179.02(-C ₂ H ₄ O ₂) 239.04 \rightarrow 167.03(-NO, -C ₂ H ₂ O)	0.04 \pm 0.02	14 \pm 6
13	Glyoxal	417.055	417.05 \rightarrow 182.02(-C ₈ H ₅ N ₅ O ₄) 417.05 \rightarrow 348.02(-C ₂ H ₃ N ₃)	0.02 \pm 0.01	6 \pm 3
15	Diacetyl	265.058 445.086	265.06 \rightarrow 218.06 (-HNO ₂) 265.06 \rightarrow 177.03(-N ₂ , -C ₂ H ₄ O ₂)	0.16 \pm 0.04	56 \pm 15
16	2,3-pentanedione	279.073 459.100	279.07 \rightarrow 176.05(-HNO ₂ , -C ₃ H ₄ O) 279.07 \rightarrow 182.02(-C ₃ H ₇ NO)	0.07 \pm 0.02	24 \pm 7
14	Methylglyoxal	431.071		0.13 \pm 0.04	46 \pm 14
17	Acetoin	267.073		0.11 \pm 0.03	55 \pm 12
18	Levulinic acid	295.069		0.07 \pm 0.02	23 \pm 8
19	Vanillin	331.069		0.14 \pm 0.05	46 \pm 19

The calculated concentrations of e-cigarette constituents characterized in this work are shown in **Table 2.2** as mass per volume or mass per ten puffs analyzed. The most abundant compounds in the blu e-cigarette aerosol for our study conditions are hydroxyacetone, formaldehyde, acetaldehyde, lactaldehyde, acrolein, and dihydroxyacetone. While, within uncertainty, the exact order of abundance is not definitive, it is clear that hydroxycarbonyls are just as important as

simple carbonyls to the composition of the e-cigarette aerosol. Hydroxyacetone (acetol) has been found to be a major, sometimes dominant, emission in other e-cigarette brands and e-liquids, as quantified by gas chromatography.^{141,165} The agreement of the high abundance of hydroxyacetone lends support to the theoretical approach in this work, which enables all carbonyls and acids to be quantified by the same method. The high abundance of hydroxyacetone may be due to its multiple formation pathways in **Scheme 2.2** and its possible role as an impurity in e-liquid, e.g., Sleiman et al.,¹⁴¹ found hydroxyacetone in concentrations of < 1% of the sum of PG and VG in the e-liquids they used. We were not able to test the e-liquid in this work due to cartridge design; thus, are unable to comment on the extent of hydroxyacetone impurity in the e-liquid, if present.

Dihydroxyacetone and lactaldehyde, in contrast, have not been regarded as major e-cigarette emissions until their unambiguous identification in this work. Their formation pathways from PG and VG (**Scheme 2.2**) are highly feasible, so their higher abundance is not unexpected. It's not clear why these compounds have not been reported earlier; we suspect analytical challenges may be a reason. As we discussed previously, lactaldehyde-DNPH co-eluted with formaldehyde-DNPH in the TIC (**Fig. 2.6**). Thus, HPLC-UV, one of most frequently used instrument for studying carbonyl compounds in e-cigarette aerosol, will not be able to identify and quantify lactaldehyde. However, the HPLC-HRMS method overcomes co-elution challenges by distinguishing compounds based on their exact mass from the SIC and mass fragmentation patterns. Dihydroxyacetone-DNPH appeared to be baseline-separated in HPLC-UV, with a retention time slightly shorter than DNPH itself; however, its unambiguous identification is not possible without HRMS and/or authentic standards. Furthermore, both of these compounds are quite polar, and thus, not conventionally compatible with gas-chromatography.

A comparison of the absolute emission concentrations of thermal degradation products between studies is not straightforward, even for the same brand of e-cigarettes,^{137, 166-167} as the puffing regimens and apparatus of reported works are all different and individual puffing parameters have non-linear effects on the thermal degradation chemistry.^{165,166-167} Klager et al.,¹³⁷ also reported high variability of carbonyl concentrations (e.g., acetaldehyde 229-1870 $\mu\text{g}/\text{m}^3$) for the same brand, puffing-regimen, and flavor, suggesting that the factors driving the thermal degradation chemistry are not yet fully understood. Our work should be primarily viewed as a demonstration of a new method to the chemical characterization of our specific e-cigarette model at the stated puffing conditions, with noted insights into the thermal degradation mechanism.

Formaldehyde, acetaldehyde, and acrolein are known to produce pathological and physiological effects on the respiratory tract. They are known to cause sensory irritation, inflammation, and changes in pulmonary function; formaldehyde is also carcinogenic.¹⁶⁸⁻¹⁷⁰ The average daily dose of aldehydes can be calculated by the amount of aldehydes per puff multiplied by the average number of puffs a user inhales per day. For example, the median puffs per day for e-cigarette users can be assumed to be 250¹⁷¹, so the average daily exposure dose of formaldehyde is 37.5 $\mu\text{g}/\text{day}$ for this e-cigarette device, e-liquid, and operating conditions. The California Office of Health Hazard Assessment (OEHHA) Chronic Reference Exposure Levels (chREL) for formaldehyde is 9 $\mu\text{g}/\text{m}^3$, which could be translated to an acceptable daily dose of 180 $\mu\text{g}/\text{day}$ (assuming the inhalation volume of 20 m^3 per day) and is higher than the e-cigarette aerosol exposure for formaldehyde in this work. In addition, OEHHA has a No Significant Risk Level (NSRL) recommendation of 40 $\mu\text{g}/\text{day}$ which is intended to protect against cancer; this NSRL level is close to the exposure dose of formaldehyde in this work. The average exposure dose of acrolein for blu

e-cigarettes is 15.2 $\mu\text{g}/\text{day}$ according to **Table 2.2**, which is higher than the OEHHA chREL value (7 $\mu\text{g}/\text{day}$). Logue et al.¹¹⁶ used a similar approach to estimate health impacts and found that both formaldehyde and acrolein can exceed maximum daily doses derived from occupational health guidelines. Differences in results are likely due to the different devices, e-liquids, and puffing regimens used.

While the reported emissions in this work may not be generalized to all e-cigarettes and use scenarios, it is informative to compare the aldehyde emissions normalized by nicotine, since e-cigarette users transitioning from traditional tobacco products (e.g., combustible cigarettes) will self-titrate nicotine intake when using e-cigarette products.¹⁷²⁻¹⁷³ In this work, the nicotine yield is $10.4 \pm 1.9 \mu\text{g}/10$ puffs. We did not observe evidence of nicotine oxidation¹⁷⁴ under the puffing conditions of this work, which will impact the ratio. The formaldehyde/nicotine ratio is $144 \pm 32 \mu\text{g}/\text{mg}$ nicotine, which is 4 times higher than the formaldehyde/nicotine ratio in combustible cigarettes ($37 \pm 7 \mu\text{g}/\text{mg}$).¹⁷⁵ The acrolein/nicotine ratio measured in this work is close to that of tobacco products ($59 \pm 13 \mu\text{g}/\text{mg}$ compared to $62 \pm 8 \mu\text{g}/\text{mg}$), while the acetaldehyde/nicotine ratio ($106 \pm 23 \mu\text{g}/\text{mg}$ compared to $663 \pm 92 \mu\text{g}/\text{mg}$) and propionaldehyde/nicotine ratio ($13 \pm 4 \mu\text{g}/\text{mg}$ compared to $60 \pm 10 \mu\text{g}/\text{mg}$) are lower than that in combustible cigarettes. Logue et al.¹¹⁶ observed similar trends using different e-cigarette products; however, the results were not normalized for nicotine so a direct comparison is not possible. Thus, we find e-cigarettes do not necessarily emit lower carbonyl compounds than tobacco products, but the comparisons may change depending on the specific e-cigarettes or tobacco products, or different puffing/smoking regimens.¹⁷⁶

Although hydroxycarbonyls are abundant in e-cigarette aerosol, a general lack of toxicological data precludes health risk assessment. Smith et al.¹⁷⁷ found that exogenous exposure to dihydroxyacetone is cytotoxic and will cause cell death by apoptosis. Glycolaldehyde is also suspected to have biological toxicity.¹⁷⁸ For hydroxyacetone and lactaldehyde, toxicology data are currently unavailable on many toxicology databases like Hazardous Substances Data Bank (HSDB), European Chemicals Agency (ECHA) and Research Institute of Fragrance Materials (RIFM).

In addition to thermal degradation products, flavoring chemicals are also found to be significant components in e-cigarette aerosol. Allen et al.⁵³ measured the concentration of diacetyl (< LOD - 238.9 $\mu\text{g}/\text{e-cigarette}$), 2,3-pentanedione (< LOD - 64.4 $\mu\text{g}/\text{e-cigarette}$), and acetoin (< LOD - 529.2 $\mu\text{g}/\text{e-cigarette}$) in 51 e-cigarettes from different brands and flavors, with the highest concentrations found for e-liquid flavors such as “Peach Schnapps.” In this work, the estimated concentrations of the flavoring chemicals diacetyl ($\sim 6.4 \mu\text{g}/\text{e-cigarette}$), 2,3-pentanedione ($\sim 2.8 \mu\text{g}/\text{e-cigarette}$), and acetoin ($\sim 4.4 \mu\text{g}/\text{e-cigarette}$) are fairly consistent with some measurements for the Classic Tobacco flavor^{137, 179} but higher than others.⁵³ Of note is that Klager et al.¹³⁷⁵³ found diacetyl concentration in 16 different e-cigarettes varies from 0.028 - 3.69 $\mu\text{g}/\text{m}^3$, while our results show a concentration of $56 \pm 15 \mu\text{g}/\text{m}^3$. It is clear that the amount of flavoring chemicals largely depend on the individual e-liquids, puffing regimen, and collection methods. In addition, two carbonyl flavoring additives (vanillin, levulinic acid) have been quantified here for the first time in e-cigarette aerosol.^{57,110} Acid additives (e.g., levulinic acid) are used to control the acidity of e-liquids.¹⁸⁰ Inhaling either diacetyl, or the related flavoring 2,3-pentanedione, has been associated with bronchiolitis obliterans (“popcorn lung”).^{181, 182} As the composition of e-cigarette aerosol is

complex and the range of products is vast, a more systematic understanding of the fundamental chemistry (e.g., the molar yield of thermal degradation products from PG and VG, the dependence on vaping temperature, the phase characteristics, the impacts of nicotine and flavorings) is needed.

Chapter 3. Impact of e-liquid composition, coil temperature, and puff topography on the aerosol chemistry of electronic cigarettes

Abstract

E-cigarette aerosol is a complex mixture of gases and particles with a composition that is dependent on the e-liquid formulation, puffing regimen, and device operational parameters. This work investigated mainstream aerosols from a 3rd generation device, as a function of coil temperature (315 – 510 °F, correspond to 157 – 266 °C), puff duration (2 – 4 s), and the ratio of propylene glycol (PG) to vegetable glycerin (VG) in e-liquid (100:0 – 0:100). Targeted and untargeted analyses using liquid chromatography high-resolution mass spectrometry, gas chromatography, in-situ chemical ionization mass spectrometry, and gravimetry was used for chemical characterizations. PG and VG were found to be the major constituents (> 99%) in both phases of the aerosol. Most e-cigarette components were observed to be volatile or semivolatile under the conditions tested. PG was found almost entirely in the gas phase, while VG had a sizable particle component. Nicotine was only observed in the particle phase. The production of aerosol mass and carbonyl degradation products dramatically increased with higher coil temperature and

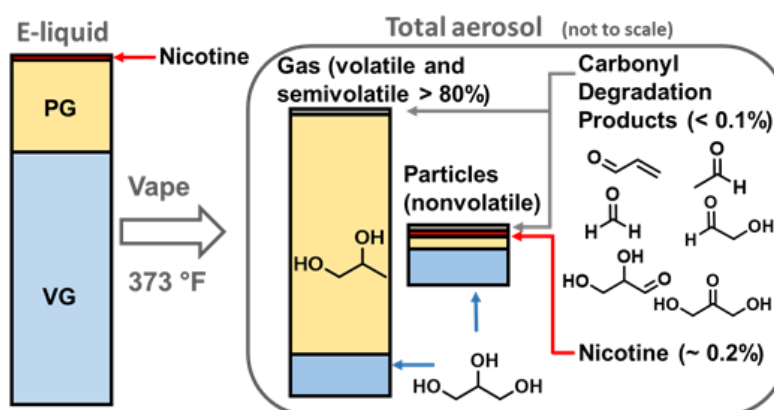


Figure 3.1 The estimated composition of e-liquid and corresponding e-cigarette aerosol at vaping temperature of 373 °F including both gas phase and particle phase.

puff duration, but decreased with increasing VG fraction in the e-liquid. An exception is acrolein, which increased with increasing VG. The formation of carbonyls was dominated by the heat-induced dehydration mechanism in the temperature range studied, yet radical reactions also played an important role. The findings from this study identified open questions regarding both pathways. The vaping process consumed PG significantly faster than VG under all tested conditions, suggesting that e-liquids become more enriched in VG and the exposure to acrolein significantly increases as vaping continues. It can be estimated that a 30:70 initial ratio of PG:VG in the e-liquid becomes almost entirely VG when 60-70% of e-liquid remains during the vaping process at 375 °F (191 °C). This work underscores the need for further research on the puffing lifecycle of e-cigarettes.

3.1 Introduction

Electronic (e-) cigarettes are battery-operated devices used to “vape” or aerosolize “e-liquid” consisting of propylene glycol (PG), vegetable glycerin (VG), nicotine, and optional flavor compounds.^{60, 88, 137, 141, 183} The global market share of e-cigarettes is rapidly growing,^{16, 102, 110, 144, 146, 173, 184-185} and e-cigarette use among young people has become a significant public health concern.¹⁸⁶⁻¹⁸⁹ Of U.S. high school students and middle school students, 27.5% and 10.5%, respectively, self-reported usage for one or more days during the past 30 days in 2019.¹⁰⁵ The design of the e-cigarette^{21, 190-191} has rapidly evolved from 1st generation “cig-a-like” pods with disposable, prefilled, e-liquid cartridges and fixed operational parameters (notably voltage and power, and correspondingly, coil temperature of the device), to 3rd generation “mods” with a refillable e-liquid tank and adjustable device operational parameters. More recently, 4th generation

“mod-pod” hybrids with fixed power output have been released. Approximately 80% of e-cigarette users primarily use 3rd or 4th generation devices today.^{10, 192-193}

E-cigarettes gas and particle emissions are composed of aerosolized PG, VG, optional flavors, and nicotine from the e-liquid, as well as free radicals, and a variety of carbonyls or hydroxycarbonyls (e.g., formaldehyde, acetaldehyde, hydroxyacetone, acrolein) formed by thermal degradation during the e-liquid heating process.^{60, 80, 137, 141, 165-166, 194-202} Recent evidence suggests hydroxycarbonyls may be more abundant than anticipated, but their impacts on health remain poorly understood.¹¹⁸ With the ability to change vaping parameters (e.g., puff duration, puff frequency, device power, etc.), coil material, and e-liquid formulations in 3rd and 4th generation devices, there exists a multitude of use combinations that can influence the composition of the inhaled e-cigarette aerosol. In particular, aerosol composition and gas/particle partitioning could greatly influence the risk of chemical exposure and aerosol deposition in the human respiratory tract.²⁰³⁻²⁰⁷ However, the ways in which e-liquids form aerosol components under different vaping parameters have not been fully elucidated in the literature.

Coil temperature and e-liquid composition will directly affect e-cigarette aerosol emissions, as heating e-liquid solutions with metal coils results in thermal degradation reactions and changes in aerosol concentration.^{141, 165, 197, 208} Coil surface area is also an important parameter that could affect thermal decomposition rates in various coil designs.¹⁹⁰ The majority of published studies have correlated e-cigarette emissions to device voltage and power, but not directly to the vaping coil temperature that governs the thermal degradation process.²⁰⁹⁻²¹² For example, Korzun et al.²⁰⁸ inferred coil temperature by airflow rate, and found higher temperatures led to higher

concentrations of formaldehyde and acetaldehyde by promoting the degradation of higher-molecular-weight products such as hydroxyacetone and glycoaldehyde in the product mixture. Uchiyama et al.¹⁶⁵ evaluated the phase distribution for a number of compounds, and found the formation of degradation products from vaping exponentially increased when the device power exceeded 40 W. However, a direct comparison between such studies is challenging. This is because the actual coil temperature is synergistically influenced by many factors, some of which are inherent to the coil, while others are a result of the conditions of operation. For example, different coils may have different resistances due to material and structural variance. Furthermore, coil temperature may also be influenced by e-liquid composition, which changes the viscosity and heat capacity, or by air flow rates in the device, as faster air flow rates have higher cooling effects.^{208, 213, 214} Thus, a single vaping device may produce different temperature ranges for the same voltage input upon minor alterations in operational scenarios.²¹⁵ In addition, the aerosol emissions will change as a result of the users' puffing regimen.^{84, 196, 216-218} Bitzer et al.¹⁶⁷ showed puff volume and duration influence the per-puff yield of nicotine, carbonyls, aerosols, and free radicals. Beauval et al.²¹⁹ also found modifications in puffing conditions lead to significant variations in the carbonyl composition of e-cigarette aerosols.

PG and VG are known to be the major contributors to the aerosol particle phase. However, there remain a number of questions concerning the fractions of PG and VG in the total e-liquid that convert to degradation products, the specific chemical mechanisms of transformation, and the ways in which e-cigarette chemical components partition between phases in response to changing vaping parameters.^{220, 221} Thus, a systematic understanding of how the carbon mass balance and chemistry of the vaping process respond to changing e-liquid formulation, major puffing

parameters, and actual coil temperatures is critically needed. Monitoring coil temperature instead of voltage/power as a standard evaluation metric may provide greater fundamental insights into the chemistry. However to do so, the coil temperature will need to be directly measured during each puff, as the temperature-controlled programs of e-cigarette devices may not be a true reflection of the actual coil temperature.²¹⁵

In the present study, a broad chemical analysis suite, volatility-based aerosol sampling, and direct measurement of coil temperatures were employed to study the aerosol emissions from a 3rd generation e-cigarette device at various coil temperatures, puff durations, and PG:VG ratios in the e-liquid solution. Flavoring compounds were deferred for future research. The loss of mass from the e-liquid conversion to aerosols was compared with independent measurements in the particle and gas phases for carbon mass closure analyses.

3.2 Experimental

3.2.1 E-cigarette sample generation and extraction

E-cigarette aerosols were generated using a 3rd generation Evolv DNA 75 Color modular vaping device (Evolv LLC., Hudson, Ohio) with replacement single mesh vaping coils (SS316L, FreeMax Technology Inc., Shenzhen, China) that have a coil resistance of *ca.* 0.12 Ohm. The stainless steel coil was selected as only limited coil materials (e.g., nickel, titanium, stainless

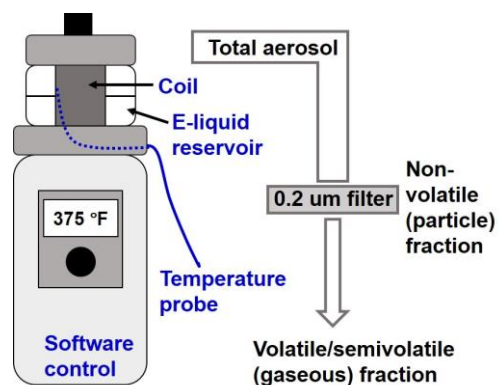


Figure 3.2 Device and sampling set up. The total aerosol and the particle fraction of total aerosol (captured by a 0.2-um pore hydrophilic-surface PTFE filter) were analyzed independently. The difference is termed the volatile/semi-volatile fraction in the gas phase.

steel) are appropriate for temperature control.²¹⁵ The device (**Fig. 3.2**) has a rechargeable battery with a variable output voltage (0.2 – 9 V) and power (0 – 75W), an atomizer coil assembly, a refillable e-liquid tank that enables e-liquid with variable formulations to be tested, and a push button to initiate puffing. The device was robotically operated by a custom linear actuator (TE-2e, Teague Enterprises Inc.,

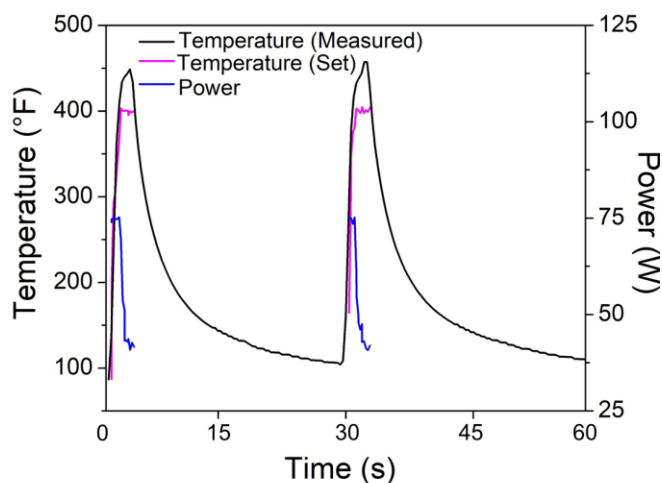


Figure 3.3 The temperature and power readings during the vaping process, as monitored by device software compared to coil temperature measured by thermocouple.

Woodland, CA) during the puffing process, which enabled precise control of the puff rate (1 – 6 puffs/minute) and puff duration (2 – 4 s) with a $\pm 3\%$ standard deviation (1σ). Evolv Escribe software (Evolv LLC., Hudson, Ohio) was used to set the power and temperature conditions to achieve the desired coil temperature (**Fig.3.3**), as measured by a flexible Kapton-insulated K type thermocouple (Oakton instrument Inc., Vernon Hills, IL) in contact with the center of the coil surface, and output to a digital readout. The puff flow rate was 1.186 ± 0.002 L/min, and the corresponding puff volume for a 3-s puff was 59.3 ± 0.1 mL, as quantified by a primary flow calibrator (A.P. Buck Inc., Orlando, FL). The puff volume and duration selected for this study is consistent with the CORESTA e-cigarette testing protocol (3 ± 0.1 s, 55 ± 0.1 mL).²²² However, puff volume larger than 100 mL and puff duration longer than 3 s have been observed in some vaping scenarios.²²³⁻²²⁴ For example, Robinson et al.²²⁵ found a typical case of puff topography with 3.7 s puff duration and 144 mL puff volume. Thus, this highlights a limitation of the current

study when extrapolated to various vaping scenarios, as an increase in the puff volume will increase the formation of aerosol and thermal degradation compounds.¹⁶⁷ The puffing protocol for the puff duration study is not based on volume, but used a variable puff duration at a fixed flow rate. **Table 3.1** shows the experimental conditions used in this work. Pure VG, PG, and nicotine (> 99 % purity, Sigma Aldrich) were used to generate e-liquids at the ratios and concentrations shown in **Table 3.1**.

Particles were collected on a hydrophilic polytetrafluoroethylene (PTFE) membrane filters (Omnipore, 0.2 μm pore size, Millipore Sigma Inc., Burlington, MA). PTFE and other types of filters have been used in sample collection for e-cigarette research.²²⁶⁻²²⁸ As hydrophobic filters were found to be incompatible with the polar compounds in e-cigarette aerosol,²²⁸ the hydrophilic PTFE filters were chosen for use because they have broad compatibility with both polar and nonpolar functional groups. Both the gas phase of total aerosol stream and the particle filters (**Fig. 3.2**) were analyzed for mass and chemical composition. The total mass lost from the e-liquid due to vaping was determined gravimetrically on a microbalance (Shimadzu Corp., 0.0001 g precision, calibrated by weight standards) by weighing the e-liquid compartment immediately before and after puffing 10 puffs, and dividing by the number of puffs at different experimental conditions. The standard deviation of the gravimetric analysis after triplicate measurements was determined to be ~ 20%, mainly due to variations in puffing. The composition of gas phase PG/VG, was analyzed by chemical ionization triple-quadrupole mass spectrometer (CIMS); a detailed description can be found in **Section 3.2.4**. The particle mass on the filter was analyzed after each collection on the microbalance, also performed in triplicate. The total mass of molecules residing

in the gas phase was determined as the difference between the total mass of e-liquid lost and the mass of the particles collected.

Table 3.1 *Experimental conditions for e-cigarette aerosol sample generation. Coil temperatures were measured by a thermocouple and controlled to within a standard deviation of 5 °F (3 °C), variable temperatures correspond to 157, 191, 216, 246, 266 °C.*

Parameters	Variable settings	Fixed settings
Coil temperature (°F)	315, 375, 420, 475, 510	PG:VG 30:70, nicotine 3 mg/mL, 3 s puff
PG:VG ratio	100:0, 70:30, 50:50, 30:70, 0:100	Temperature 375 °F, nicotine 3 mg/mL, 3 s puff
Puff duration (s)	2, 3, 4	Temperature 375 °F, PG:VG 30:70, nicotine 3 mg/mL

E-cigarette aerosols are known to be semivolatile at room-temperature, i.e., the chemicals can exist in both gas and particle phases under various conditions (slight temperature and humidity variance, condensable surface area, dilution air, etc.), and are highly unstable mixtures that undergo continuously change of size, number concentration and chemical composition by coagulation, evaporation/condensation of individual components, wall deposition and potentially water uptake.^{229, 230} Thus, there is no perfect sampling protocol for such a dynamic mixture. Sampling with particle filters may either underestimate or overestimate total nonvolatiles. Underestimation may occur if fine particles break through the filter. Overestimation could result if the filter has a higher surface area than in realistic vaping scenarios, or if the filter is saturated with an organic film, into which the semivolatiles can partition during sampling. Our particle size distribution analysis with a scanning mobility particle sizer (SMPS, TSI Inc) that measures a size range of 0.014 - 0.671 μm diameter (**Fig. 3.4**) showed that particle breakthrough for Omnipore filter at a 0.2- μm pore size may not be significant for this work. However, the diameter of aerosol will go through a size change process caused mainly by coagulation and evaporation that could occur during the aerosol collection and measurement steps.²²⁹ Zhang et al.²³¹ found that the count median diameter (CMD) of e-cigarette aerosols is 120 – 180 nm when counted immediately after

emission from the e-cigarette. The CMD changes to 400 nm for the measurement of droplets at steady-state. Furthermore, we confirmed that the collection efficiency for the filter was > 97.5% based on consecutive collections in series. Thus, we believe this method minimized the possible underestimations of the particle phase. We then tested a denser structure or higher surface area particle filtering material. A high-flow (no pressure drop) High Efficiency Particulate-free Air (HEPA) capsule (Pall Corp., 121144) upstream of our chemical analyses removed 99.9% of all particles (**Fig. 3.4**). However, the HEPA capsule also removed 50-100% of gaseous formaldehyde, hydroxyacetone, acetone, acetaldehyde, and dihydroxyacetone gas standards that were evaporated and diluted directly into a 100-L Teflon FEP bag using chemical standards, which would overestimate the particle phase.

For the purpose of this work, particles that are trapped by hydrophilic PTFE filter are termed the “nonvolatile (NV)” or “particle” fraction and the difference between the total aerosol and the NV fraction is termed the “volatile/semivolatile” or “gas” fraction. Although particles are termed nonvolatile, it does not mean that they cannot partition to the gas phase under conditions different than

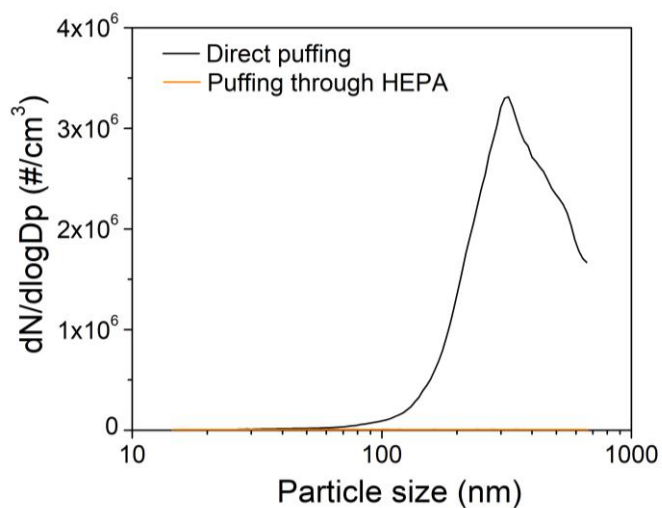


Figure 3.4 Particle size and distribution of e-cigarette aerosol, as sampled via direct puffing into a 100 mL glass bulb (black) and sampling the same mixture through a HEPA filter (orange). The HEPA filter particle removal efficiency is estimated to be > 99.8%.

the ones we tested (e.g., with a dilution stream of gas). Likewise, semivolatiles emitted in the gas

phase directly from the mainstream can condense onto surfaces (e.g., respiratory passageways) that have higher condensable surface area than used our study.

3.2.2 Particle-phase PG, VG, and nicotine characterized by GC-MS

The particle filters were analyzed by an Agilent 6890N gas chromatograph coupled to an Agilent 5973N quadrupole mass spectrometer (GC-MS, Agilent Technologies Inc., Santa Clara, CA). Filters were extracted by a 10-mL 1:1 mix of methanol and ethyl acetate (Fisher Scientific Inc., Hampton, NH). The method for the analysis of PG, VG, and nicotine was adapted from Williams et al.²³² The components were separated on a DB-wax capillary column (30 m, 0.25 mm ID, 0.25 μ m film, Agilent Technologies Inc., Santa Clara, CA) with ultra-high purity (UHP) grade Helium at a constant flow of 1.1 mL/min. The temperature program was 50 °C (0.5 min), 8 °C /min to 160 °C, 5 °C /min to 170 °C, then 170 °C (15 min). Electron impact mass spectra for PG, VG, and nicotine were > 90% matched to the National Institute of Standards and Technology (NIST) database. PG, VG, and nicotine standards (purity \geq 99%, Sigma-Aldrich Inc.) were used for GC-MS calibration.

3.2.3 Carbonyls and organic acids characterized by high performance liquid chromatography-high resolution mass spectrometry (HPLC-HRMS)

Details of the identification and quantification methods have been previously described in detail.⁴⁰ Briefly, carbonyls are derivatized *in-situ* into hydrazones with 2, 4-dinitrophenylhydrazine (2,4-DNPH) cartridges (Supelco Inc., 350 mg DNPH) and extracted with 2 mL acetonitrile (Fisher Scientific Inc., LC-MS grade, Hampton, NH) prior to analysis. Consecutive sampling with three DNPH cartridges in series showed that >98.4% of carbonyls were

captured in the first cartridge. Consecutive solvent extractions of DNPH cartridges for samples confirmed that > 97% of both DNPH and its hydrazones were extracted after the first 2-mL volume of acetonitrile. Carbonyl-DNPH extracts were analyzed for molecular composition using an Agilent 1100 HPLC with an Agilent Poroshell EC-C18 column (2.1 × 100 mm, 2.7 μm, 120 Å) coupled to a linear-trap-quadrupole Orbitrap (LTQ-Orbitrap) mass spectrometer (Thermo Corp., Waltham, MA) at a mass resolving power of ~ 60,000 $m/\Delta m$ at m/z 400. All analyses were performed in triplicate. A total of 30 puffs were collected for each analysis, which was verified to be within the linear dynamic range of the measurement. Concentrations of formaldehyde, acetaldehyde, acetone, acrolein, and propionaldehyde in e-cigarette aerosols were quantified by analytical standards, and those of other carbonyls were quantified using theoretical calculations of relative sensitivity in the ESI negative mode ionization.⁴⁰ The $\pm 1\sigma$ uncertainty of the analysis is 10-20% when using analytical standards and 30-50% when using the theoretical model. The HPLC-HRMS data for carbonyls derivatized as hydrazones were corrected to remove the mass contribution of DNPH.

3.2.4 Volatile/semivolatile PG and VG characterized by chemical ionization triple quadrupole mass spectrometer (CIMS)

The volatile/semivolatile concentrations of PG and VG were quantified by custom trifluoromethanolate (CF_3O^-) CIMS at a 5-min time resolution, which analyzes the *in-situ* mixing ratios of polar volatiles in the gas phase.²³³⁻²³⁶ One puff was introduced into a Teflon pillow bag that was filled with 100 L of ultra-zero air via a calibrated mass flow controller. The CIMS flow tube diluted the mixture by a factor of 9 with UHP nitrogen. The particulate fractions of aerosols are lost through the flow introduction method to the CIMS, which uses a small pinhole orthogonal

to a fast straight flow. The ionization mechanism for PG and VG in the negative mode is cluster formation ($M + CF_3O^-$). Direct calibration is not possible due to lower Teflon permeation efficiencies and unavailability of fourier-transform infrared (FT-IR) spectra for PG and VG; thus, quantification of PG and VG was performed based on ethylene glycol as a proxy calibrant. The ethylene glycol sensitivity was obtained by gravimetric measurements of a permeation tube of the pure standard with a stable permeation rate over several months, achieved by constantly flowing 25 sccm of UHP nitrogen past the permeation tube in a custom flow chamber kept in a 40 °C bath. The effect of an additional hydroxy ($-OH$) group and methyl ($-CH_3$) group on the CIMS sensitivity was estimated based on the sensitivities of other calibrant compounds (e.g., formic acid vs. acetic acid, and hydroxymethylhydroperoxide vs. methylhydroperoxide). Analytical uncertainties of 40-50% were estimated based on the range of possible sensitivities, with PG having lower uncertainty. The CIMS signal for PG and VG were normalized by the reagent signal before applying their sensitivities, then dilution-corrected to obtain the gas-phase mixing ratios in the bag. Multiplying by the exact volume of gas in the bag gave the quantity in one puff.

The limitation of this technique for e-cigarette aerosols is that semivolatiles may evaporate from particles during the dilution process. Thus, the technique may overestimate the volatile/semivolatile fractions in comparison to the filter method. Thus, we limited the interpretations of CIMS to the following: (1) observations of gaseous nicotine, which may be observed in the positive mode as a protonated ion if it existed in the mixture (we did not observe this signal); (2) a rough mass balance closure — estimations of whether the gaseous fraction (gravimetric difference between total mass loss from the e-liquid and the particulate fraction) can be attributed to PG, VG, or other compounds such as hydroperoxides and organic acids that the

CIMS can quantify well; and (3) the relative abundance of PG and VG compared to carbonyls, such as hydroxyacetone, that the CIMS also detects with high sensitivity.

3.3 Result and discussion

3.3.1 Coil temperature

The particle mass was strongly correlated to the measured coil temperature (**Fig. 3.5a**, $R^2 \sim 0.8$), and was independent of coil identity. In contrast, the production of particle mass was not well-

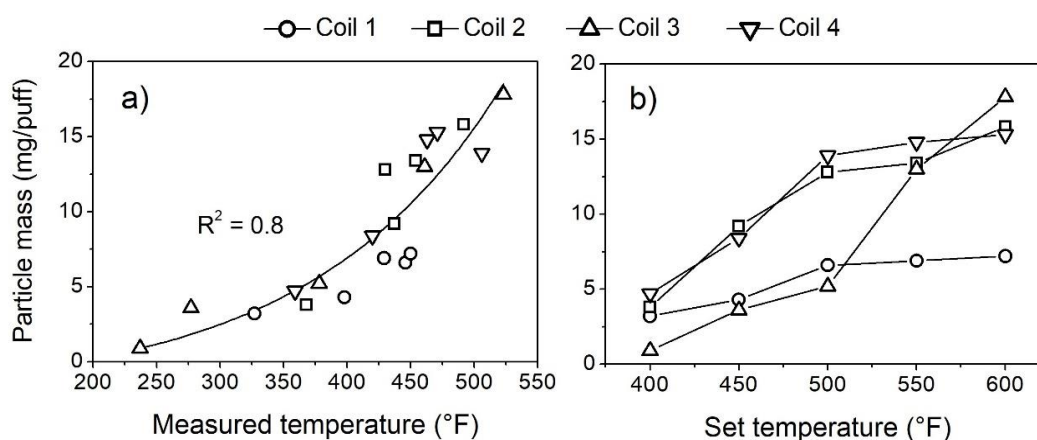


Figure 3.5 The relationship between the production of particle mass and **a)** measured coil temperatures, or **b)** temperatures set by the Evolv software for four different coils using e-liquid with a 30:70 PG:VG ratio by volume and 3 mg/mL nicotine.

correlated to the temperature set by the Evolv program when different coils were used from the same manufacturer, model, and batch (**Fig. 3.5b**). Repeated replacement of the coil in the device was also found to change the measured temperature response for the same power and temperature settings. Our findings demonstrated significant variations were present between different coils.²¹⁵ The particle mass range of 0.9 – 17.2 mg/puff for the temperatures examined in this study was within the range studied by Gillman et al. (1.5 – 28 mg/puff) for five different devices.²⁰⁹ The exponential dependence shown **Fig. 3.5a** is in large measure consistent with the few limited studies of particle production with device power, which generally show a positive relationship, albeit with

limited data points.^{211, 237} A more thorough comparison of the present findings to others is challenging, as coil temperatures are typically not reported in the literature.

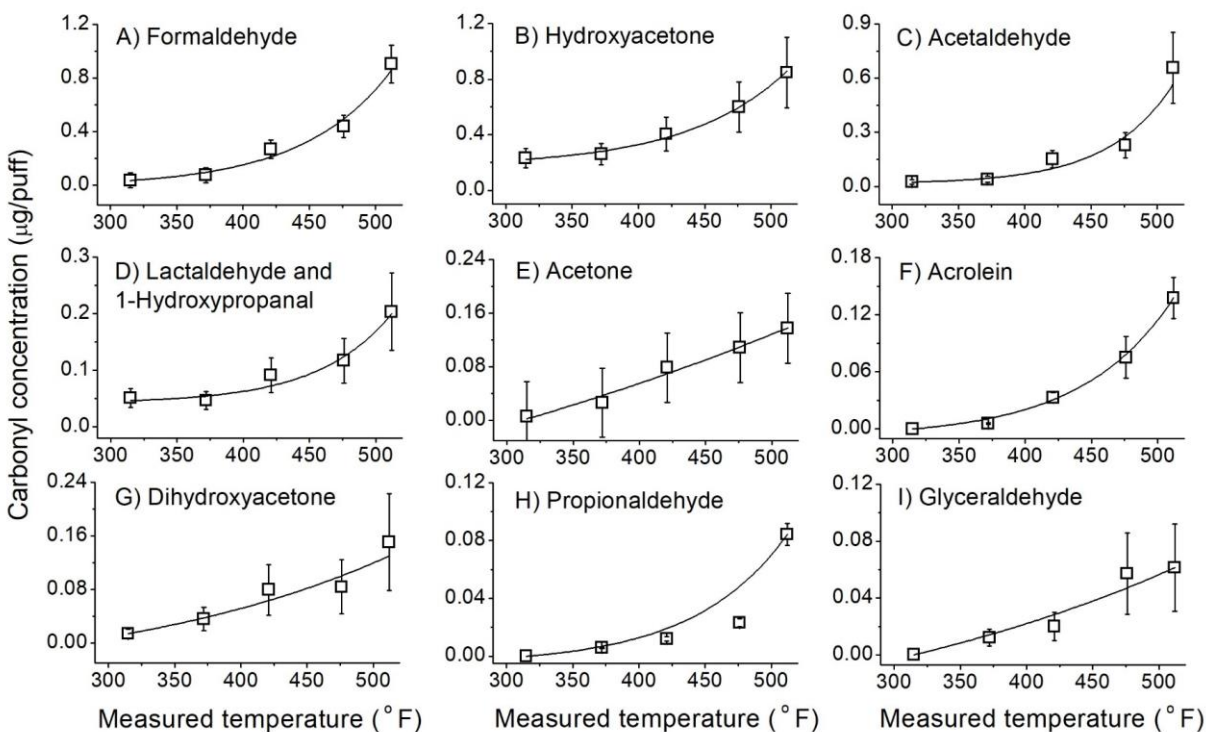
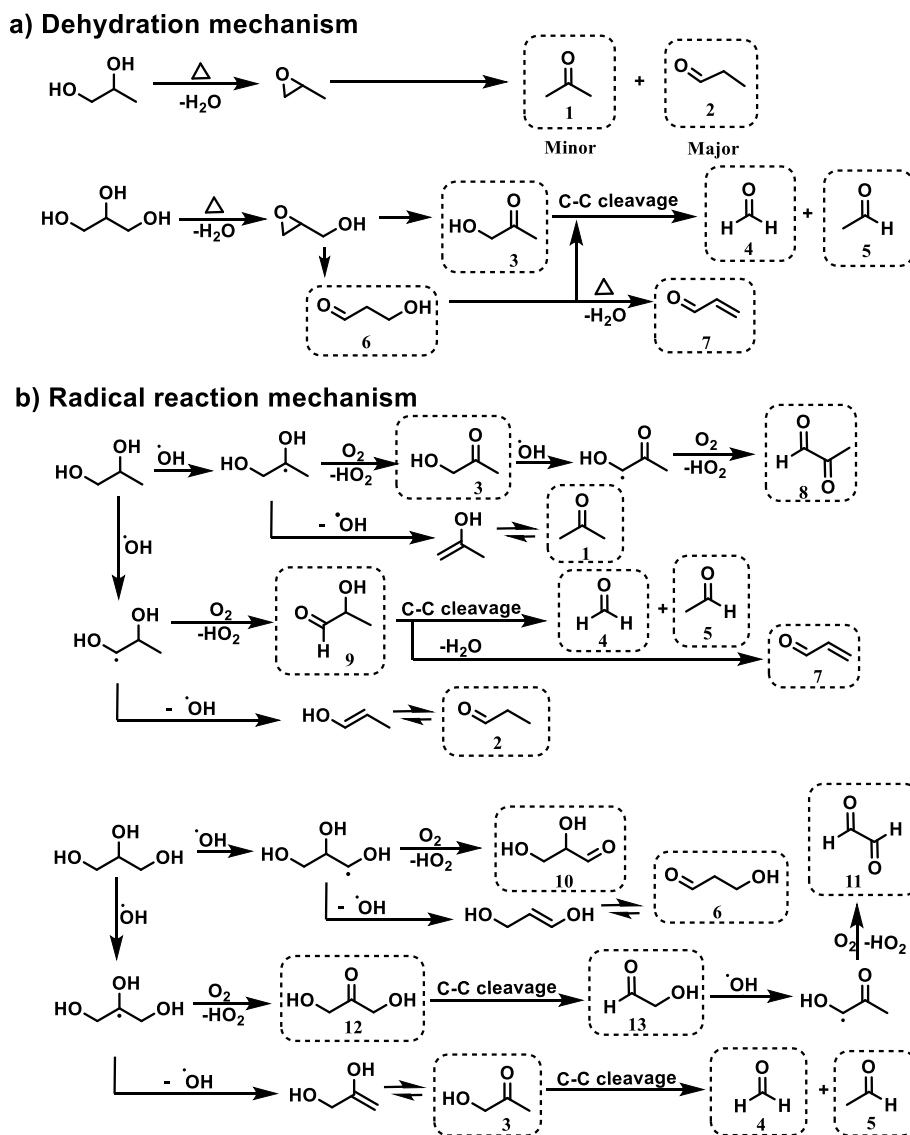


Figure 3.6 The production of representative carbonyl compounds and various coil

The production of carbonyls from vaping (**Fig. 3.6**) had a strong dependence on coil temperature and, in general, a vertical offset around zero (i.e., they were not formed without heat). Hydroxyacetone (**Fig. 3.6B**) was the only compound observed with a substantial concentration at a coil temperature of 315 °F (157 °C). This finding is consistent with Sleiman et al.,¹⁴¹ who reported hydroxyacetone exists in PG/VG e-liquid without thermal degradation, as a possible minor impurity. In general, we found exponential relationships between carbonyl formation and temperature, which reflect that of particle mass production, and are consistent with Arrhenius kinetics given that the formation of carbonyls is a chemical process.²³⁸⁻²⁴⁰ All data for carbonyls and organic acids (also captured by the DNPH cartridge) are reported in **Table 3.1**. The temperature dependencies for formaldehyde, hydroxyacetone, acetaldehyde, acrolein, and



Scheme 3.1 Proposed mechanism of PG and VG degradation in the e-cigarette device from (a) heat induced dehydration and (b) radical reaction pathways, with further oxidation and bond cleavage to form final products. Legend key: 1) acetone, 2) propionaldehyde, 3) hydroxyacetone, 4) formaldehyde, 5) acetaldehyde, 6) 1-hydroxypropanal, 7) acrolein, 8) methylglyoxal, 9) lactaldehyde, 10) glyceraldehyde, 11) glyoxal, 12) dihydroxyacetone, 13) glycolaldehyde.

propionaldehyde (**Fig. 3.6A, B, C, F, G, and H**) were more steeply exponential than those observed for others. The trends for acetone, dihydroxyacetone, and glyceraldehyde (**Fig. 3.6E, G, I**) were nearly linear (or at least, within the linear part of the exponential curve that would manifest

when a greater temperature range is used). We believe the different response curves were due to the different chemical pathways forming specific carbonyls.

Two major pathways have been proposed for the thermal degradation of PG and VG in e-cigarette devices, including heat-induced dehydration (**Scheme 3.1a**)^{137, 75, 141, 76} and H-abstraction by radicals such as OH (**Scheme 3.1b**),^{80,196,77,81} both followed by further oxidation and bond cleavage. The more exponential temperature-dependent carbonyl compounds (e.g., formaldehyde, acetaldehyde, acrolein, hydroxyacetone, 1-hydroxypropanal) are formed primarily through heat-induced dehydration pathways since they are directly affected by heat. The carbonyls formed from the radical reaction pathway (e.g., dihydroxyacetone and glyceraldehyde, **12** and **10** in **Scheme 3.1**) have trends that are more linear because they only have a secondary dependence on heat; their direct dependence is on radical concentrations. Bitzer et al.²⁴¹ found that the formation of free radicals from e-cigarettes is linear within the temperature range (315 – 510 °F, correspond to 157 – 266 °C) of the present study. Thus, the radical-derived products will mirror this temperature dependence. It is not clear from Bitzer et al. or our data what temperature inflection point will cause a more exponential formation of radicals, as higher temperatures are outside the range for our device. However, computational modeling data predict radical formation may start dominating at 680 °F (360 °C) for VG.²⁴² Acetone (**1**), in particular, has a linear temperature trend, even though it can be formed through the same PG dehydration pathway (**Scheme 3.1a**) as propionaldehyde (**2**). Acetone is a minor product of PG dehydration due to the selectivity of the rearrangement of the propylene oxide intermediate, as the energy barrier for acetone is significantly higher (> 8 kcal/mol) than for the main product, propionaldehyde.⁷⁶ Thus, either radical-initiated reaction from

PG may dominate over the dehydration, which is unlikely based on known rates,²⁴³ or other unknown radical mechanisms exist from VG.

The linear temperature dependences of dihydroxyacetone (**12**) and glyceraldehyde (**10**) support that they are from the same radical pathway of VG (**Scheme 3.1b**). Furthermore, the product ratio between them, a factor of 2-3 in favor of dihydroxyacetone, is consistent with the thermodynamic stability of alkyl radicals,²⁴⁴⁻²⁴⁶ wherein a secondary alkyl radical that eventually forms dihydroxyacetone is thermodynamically preferred compared to the primary alkyl radical that will form glyceraldehyde.

The compounds 1-hydroxypropanal (**6**) and lactaldehyde (**9**) coeluted in the chromatography because they are isomeric with very similar polarity. While 1-hydroxypropanal can only be formed by VG by heat-induced dehydration, lactaldehyde can only be formed by PG from radical reaction. We show later, in the e-liquid formulation data (**Fig.3.8**) that 1-hydroxypropanal is more efficiently produced than lactaldehyde. This conforms with the overall exponential temperature trend that is more consistent with heat-induced dehydration, as 1-hydroxypropanal is a hydroxyacetone coproduct from the hydroxypropylene oxide intermediate in VG dehydration (**Scheme 3.1a**).

There are a number of compounds, such as formaldehyde (**4**), hydroxyacetone (**3**), and acrolein (**7**), that can be formed from either heat-induced dehydration of VG or radical pathways from both PG and VG. The exponential temperature dependence data suggest that the heat-induced dehydration pathway is more efficient for **3**, **4**, and **7** under the studied conditions. Our data agree

with the modeling work of Buhler et al.,²⁴² which predicts a preference for VG dehydration at the lower temperatures employed in the present study and a preference for radical chemistry at higher temperatures (e.g., above 680 °F, corresponds to 360 °C). It is unlikely that vaping devices will reach the temperatures that favor predominant radical chemistry for VG. Thus, our findings demonstrate that heat-induced dehydration of VG will dominate most vaping scenarios. Based on the significant abundance of dihydroxyacetone (**12**) and glyceraldehyde (**10**), however, it is clear that radical chemistry for VG in e-cigarette vessels is not negligible.

With regard to phase partitioning, most of the simple carbonyls including formaldehyde, acetaldehyde, acetone, and acrolein can be considered volatile or semivolatile and exist primarily in the gas phase, as they were not captured by the hydrophilic PTFE filter. Nearly 100% of the mass was recovered after the filter. These data are not shown, as a more thorough study on phase partitioning is forthcoming. In contrast, hydroxyacetone was captured at ~ 20% in the particle phase. The differences between simple and hydroxylated carbonyls is likely due to hydrogen bond interactions with PG and VG in the particles, which will keep a fraction of hydroxycarbonyls from partitioning to the gas phase.²⁴⁷⁻²⁵⁰ We emphasize that these phase partitioning results apply to the mainstream aerosol that is directly released from the device, and gas/particle partitioning may change toward more evaporation or condensation on surfaces as the aerosol travels in the respiratory system.²²⁹

The partitioning of carbonyl compounds between the gas and particle phase is influenced by many factors (e.g., relative humidity, temperature, collection method) and has been subject of numerous studies in cigarette smoke. For example, John et al.²⁵¹ found the fraction of particulate

formaldehyde ranges from 35% - 61% at temperatures of 298 – 323 K. Acetaldehyde is found mainly in the gas phase (98%), and the acrolein concentrations in the particle phase ranges from 0% - 33% in different studies.²⁵²⁻²⁵⁴ Uchiyama et al.¹⁶⁵ recently studied the phase distribution for select carbonyl compounds. They reported approximately half of the formaldehyde in the particle phase, whereas our PTFE filters did not trap formaldehyde. Formaldehyde is a well known volatile organic compound with a very high vapor pressure (> 0.8 atm at -20 °C;²⁵⁵ thus, it should be in the gas phase at room temperature in the carbonyl form. However, it can also exist in aqueous-like solutions to some extent as methanediol, which will lower its vapor pressure. When we collected formaldehyde gas with our high-flow HEPA filter, we captured ~ 90% of formaldehyde. It is possible the Cambridge filter pads used by Uchiyama et al.¹⁶⁵ had a surface area between our HEPA filter and hydrophilic PTFE filter, that there was substantial organic loading on their filter (i.e., if a high number of puffs was collected), or that the commercial e-liquid used in their work contains some water, which helps formaldehyde condense. Similarly, Uchiyama et al.¹⁶⁵ reported most of the hydroxyacetone is in the particle phase, while we captured only 20% on the filter. The limited volatility results for carbonyls in the present study are consistent with calculations by Pankow et al.^{256, 55} for gas/particle partitioning in electronic cigarettes.

Another discrepancy arose in the total mass of carbonyl compounds, where the Uchiyama work reported much higher carbonyl formation (in the mg/puff range) than found in the present and other studies (e.g., Geiss et al.²⁵⁷ and references therein), including those that used flavored e-liquid.⁶⁰ The reasons for these discrepancies are unclear. However, our results for nicotine are consistent with Uchiyama et al.¹⁶⁵, who reported it exclusively in the particle phase. Prior research found that nicotine is almost entirely in the particle phase of cigarette smoke, and the partitioning

coefficient of nicotine between the gas and particle phase is related to the pH of the aerosol, as nicotine can exist in both free base form and protonated form.^{258, 259} Lisko et al.²⁶⁰ found that the pH of e-liquids with PG and VG is pH ~ 6, suggesting that most of the nicotine in our study will be protonated, which will suppress its partitioning into the gas phase. El-Hellani et al.²⁶¹ found that some flavored e-liquids have high pH, such that a significant fraction of nicotine may exist as free base for some commercial e-liquids.

3.3.2 E-liquid formulation

Table 3.2 Total mass of e-cigarette aerosol and particle phase composition from e-liquids of different PG/VG ratios and temperatures. ^(a)

PG:VG ratio	Temp. (°F)	Total mass (mg/puff)	Particle mass (mg/puff)	Particle PG (mg/puff)	Particle VG (mg/puff)	Nicotine (mg/puff)	Particle PG (%)	Particle VG (%)	Nicotine (%)
100:0	375	150 ± 34	17.5 ± 1.8	17.3 ± 1.4	N.D.	0.07 ± 0.01	99 +1/-8	---	0.4 ± 0.1
70:30	375	121 ± 27	16.2 ± 1.6	9.1 ± 0.9	6.3 ± 0.8	0.04 ± 0.01	56 ± 6	39 ± 5	0.25 ± 0.06
50:50	375	50 ± 12	6.9 ± 0.7	2.7 ± 0.3	3.7 ± 0.6	0.01 ± 0.002	40 ± 2	54 ± 9	0.15 ± 0.03
30:70	375	26 ± 6	3.9 ± 0.4	0.8 ± 0.2	3.0 ± 0.3	0.007 ± 0.002	20 ± 4	76 ± 9	0.17 ± 0.03
0:100	375	19 ± 4	3.0 ± 0.3	N.D.	2.9 ± 0.3	0.01 ± 0.002	---	96 +4/-9	0.3 ± 0.07
30:70	525	135 ± 28	14.1 ± 1.4	2.9 ± 0.3	11.2 ± 1.9	0.01 ± 0.002	20 ± 2	78 ± 13	0.08 ± 0.02

^(a) Nicotine concentration was 3 mg/mL in all e-liquids. N.D. = not detected. The uncertainty in the control of measured coil temperature is ± 5 °F (3 °C). Temperature 375, 525 °F correspond to 191, 274 °C.

The total aerosol mass production, particle mass production, and composition of the aerosol are affected by the PG:VG ratio in the e-liquid due to the fact that VG and PG have different vaporization, aerosolization, and/or degradation rates at any particular temperature. When the VG content increased in the e-liquid mixture, a decrease was found for the production of total aerosol mass and corresponding particle mass (**Table 3.2**). This has also been observed elsewhere.^{42, 122, 262} The trend held for all of the major components of the particle phase as well, including PG, VG, and nicotine. Clearly, PG is easier to aerosolize than VG. This is due to the differences in chemical structure, and correspondingly, viscosity, vapor pressure, and boiling point. VG has one more OH group than PG, which results in stronger hydrogen bond intermolecular forces in the e-

liquidsolution. The order of magnitude higher viscosity of VG at room temperature,^{263, 264} requires more energy for vaporizing the solution.²⁶⁵ Moreover, the coil temperatures in **Table 3.2** already surpass the boiling point of PG (372.2 °F, corresponds to 189 °C) but are below the boiling point of VG (557.6 °F, corresponds to 292 °C). This is consistent with the high aerosol production when pure PG was used,²⁶⁶ and the high PG fraction in the gas phase (discussed later, in **Section 3.3.4**)

The difference in total aerosol mass when vaping pure PG versus pure VG e-liquids at 375 °F (191 °C), 150 mg/puff vs. 19 mg/puff, **Table 3.2**) suggests that PG was lost from the e-liquid at 8 times the rate of VG. This observation was corroborated in the mixed e-liquid (PG:VG = 30:70) using the gaseous CIMS and particle filter GC-MS data for PG and VG. The combined analytical uncertainties from CIMS (gas phase data) and CG-MS (particle phase data) are larger than for the

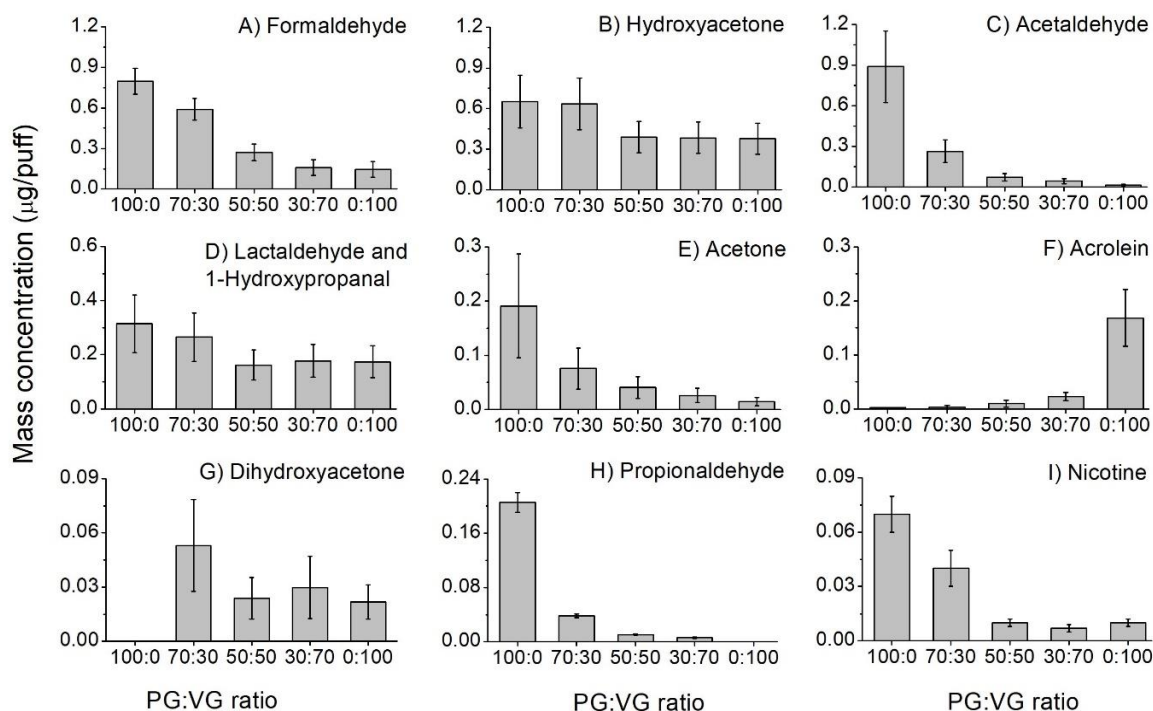


Figure 3.7 The absolute concentrations of representative carbonyl compounds and nicotine observed in aerosols from vaping e-liquid at various PG:VG ratios at a coil temperature of 375 °F (191 °C).

pure gravimetric analysis, but also suggested a significant acceleration of PG loss compared to VG by a factor of ~9.

Figure 3.7 shows representative carbonyl compounds (**Fig. 3.7A-H**) and nicotine (**Fig. 3.7I**) emitted from vaping e-liquid with different PG:VG ratios. Generally, carbonyl and nicotine concentrations decrease as the VG percentage increases in the mixture; although the hydroxycarbonyls do not decrease as dramatically as the simple carbonyls. This is likely due to the lower total aerosol and particle mass production overall as VG content increases in the e-liquid (**Table 3.2**). A notable exception is acrolein (**Fig. 3.7G**), which is the only compound whose formation increased with increasing VG, even as total aerosol mass decreased. Thus, for the 100% VG e-liquid, acrolein was one of the most concentrated carbonyls inhaled, and its relative production exceeded that of formaldehyde. The enhancement of acrolein between 30:70 and 0:100

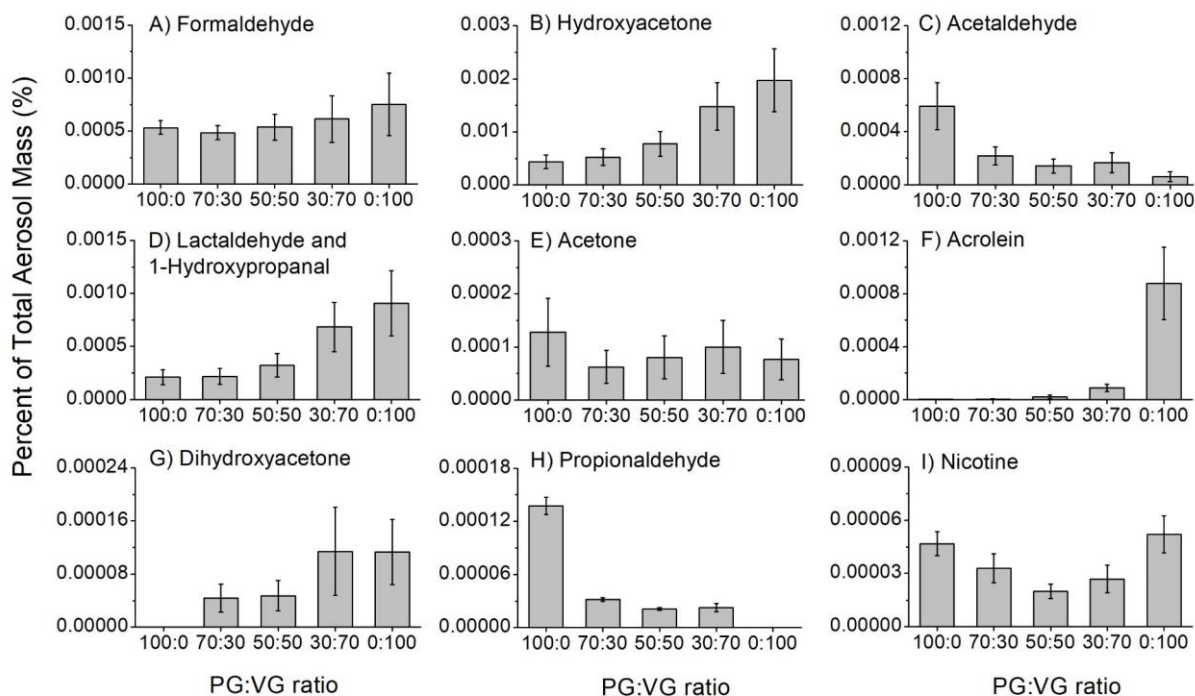


Figure 3.8 The production yield percent of representative carbonyl compounds and nicotine, as normalized by total aerosol mass, from vaping e-liquid at various PG:VG ratios at a coil temperature of 375 °F (191 °C).

PG:VG e-liquid was a factor of 7 – 30 considering all analytical and sampling uncertainties from concentration error bar (**Fig. 3.7F**). This was higher than the VG increase would predict, suggesting that the intermolecular interactions of PG and VG in the e-liquid may alter the thermal degradation chemistry.

Mechanistic differences were more apparent when carbonyl formation was normalized by the total aerosol mass (**Fig. 3.8**). The normalized trends reverse the absolute trends for some compounds, such as hydroxyacetone (**Fig. 3.8B**). Although hydroxyacetone can be generated from both PG (through radical reaction) and VG (through dehydration), the increase in relative aerosol fraction of hydroxyacetone with higher VG percentage in the e-liquid suggests that it is more efficiently formed from VG through the dehydration mechanism. This is consistent with the previous discussion that the heat-induced pathway is much more favorable for VG at the vaping temperatures we tested, and supports the exponential temperature dependence of hydroxyacetone (**Fig 3.6B**). Likewise, formaldehyde emissions were inversely proportional to VG content (**Fig 3.6A**), but increased slightly when normalized by aerosol mass (**Fig 3.8A**). Formaldehyde can originate from both PG and VG and from either thermal or radical pathways. The data suggest that it is formed at similar efficiencies from both precursors, perhaps slightly favoring VG, which is consistent with more pathways available from VG (**Scheme 3.1**).

The relative production trends clearly showed that PG decomposition was responsible for all of the propionaldehyde (**Fig. 3.8H**) and most of the acetaldehyde (**Fig. 3.8C**), while VG decomposition was responsible for all of the dihydroxyacetone (**Fig. 3.8E**) and nearly all of the acrolein (**Fig. 3.8G**). The VG source of acrolein is well-studied, and is leveraged in the conversion

of biomass to fuels.²⁶⁷ Although acrolein can be formed by PG, it is a secondary product of a minor compound that is formed by the primary alkyl radical intermediate instead of secondary (**Scheme 3.1b**), which limits the importance of the PG source. The isomeric lactaldehyde and 1-hydroxypropanal (co-eluted) likely had opposite trends that overlapped since they are solely formed by PG and VG, respectively (**Scheme 3.1**). Given the higher formation of the sum of lactaldehyde and 1-hydroxypropanal with increased VG percentage (**Fig. 3.8D**), it appears that the formation of 1-hydroxypropanal from VG dominates over lactaldehyde formation from PG. These data support the exponential temperature trends (**Fig. 3.6D**) of the lactaldehyde/1-hydroxypropanal pair, given that 1-hydroxypropanal is formed via heat-induced dehydration from VG.

So far, most of the data are consistent with PG/VG mechanisms from the literature as shown in **Scheme 3.1**. However, notable deviations may exist for acetaldehyde and acetone. Acetaldehyde is thought to be a coproduct of formaldehyde in the VG dehydration,⁸⁰ which would elevate it to be a major VG product, yet it appeared to be formed almost exclusively from PG (**Fig. 3.8C**). From PG, there was a suggested acetaldehyde source via radical reaction, instead of heat-induced dehydration. Thus, there was no reason to expect such a large abundance, or an exponential temperature curve (**Fig. 3.8C**). These observations, together with the fact that propionaldehyde (the main PG dehydration product expected from **Scheme 1** was observed in quite low abundance, suggests that there is at least one missing PG dehydration pathway to form acetaldehyde. We rule out the idea that PG radical reaction may be more efficient than dehydration, as the OH rate coefficient of PG is slightly lower than VG in aqueous solution.²⁴³ The results for acetone were also interesting (**Fig. 3.8F**). Acetone is known to be formed by PG; however, the data suggest that it can be formed by both PG and VG at roughly equal efficiencies. The temperature results (**Fig.**

3.6E) also suggest a radical mechanism is dominant for acetone formation. Combined with the relative production trends, it would suggest that a radical formation mechanism from VG is missing from **Scheme 3.1**. We are not aware of any proposed mechanism in the literature stemming from VG, especially one that is radical-initiated. The nicotine percentage in the particle phase (0.15% - 0.4%) at the same vaping temperature (375 ± 5 °F, corresponds to 191 ± 3 °C) fluctuated with different PG:VG ratios (100:0 – 0:100). The nicotine concentration range observed in the particle phase is comparable to that in the original e-liquid (0.24% - 0.29%). These results are consistent with those of Baassrir et al.¹²² and the trials organized by the Cooperation Centre for Scientific Research Relative to Tobacco (CORESTA).²⁶⁸ A 3-mg/mL concentration of nicotine in the e-liquid translated to 1.2 – 3.4 mg/mL nicotine in the particle phase, with the lowest nicotine percentage for the 50:50 mixture and increasing in both directions (**Fig. 3.8I**). More research is needed to understand the robustness of, and underlying reasons for, this trend and whether it is conserved with different nicotine content in the e-liquid. Approximately 0.3 mg/mL nicotine was observed in the total aerosol compared to 3 mg/mL used in e-liquid.

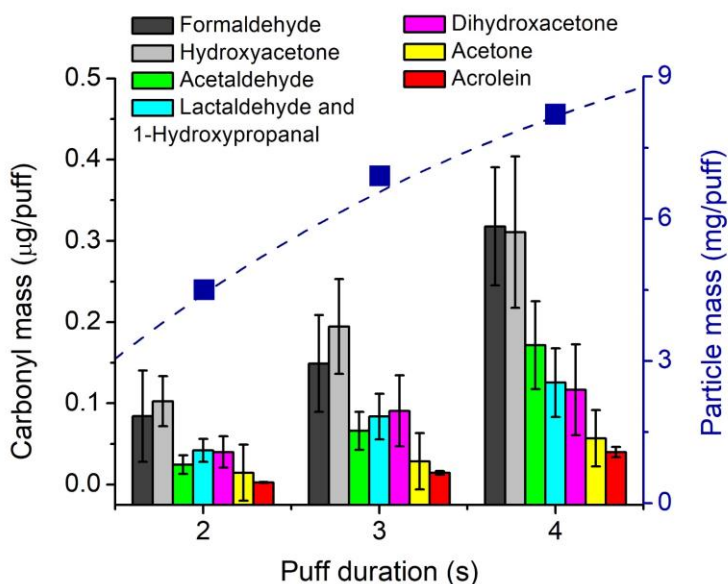


Figure 3.9 Particle mass (blue filled squares) and representative carbonyl compounds produced during vaping with various puff durations, at a 375 °F (191 °C) coil temperature and 30:70 PG/VG e-liquid ratio by volume. A non-linear best fit relationship for particle mass is shown.

3.3.3 Puff Duration

Figure 3.9 shows that the mass of the particles and representative carbonyl

compounds generally increased with puff duration, as expected. Given the simultaneous increase in both particle mass and carbonyl mass with puff duration at the same flow rate, which would increase the puff volume, the carbonyl mass yield as normalized by aerosol mass would more or less be invariable. Both linear and non-linear fits would have yielded acceptable correlation coefficients within the studied range of only three data points. As puff durations in realistic use cases are unlikely to exceed this range,²⁶⁹ we did not test further. The relative increase between carbonyl compounds were roughly the same, within uncertainty. These results agree with Son et al.,²¹¹ who found that increases in puff duration will increase the formation of carbonyl compounds, OH radicals, and nicotine.

3.3.4. Mass Balance Closure and Volatility

Most of the aerosol mass ended up in the gas phase (84 - 88 %, **Fig. 3.10**), i.e., not captured on the hydrophilic PTFE filter, regardless of the temperature or PG:VG ratio tested (**Table 3.2**). It is challenging to understand how the carbon mass from the e-liquid loss was distributed in the gas phase because there is no

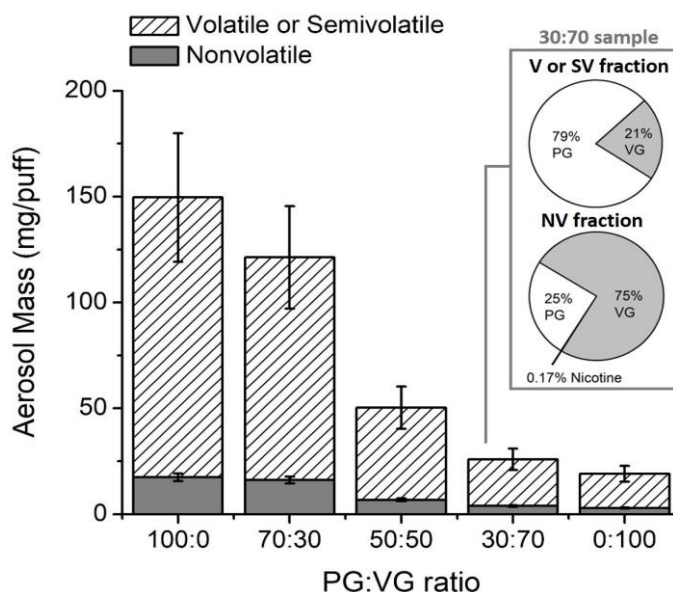


Figure 3.10 Distribution of total mass loss from the e-liquid as nonvolatile (NV) particles captured by a filter or volatile/semivolatile (V/SV) compounds at different PG:VG ratios and a measured coil temperature of 375 °F (191 °C), 3 s puff duration and 3 mg/ml nicotine concentration. For the 30:70 PG:VG ratio sample (insert), the V/SV fraction was measured by CIMS to be primarily PG, and the nonvolatile (NV) fraction was measured by GC-MS to be primarily VG. The measured V/SV mass closed the balance of mass determined from gravimetric analysis.

conventional analytical technique to quantify PG and VG in the gas phase due to the semivolatile nature of these compounds. The results from CIMS (**Fig. 3.11**), demonstrated that the majority of the gas phase was PG and VG instead of unknown compounds (e.g., peroxides, CO, CO₂, etc.) that are not well-measured by targeted techniques. This is consistent with findings that CO and CO₂ are not abundant e-cigarette emissions.^{270,271} The CIMS spectra also showed that PG and VG were orders of magnitude larger in concentration than hydroxycarbonyls, a result that is consistent with the carbonyl-DNPH analysis. For the 30:70 PG:VG condition at 375 °F (191 °C) coil temperature, the sum of PG (22.5 ± 8 mg/puff) and VG (4 ± 2 mg/puff) obtained by CIMS in the gas phase accounted for the missing mass that was not captured by the particle filter (22 ± 5 mg/puff) within uncertainty (**Fig. 3.11**). As discussed in **Section 3.2.4**, CIMS may overestimate semivolatile distribution in the gas phase due to evaporation during the sample dilution (which was necessary as the instrument is highly sensitive). However, it is clear from the CIMS spectra that the gas phase was dominated by mainly PG (even after accounting for the higher sensitivity of CIMS to VG).

GC-MS analysis of filters also showed that PG and VG were dominant

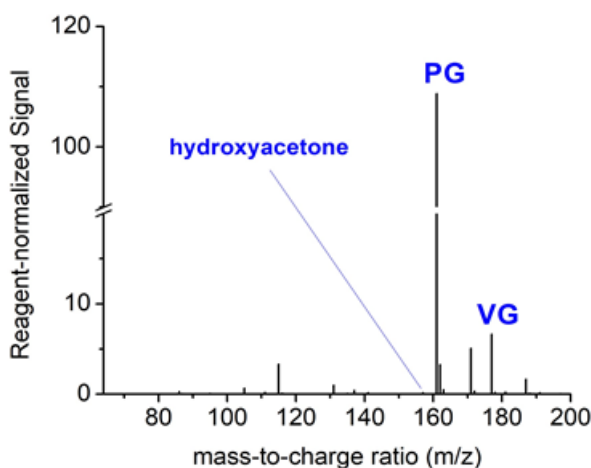


Figure 3.11 CIMS mass spectrum for the e-cigarette aerosol, after the background signal in the lab air has been subtracted. The spectra shows that the major content is PG (detected as PG•CF₃O, m/z 161) and VG (detected as VG•CF₃O, m/z 177). The relative sensitivity of VG is higher than PG, which is not accounted for in this plot. After all dilution corrections and sensitivity calibrations, the concentrations of PG (22.5 ± 8 mg/puff) and VG (4 ± 2 mg/puff) are obtained. Hydroxycarbonyls such as hydroxyacetone are well-observed by CIMS, but had negligible signal.

components in the particle phase, with nicotine making up much less than 1%. In the 30:70 sample (**Fig. 3.10**, insert), approximately three-fourths of the particulate fraction was VG and three-fourths of the gaseous fraction was PG. The particle-phase composition roughly mirrored the e-liquid composition (note that a 30:70 volume ratio of PG:VG translates to a 26:74 ratio by mass according to their densities). The particle phase content of nicotine at 2.2 mg/mL was also similar to the e-liquid composition. Our particle-phase results are consistent with other accounts that PG, VG, water and nicotine are the main components of e-cigarette droplets,^{220, 221, 272} and that nicotine is a small fraction of the total aerosol and only found in the particle phase (regardless of whether free-base or nicotine salts were used).^{61, 273} Thermal degradation products of nicotine (e.g., nicotyrine, nor nicotine) have been reported in other works,^{88, 198} but were not found in the present study even though the GC-MS method we used can detect nicotine products.

3.3.5. Health Impacts

It can be assumed that regular e-cigarette users intake a median of 200 puffs per day.¹²⁶ This translates to an exposure dose of approximately 4.5 g PG/day and 0.8 g VG/day through inhalation of e-cigarette aerosols produced from vaping 30:70 PG:VG e-liquid at a coil temperature of 375 °F (191 °C) for a duration of 3 seconds. Although the PG exposure is fairly high compared to other aerosol components, animal and human studies demonstrate that PG has low toxicity even at relatively high doses.²⁷⁴⁻²⁷⁶ Mild sensory and respiratory irritation effects may result at concentrations of > 871 mg/m³ for particle plus gas phase PG, which translates to ~ 17.5 g/day exposure assuming 20 m³ air intake per day for a 70 kg adult.²⁷⁷ VG has similarly weak irritation effects, which is supported by the German occupational exposure limit (MAK) of 200 mg glycerin/m³ to protect against sensory irritation effects in the workplace.²⁷⁸

In contrast, the thermal degradation products, such as carbonyls, are a concern for potential risk of acute and chronic adverse human health effects despite their low absolute concentration in our study (< 0.5% by mass under all tested conditions). Carbonyls may be further enhanced in flavored e-liquid,⁶⁰ and may approach or exceed unhealthy doses for toxicological exposure with or without additional flavors. Formaldehyde, acetaldehyde, and acrolein are classified as known or probable human carcinogens.²⁷⁹ The more abundant hydroxycarbonyls in e-cigarette aerosols, such as hydroxyacetone, do not have available toxicology data. Carbonyls are also found in combustible cigarettes, so it is informative to discuss carbonyl exposure risk compared to combustible cigarettes and normalized to nicotine, as e-cigarette users have been reported to self-titrate for nicotine intake.^{173, 172}

Ashton et al.²⁸⁰ reported a mean nicotine production of 1.4 mg/cigarette (The maximum legal content for nicotine is 1.0 mg/cig in the European Union),²²³ and cigarette smokers can consume a range of 1 – 30 cigarettes per day (average 15 cig/day);^{281, 282} With an observed

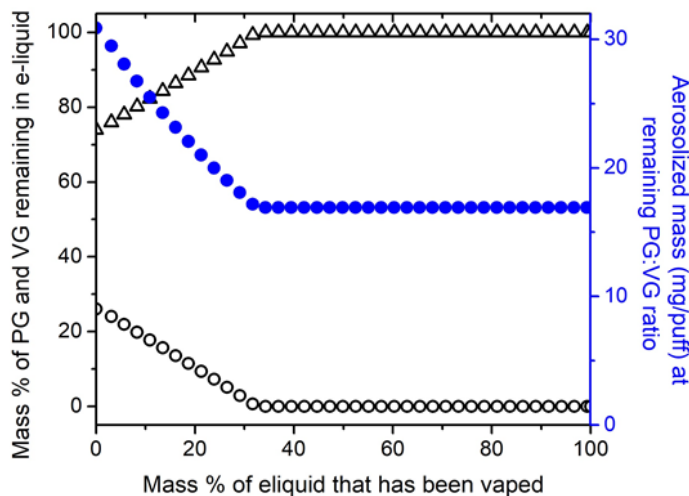


Figure 3.12 Simplified model of mass loss during e-cigarette vaping. The VG percent (black open triangles) in the e-liquid, PG percent (black open circles) in the e-liquid, and aerosolized mass (blue filled circles) all change during vaping. The model starts with 1000 mg e-liquid at 30:70 PG:VG volume ratio (26:74 mass ratio), and losing mass per puff as reported in Table 2 as a function of e-liquid PG content ($f(\text{PG}\%) = 16.92e^{(0.0231 \times \text{PG})}$) that is remaining in the e-liquid, and assuming an 8:1 mass loss ratio for PG:VG as measured by total mass loss for 100% PG compared to 100% VG e-liquid.

formaldehyde/nicotine ratio range of 11 – 90 $\mu\text{g}/\text{mg}$ in the coil temperature range of 315 – 510 °F (157 – 266 °C), there exists vaping conditions in this study that exceed the 37 $\mu\text{g}/\text{mg}$ of formaldehyde/nicotine in combustible cigarettes.¹⁷⁵ However, we found that the acetaldehyde/nicotine ratio (6 - 66 $\mu\text{g}/\text{mg}$), acrolein/nicotine ratio (1 – 20 $\mu\text{g}/\text{mg}$), and propionaldehyde/nicotine ratio (1 – 9 $\mu\text{g}/\text{mg}$), at the coil temperature range of 315 – 510 °F (157 – 266 °C) and the 30:70 PG:VG e-liquid composition, were all lower than combustible cigarettes (580 $\mu\text{g}/\text{mg}$ for acetaldehyde, 62 $\mu\text{g}/\text{mg}$ for acrolein, and 59 $\mu\text{g}/\text{mg}$ for propionaldehyde).

At a VG content of 100% in the e-liquid, exposure to VG products (**Fig. 3.7**) such as hydroxyacetone, 1-hydroxypropanal, and acrolein become increasing important. At 100% VG, the acrolein/nicotine ratio range increased by a factor of 20 (range 17 – 408 $\mu\text{g}/\text{mg}$) compared to the 30:70 e-liquid at the same coil temperature range of 315 – 510 °F (157 – 266 °C), which exceeds the acrolein/nicotine ratio in combustible cigarettes (50 - 70 $\mu\text{g}/\text{mg}$)^{175 176} under some temperature conditions. A Chronic Reference Exposure Levels (chREL) value of 0.35 $\mu\text{g}/\text{m}^3$ was set by the California Office of Health Hazard Assessment (OEHHA) for acrolein. If this is multiplied by 20 m^3 inhaled volume of per day for a 70 kg adult,²⁷⁷ then a threshold of 7 $\mu\text{g}/\text{day}$ may be considered safe for chronic exposure. However, at 100% VG, the acrolein e-cigarette exposure that is equivalent to replacing only 1 cigarette/day exceeds chREL threshold at all tested temperatures. Given the lower aerosol and nicotine production at high VG ratios in the e-liquid (**Table 3.2**), users may increase temperatures, puff duration, or puff frequencies to achieve higher aerosolization rates, which will significantly increase carbonyl exposure.

Although e-liquids with 100% VG can be readily found commercially, they also may be formed during the dynamic vaping process. Our data suggest, because the total e-liquid mass loss from PG was 8 times that of VG (**Table 3.2**, total aerosol mass), the e-liquid will be more enriched in VG as vaping continues. This will shift the e-cigarette aerosol composition toward VG and its degradation products, particularly acrolein, as VG enrichment occurs. Relative formation of formaldehyde will stay fairly uniform as VG enrichment occurs. Likewise, total aerosol mass and total nicotine will decrease during the lifespan of the e-liquid. We can build a simple model (**Fig. 3.12**) to predict the e-liquid mass remaining when 100% enrichment occurs. The model assumes that, as the PG and VG ratio changes during vaping, the total amount of e-liquid lost also changes in accordance with the total aerosol data (**Table 3.2**, with a fit function of $f(\text{PG}\%) = 16.92e^{(0.0231 \times \text{PG})}$). Thus, for an 8:1 aerosolization ratio (by mass) for PG:VG, and for a 30:70 (by volume) ratio PG:VG mixture, it can be estimated that approximately 30-40% of e-liquid mass will be consumed by the time the e-liquid reaches 100% VG (**Fig. 3.12**). In other words, the e-liquid will be entirely VG well before the e-liquid reservoir is depleted. The predicted percent of e-liquid remaining at full VG enrichment in the model is fairly insensitive to starting volume in the e-liquid but is sensitive to starting PG:VG ratio and temperature, as expected. Thus, a user may be inhaling high relative concentrations of acrolein (**Fig. 3.8G**) and other predominant VG products in the aerosol for a significant amount of time during the e-liquid cartridge or reservoir lifespan.

3.4 Conclusion

The vaping process for e-cigarettes is complex and dynamic, possibly more so than currently appreciated. Coil temperature, puff duration, and PG:VG ratio all significantly affect both the

aerosol production and the composition. Most of the mass that was lost from the e-liquid could be accounted for as PG and VG. Furthermore, volatile/semivolatile compounds dominated the total aerosol. Caution should be exercised when collecting particles with dense filter material or with overloaded filters for studying the particle phase, as the semivolatiles can be trapped and interpreted as particulates. In general, the chemical mechanisms for forming carbonyls appear to be well understood, and consistent with the numerous insights gained from interpreting the carbonyl mass yield as normalized by aerosol mass. Some exceptions include acetone, for which there may be a radical pathway from VG not currently accounted for, and acetaldehyde, for which there may be a thermal pathway from PG. The thermal pathways appeared more efficient under the temperature conditions tested. Importantly, the user's exposure to toxic carbonyls such as acrolein may change during the vaping process, and the user may be exposed to high relative content of VG and its degradation products as the e-liquid is depleted. These findings support the need for further research into aerosol composition and toxicology as a function of the e-cigarette puffing lifecycle, in addition to e-liquid composition, puffing regimen, and vaping device operational conditions.

Chapter 4. Vaping aerosols from Vitamin E Acetate and Tetrahydrocannabinol oil: chemistry and composition

Abstract

The popularity of vaping cannabis products has increased sharply in recent years. In 2019, a sudden onset of electronic cigarette/vaping-associated lung injury (EVALI) was reported, causing thousands of cases of lung illness and dozens of deaths due to the vaping of tetrahydrocannabinol- (THC) containing e-liquids that were obtained on the black market. A possible cause of EVALI was attributed to the illicit use of vitamin E acetate (VEA) as a diluent, an ingredient not found in legal cannabis vapes. However, the thermal chemistry that can modify VEA and THC under actual vaping conditions, potentially producing toxic byproducts, is not well understood. In this work we identified over 50 kinds of carbonyls, organic acids and cannabinoids in the vaping aerosol of pure VEA, extracted THC oil, and the 1:1 mixture of VEA and THC oil. Accordingly, we propose the thermal degradation pathways for VEA and cannabinoids, including Δ^9 -THC and CBG. The oxidation and bond cleavage of the aliphatic side-chains of both VEA and cannabinoids were found to be important decomposition pathways during the vaping process, which will cause the formation of a series of smaller carbonyls. Oxidation may also occur on the ring positions of cannabinoids to form various oxidative products. The production of some unexplained compounds in the vaping aerosol of extracted THC oil may be related to the thermal degradation of terpenes that exist in the e-liquid. We show that THC oil has a stronger tendency to aerosolize and degrade than VEA, and adding VEA into extracted THC oil will suppress the thermal degradation and the generation of vaping particles compared to only THC oil. However, certain potentially more toxic (e.g., carcinogenic) carbonyls including formaldehyde, hexanal/4-methylpentanal, glyoxal,

diacetyl/3-oxobutanal are more likely to be formed from VEA, when normalized by collected particle mass.

4.1 Introduction

The unexpected outbreak of e-cigarette or vaping-associated lung injury (EVALI) was reported nationwide starting in September 2019, causing more than 2800 hospitalizations and 60 deaths.²⁸³⁻
²⁸⁶ The specific biological mechanisms of EVALI, as well as the chemical causes, are still under investigation.²⁸⁷⁻²⁹⁰ Emerging evidence shows that EVALI is associated with vaping tetrahydrocannabinol (THC) containing e-liquid cartridges that were obtained on the black market.^{112, 291-293} Although adverse health effects of vaping THC cartridges have been found to include abdominal pain, nausea, chest pain, shortness of breath, and acute respiratory distress,²⁹⁴⁻
²⁹⁶ they have not to date been fatal. The sudden deaths and hospitalizations from EVALI are, instead, strongly linked to a compound called vitamin E acetate (VEA), the chemically-stable esterified form of vitamin E (VE).^{285, 297-299} VEA is thought to be used as a cutting agent in THC cartridges because it has a similar viscosity to THC oil, so that the adulteration will not be visually evident. FDA labs confirmed that VEA was present in 81% of THC-containing vaping cartridges confiscated from 93 EVALI patients. VEA was also found in the bronchoalveolar (BAL) fluid samples from 48 of 51 patients, but not found in samples from the healthy comparison control group.³⁰⁰⁻³⁰² The VEA fraction in vaping cartridges confiscated from EVALI patients range from 23% - 88%.^{299,303} The interaction between aerosolized VEA with lung surfactant,³⁰⁴ the toxicity of VEA thermal degradation products,^{92,93} or other components in the vaping aerosol of extracted THC oil^{98,26} have been hypothesized to explain the association of VEA to EVALI. It should be noted that there is currently not sufficient evidence to rule out the contribution of other diluents

(e.g., squalene oil, medium chain triglyceride), flavoring additives, pesticide residues, or other ingredients found in THC cartridges.^{70,98} It's also not known if VEA has a synergistic effect with THC oil components that may lead to EVALI.

A limited number of recent research publications has focused on either the physical and chemical properties, or the biological effects of the vaping aerosol from VEA. DiPasquale et al.³⁰⁴ observed VEA was capable of reducing the elastic properties of pulmonary surfactant and thus cause lung dysfunction by alveolar collapse or atelectasis. Lanzarotta et al.³⁰³ found evidence for hydrogen bonding between VEA and THC in both vaping aerosol and unvaped e-liquid, suggesting they may synergistically cause EVALI. Wu et al.⁹³ showed that the toxic gas ketene, as well as carcinogenic alkenes and benzene are generated from the thermal degradation of VEA. Riordan-Short et al.⁹² found that pure VEA starts to decompose at an incubation temperature of 240 °C and identified over 40 kinds of thermal degradation product at an incubation temperature of 300 °C, 30 of which are carbonyls and acids. However, the experiments of Riordan-Short was done under heated headspace sampling as a surrogate vaping environment, instead of a real vaping environment in an e-cigarette tank with metal coil, where temperature gradients exist due to localized coil heating.^{215,21} Furthermore, different coil material and surface area will have different effects on thermal degradation chemistry.¹⁹⁰ Jiang et al.⁷⁰ reported a total of 35 toxic byproducts (e.g., quinones, carbonyls, esters, and alkyl alcohols) during the vaping of commonly used diluents including VEA; over 25 of them are carbonyl compounds.

Compared to VEA, there is less research available on the vaping chemistry of THC oil extracts and other cannabinoids due to DEA regulations, even though the metabolism of THC has been

well studied.³⁰⁵⁻³⁰⁷ Meehan-Atrash et al.⁹⁴ hypothesized that THC emits similar thermal degradation products to terpenes given their terpenoid backbone; however, terpenes are also found in cannabis plants and can be used as additives in e-liquids, such that the degradation products may be difficult to distinguish from THC.³⁰⁸ It was also found that vaping and dabbing cannabis oil including terpenes may cause exposure to concerning degradants such as methacrolein, benzene, and methyl vinyl ketone.⁹⁸ Adding terpenes to THC oil led to higher levels of gas-phase products compared to vaping THC alone.²⁶ Since vaping is a complex and dynamic process, a systematic understanding of the chemistry occurring during the vaping process is needed to assess potential factors that may contribute to EVALI, as well as other potential adverse health effects.

In this work, a temperature controlled vaping device with accurate coil temperature measurement was used to vape e-liquids of VEA, extracted THC oil, and their mixture under typical vaping conditions consistent with the CORESTA standard.²²² Gravimetric analysis was used to evaluate the aerosolization efficiency, while the high performance liquid chromatograph coupled with high resolution mass spectrometry (HPLC-HRMS) was used to characterize thermal degradation products including carbonyl compounds, acids, and cannabinoids using the methods developed by Li et al.⁴⁰ A comprehensive thermal degradation mechanism for THC and VEA are proposed, which could be useful for regulation and further research.

4.2 Experimental

4.2.1 Vaping aerosol generation and extraction

A temperature-controlled third generation Evolv DNA 75 modular e-cigarette device (Evolv LLC, Hudson, OH) with a refillable e-liquid tank and single mesh stainless steel coils (SS316L,

FreeMax Inc., Shenzhen, China) was used for aerosol generation (hereinafter referred to as the “mod”, Fig. 1). The mod enabled variable output voltages (0.2 – 9 V) with coil resistance of ~0.12 ohm. Evolv Escribe software (Evolv LLC, Hudson, OH) was used to customize the power output (0 - 75 W) in order to achieve the desired coil temperature. The coil temperatures were measured by a flexible Kapton-insulated K type thermocouple (Oakton instrument Inc., Vernon Hills, IL) in contact with the center of the coil surface and output to a digital readout. The

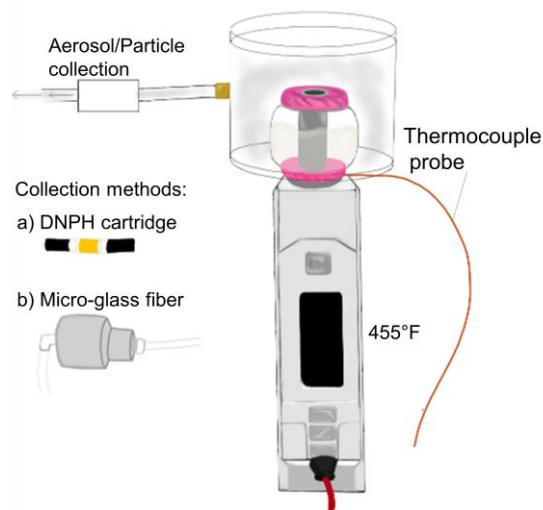


Figure 4.1 The setup of vaping device (mod) and collection system. Particles fraction of vaping aerosol will be collected by micro-glass fiber. Carbonyls, acids and cannabinoids in aerosol will be collected on 2,4-DNPH cartridge for the HPLC-HRMS analysis.

temperature set by the device is not truly representative of the measured coil temperature,²¹⁵ as often, the device flow rate, e-liquid viscosity, and coil resistance changes will alter the relationship between applied power and output coil temperature that drives chemistry. The puff duration is 3 s with a flow rate of 1.20 ± 0.05 L/min, quantified by a primary flow calibrator (A.P. Buck Inc., Orlando, FL), corresponding to puff volume of 60 ± 2.5 mL. The puff volume and puff duration selected in this work is consistent with e-cigarette test protocols applied to propylene glycol (PG)/vegetable glycerin (VG) based e-cigarettes.²²² The e-liquids used for vaping in this work are: (1) pure VEA (purity ≥ 96 %, Sigma Aldrich, St. Louis, MO) that was used as purchased, (2) extracted THC oil that is commercially obtained from Biopharmaceutical Research Company (BRC, Castroville, CA), and (3) the mixture of the two ingredients (volume ratio of 1:1). All THC experiments are performed at the BRC facility under an active DEA Schedule 1 license. The

composition analysis by gas chromatography of unvaped extracted THC oil showed that the most abundant cannabinoids are: Δ^9 -tetrahydrocannabinol (THC, mass percentage of 32.8%), Δ^9 -tetrahydrocannabinol acid (THCA, mass percentage of 32.8%) and cannabigerol acid (CBGA, mass percentage of 10.7%), while other cannabinoids were identified below 3% of the total peak area (e.g., cannabidiol, cannabigerol, tetrahydrocannabivarin, cannabichromene, etc.). Δ^8 -THC, which can be observed at 0.3 minutes after the Δ^9 isomer, was not detected in the mixture. A total of over 50% of mass in unvaped extracted THC oil remain uncharacterized, but presumably contains terpenoids and potentially other alkanes and alkenes. Three temperatures (315, 455, 545 °F (157, 235, 285 °C)) were chosen for the particle generation, with a temperature measurement deviation of 10 °F. The quantification of carbonyls is only reported at 455 °F.

During the sample collection, a total of 10 puffs of aerosol with a frequency of 2 puffs/min were collected for each sample. Carbonyls, acids and cannabinoids in vaping aerosols (both gas and particles), which represent a large portion of expected products,^{70, 92} were collected onto 2,4-dinitrophenylhydrazine (2,4-DNPH) cartridges (Supelco Inc., 350 mg DNPH, Bellefonte, PA) for HPLC-HRMS analysis. The consecutive sampling with three DNPH cartridges shows a collection efficiency >98.4% for carbonyl-DNPH adducts in the first cartridge.⁴¹ Excess DNPH is conserved in the cartridge after the collection to maximize collection efficiency. DNPH cartridges were extracted with 2 mL of acetonitrile (Fisher Scientific Inc., LC-MS grade, Hapton, NH) into auto-sampler vials and analyzed by HPLC-HRMS. Consecutive extractions of DNPH cartridges for samples confirmed that >97% of both DNPH and its hydrazones were extracted after the first 2 mL volume of acetonitrile. The collection efficiency for cannabinoids is unknown, since only a limited amount of THC oil was available for experiment and not for quality control

characterizations. The high resolution mass data of cannabinoids is only used for identification in this work. Details on the collection method are described elsewhere.⁴¹ Moreover, glass fiber filters (Pall Corp., New York) were used to collect the particles, as has been done in other e-cigarette studies.²²² The particle mass collected on filters was determined gravimetrically on a microbalance (Mettler Toledo Inc., 0.001 g precision, calibrated by weight standards) by weighing the filter mass immediately before and after puffing at different experimental conditions. The standard deviation of the gravimetric analysis after triplicate measurements was determined to be ~20%, mainly due to variations in puffing. The sample collection and analysis were performed in triplicate.

4.2.2 Thermal degradation carbonyls, acids, and cannabinoids characterized by HPLC-HRMS

Carbonyl compounds and acids from the thermal degradation of VEA and THC were derivatized by 2,4-DNPH to form carbonyl(acid)-DNPH compounds during the collection process. The detailed mechanism and method of identification for each carbonyl were described in previous work.⁴⁰ Beside DNPH adducts, HRMS has been proven to be an effective tool for the detection of cannabinoids and their oxidative products, as the phenolic hydroxyl group in cannabinoids can be ionized in both electrospray ionization (ESI) positive and negative modes, while the high mass precision enables the analysis of elemental composition.³⁰⁹ Negative mode was applied for the detection in this work as both carbonyl(acid)-DNPH adducts and cannabinoids can form negative ions by deprotonation. An external mass calibration was performed using the carbonyl-DNPH standard solution (M-1004-10X, Accustandard, Inc., New Haven, CT) immediately prior to the MS analysis, such that the mass accuracy was adjusted to be approximately 1 ppm for standard compounds, the mass calibration was then applied to a molecular formula assignment for unknown

compounds. All molecular assignments were analyzed by the MIDAS v.3.21 molecular formula calculator (Florida State Univ.). Carbonyl(acid)-DNPH adducts and cannabinoids in extracts solution were separated and analyzed using an Agilent 1100 HPLC with an Poroshell EC-C18 column (2.1×100 mm, $2.7 \mu\text{m}$, 120 \AA , Agilent Inc.) coupled to a linear-trap-quadrupole Orbitrap (LTQ-Orbitrap) mass spectrometer (Thermo Corp., Waltham, MA) with an ESI source at a mass resolving power of $\sim 60\,000$ $m/\Delta m$ at m/z 400. The mobile phase of LC-MS grade water with 0.1% formic acid (A) and acetonitrile (B) were applied in the chromatography method. The analytes were eluted over the course of 45 min at 0.27 mL/min with the following gradient program: 40% B (3 min), 50% B (14.3 min), 60% B (20 min), 80% B (40 min), and 40% B (42 min). After separation by chromatography, single ion chromatography (SIC) of each compound were extracted for the quantification of specific carbonyl compounds based on their calibrated m/z . Formaldehyde, acetaldehyde, acetone, butyraldehyde, valeraldehyde, hexanal were quantified using the analytical carbonyl-DNPH standards. The SIC peak separation between isomers of butyraldehyde/isobutyraldehyde, valeraldehyde/isovaleraldehyde hexanal/4-methylpentanal cannot be achieved, so the concentration of all isomers were calculated as a total amount. The concentrations of glyoxal, methylglyoxal, diacetyl were calculated by an estimated ESI sensitivity as described by Li et al.⁴⁰

4.3 Results and discussion

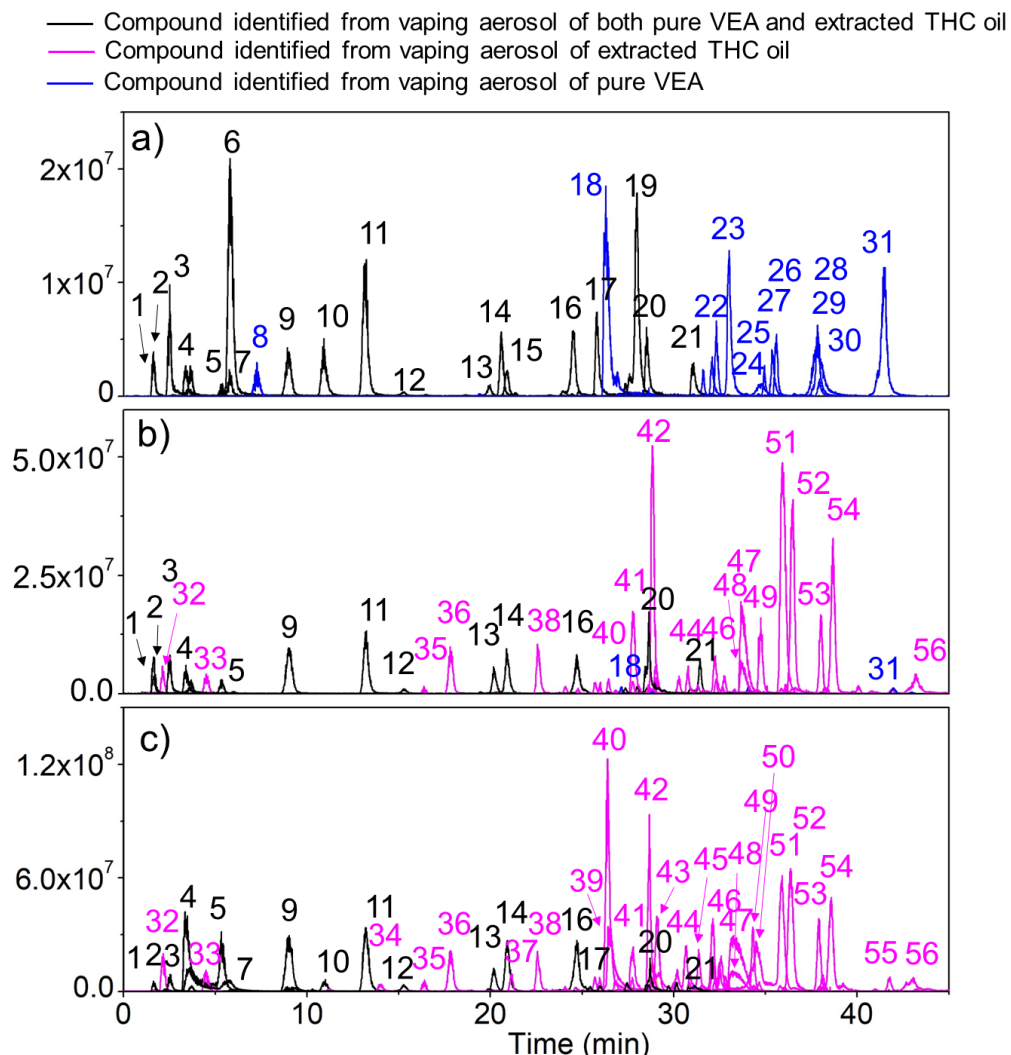


Figure 4.2. Stacked single ion chromatogram (SIC) of the main thermal degradation products and aerosolized components from the vaping aerosol of **a)** VEA, **b)** VEA/extracted THC oil = 1:1, **c)** extracted THC oil at $455 \pm 10^\circ\text{F}$ (235°C). Numbers correspond to the proposed assignments shown in Table 4.1.

The thermal degradation of both VEA and THC was observed at the measured coil temperature of $455 \pm 10^\circ\text{F}$ (235°C), which is close to temperature that VEA started to degrade in the work of Riordan-Short et al.⁹² The information given by the total ion chromatogram (TIC) is limited because of its complexity caused by co-elution and background noise. Instead, single ion chromatograms (SIC) of different mass to charge ratios were extracted for isolating peaks of

individual compounds, while avoiding co-elution and background noise. The stacked SIC of different thermal degradation compounds or aerosolized components from vaping aerosols of **a)** pure VEA, **b)** the mixture of VEA and extracted THC oil, **c)** extracted THC oil were shown in **Figure 4.2**. The black line represents the carbonyl/acids that can be generated from the thermal degradation of both VEA and extracted THC oil, the blue line represents the carbonyl/acids only from the thermal degradation of VEA, while the magenta line represents the thermal degradation carbonyls as well as cannabinoids only from the vaping aerosol of THC oil. Although the SICs were able to separate the co-eluting peaks with different m/z ratios, the isomers having identical m/z with similar structures and polarity are still not able to be separated or clearly identified. For example, multiple peaks are observed for $C_6H_{12}O$ (#19, assignable to either hexanal or 4-methylpentanal) in the vaping aerosol of mixture of VEA and THC oil (the peaks are very small and invisible in **Fig. 4.2b**). While hexanal can be formed from terpenes,⁹⁷ 4-methylpentanal could be formed from the thermal degradation VEA according to the proposed thermal degradation pathway in **Scheme 4.1**. However, since $C_6H_{12}O$ is highly enhanced in the VEA aerosol (**Fig. 4.2a**), we assign the majority of this emission to 4-methylpentanal.

Table 4.1 Calibrated m/z , correspond ion and molecular formula, proposed thermal degradation products from VEA and THC

Peak labeled in chromatograph	Calibrated m/z	Corresponding ion	$\Delta m/z$ (ppm)	Molecular formula	Proposed compound
Compound identified from vaping aerosol of both pure VEA and extracted THC oil					
6	209.032	$C_7H_5N_4O_4^-$	-0.1	CH_2O	Formaldehyde
9	223.047	$C_8H_7N_4O_4^-$	0.1	C_2H_4O	Acetaldehyde
1	225.027	$C_7H_5N_4O_5^-$	0.3	CH_2O	Formic acid
11,12	237.063	$C_9H_9N_4O_4^-$	0.3	C_3H_6O	Acetone, Propionaldehyde
2,3	239.042	$C_8H_7N_4O_5^-$	0.4	$C_2H_4O_2$	Acetic acid Glycoaldedehyde
14	249.063	$C_{10}H_9N_4O_4^-$	-0.5	C_4H_6O	Methacrolein
7	251.042	$C_9H_7N_4O_5^-$	-0.4	$C_3H_4O_2$	Methylglyoxal

13,15	251.078	$C_{10}H_{11}N_4O_4^-$	-0.3	C_4H_8O	Butyraldehyde or isobutyraldehyde, 2-Butanone
4,5	253.058	$C_9H_9N_4O_5^-$	1.0	$C_3H_6O_2$	Hydroxyacetone, Lactaldehyde or 1-hydroxypropal
10	265.058	$C_{10}H_9N_4O_5^-$	-0.2	$C_4H_6O_2$	Diacetyl
21	445.086	$C_{16}H_{13}N_8O_8^-$	0	$C_4H_6O_2$	Diacetyl
16	265.094	$C_{11}H_{13}N_4O_4^-$	-0.5	$C_5H_{10}O$	Valeraldehyde or isovaleraldehyde
19	279.110	$C_{12}H_{15}N_4O_4^-$	0.1	$C_6H_{12}O$	Hexanal or 4-methylpentanal
17	417.054	$C_{14}H_9N_8O_8^-$	0.2	$C_2H_2O_2$	Glyoxal
20	431.070	$C_{15}H_{11}N_8O_8^-$	-0.3	$C_3H_4O_2$	Methylglyoxal

Compound identified from both original and vaping aerosol of extracted THC oil

	309.185	$C_{21}H_{25}O_2^-$	0	$C_{21}H_{26}O_2$	Cannabinol (CBN)
48	313.218	$C_{21}H_{29}O_2^-$	0.3	$C_{21}H_{30}O_2$	Tetrahydrocannabinol (THC) Cannabidiol (CBD) Cannabichromene (CBC)
42,47	359.222	$C_{22}H_{31}O_4^-$	0.6	$C_{21}H_{30}O_2^a$ $C_{22}H_{32}O_4$	Tetrahydrocannabinol (THC) Cannabiglendol acid (CBGA)
52,53	357.206	$C_{22}H_{29}O_4^-$	-0.9	$C_{22}H_{30}O_4$	Tetrahydrocannabinol acid (THCA)
	315.233	$C_{21}H_{31}O_2^-$	0.5	$C_{21}H_{32}O_2$	Cannabigerol (CBG)

Compound identified from vaping aerosol of extracted THC oil

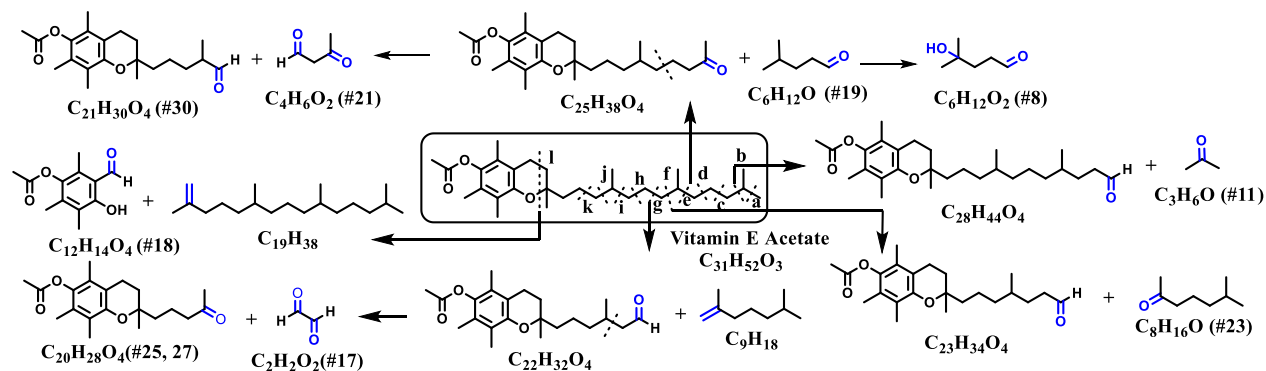
32	269.053	$C_9H_9N_4O_6^-$	-0.2	$C_3H_6O_3$	Dihydroxyacetone
45	293.126	$C_{13}H_{17}N_4O_4^-$	0.2	$C_7H_{14}O$	Heptanol
34	295.068	$C_{11}H_{11}N_4O_6^-$	-0.7	$C_5H_8O_3$	Proposed in Scheme 4.3
39,44,46,50,51	329.211	$C_{21}H_{29}O_3^-$	-0.7	$C_{21}H_{30}O_3$	Proposed in Scheme 4.3
35,40,43	331.227	$C_{21}H_{31}O_3^-$	-0.2	$C_{21}H_{32}O_3$	Proposed in Scheme 4.3
33	339.131	$C_{14}H_{19}N_4O_6^-$	0	$C_8H_{16}O_3$	Proposed in Scheme 4.3
36,38	345.207	$C_{21}H_{29}O_4^-$	-0.4	$C_{21}H_{30}O_4$	Proposed in Scheme 4.3
54	373.237	$C_{23}H_{33}O_4^-$	-0.6	$C_{23}H_{34}O_4$	10-ethoxy-9-hydroxy-THC
55,56	399.203	$C_{21}H_{27}N_4O_4^-$	-0.9	$C_{15}H_{24}O$	unidentified
49	399.290	$C_{26}H_{39}O_3^-$	-0.4	$C_{26}H_{40}O_3$	unidentified
41	425.147	$C_{21}H_{21}N_4O_6^-$	-0.1	$C_{15}H_{18}O_3$	Cannabispiran
37	303.196	$C_{19}H_{27}O_3^-$	-0.9	$C_{19}H_{28}O_3$	Cannabiglendol
	279.073	$C_{11}H_{11}N_4O_5^-$	-0.3	$C_5H_8O_2$	Proposed in Scheme 4.3
	423.131	$C_{21}H_{19}N_4O_6^-$	0	$C_{15}H_{16}O_3$	Cannabispirone-A
	321.120	$C_{14}H_{17}N_4O_5^-$	-0.4	$C_8H_{14}O_2$	Proposed in Scheme 4.3
	305.125	$C_{14}H_{17}N_4O_4^-$	-0.1	$C_8H_{14}O$	Proposed in Scheme 4.3

	325.181	$C_{21}H_{25}O_3^-$	-0.1	$C_{21}H_{26}O_3$	OH-Cannabinol
	347.223	$C_{21}H_{31}O_4^-$	-0.2	$C_{21}H_{32}O_4$	Proposed in Scheme 4.3
	367.118	$C_{21}H_{19}O_6^-$	-0.8	$C_{21}H_{20}O_6$	Cannflavin B
	377.233	$C_{22}H_{33}O_5^-$	0.1	$C_{21}H_{32}O_3^a$	Proposed in Scheme 4.3
	393.228	$C_{22}H_{33}O_6^-$	-0.6	$C_{21}H_{32}O_4^a$	Proposed in Scheme 4.3
	401.146	$C_{19}H_{21}N_4O_6^-$	-0.4	$C_{13}H_{18}O_3$	Proposed in Scheme 4.3
	415.162	$C_{20}H_{23}N_4O_6^-$	-0.3	$C_{14}H_{20}O_3$	unidentified
	507.224	$C_{27}H_{31}N_4O_6^-$	0.2	$C_{21}H_{28}O_3$	Proposed in Scheme 4.3
Compound identified from vaping aerosol of pure VEA					
8	295.105	$C_{12}H_{15}N_4O_5^-$	0	$C_6H_{12}O_2$	Proposed in Scheme 4.1
23	307.141	$C_{14}H_{19}N_4O_4^-$	-0.9	$C_8H_{16}O$	Proposed in Scheme 4.1
26	321.157	$C_{15}H_{21}N_4O_4^-$	-0.7	$C_9H_{18}O$	Proposed in Scheme 4.1
29	335.172	$C_{16}H_{23}N_4O_4^-$	-0.2	$C_{10}H_{20}O$	Proposed in Scheme 4.1
31	349.188	$C_{17}H_{25}N_4O_4^-$	0.2	$C_{11}H_{22}O$	Proposed in Scheme 4.1
24,28	377.219	$C_{19}H_{29}N_4O_4^-$	-0.9	$C_{13}H_{26}O$	Proposed in Scheme 4.1
18	401.110	$C_{18}H_{17}N_4O_7^-$	-0.2	$C_{12}H_{14}O_4$	Proposed in Scheme 4.1
22	483.189	$C_{24}H_{27}N_4O_7^-$	0.6	$C_{18}H_{24}O_4$	Proposed in Scheme 4.1
25,27	511.220	$C_{26}H_{31}N_4O_7^-$	0.7	$C_{20}H_{28}O_4$	Proposed in Scheme 4.1
30	525.236	$C_{27}H_{33}N_4O_7^-$	0.4	$C_{21}H_{30}O_4$	Proposed in Scheme 4.1
	469.173	$C_{23}H_{25}N_4O_7^-$	-0.6	$C_{17}H_{22}O_4$	Proposed in Scheme 4.1
	539.252	$C_{28}H_{35}N_4O_7^-$	0.7	$C_{22}H_{32}O_4$	Proposed in Scheme 4.1
	553.267	$C_{29}H_{37}N_4O_7^-$	0.6	$C_{23}H_{34}O_4$	Proposed in Scheme 4.1
	581.299	$C_{31}H_{41}N_4O_7^-$	1.3	$C_{25}H_{38}O_4$	Proposed in Scheme 4.1

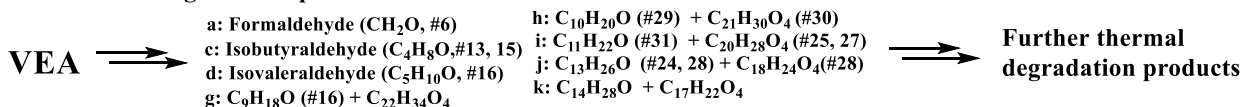
a: the detected ion is the cluster ion of molecule and $HCOO^-$

Over 30 thermal degradation products from VEA were identified. (**Fig. 4.2a**) All of the reported thermal degradation products from VEA are carbonyls/acids in this work, consistent with other accounts.⁹² Riordan-Short et al.⁹² also identified several esters and alkanes with GC-MS (confirmed by standard spectra in the NIST database). While around 10 carbonyls and acids (e.g., formaldehyde, isovaleraldehyde, acetic acid) are identified both by us and Riordan-Short et al.,⁹² carbonyls with VEA-specific structures (e.g., $C_{12}H_{14}O_4$ in **Table 4.1**) have only been identified in this work. The VEA-derived stable products are extremely informative for developing the proposed mechanism. The lack of standard spectra for these VEA-derived compounds in GC-MS libraries may have prevented identification of peaks in the chromatograms of Riordan-Short et al.

Moreover, some carbonyls identified by Riordan-Short et al. were not found in this work (e.g., 3,6-heptanedione). The cause for discrepancy is unknown; however, we hypothesize it may be partially due to the difference in vaporization method (ours using a heated coil in a third-generation vaping device, while Riordan-Short used a surrogate vaping environment).

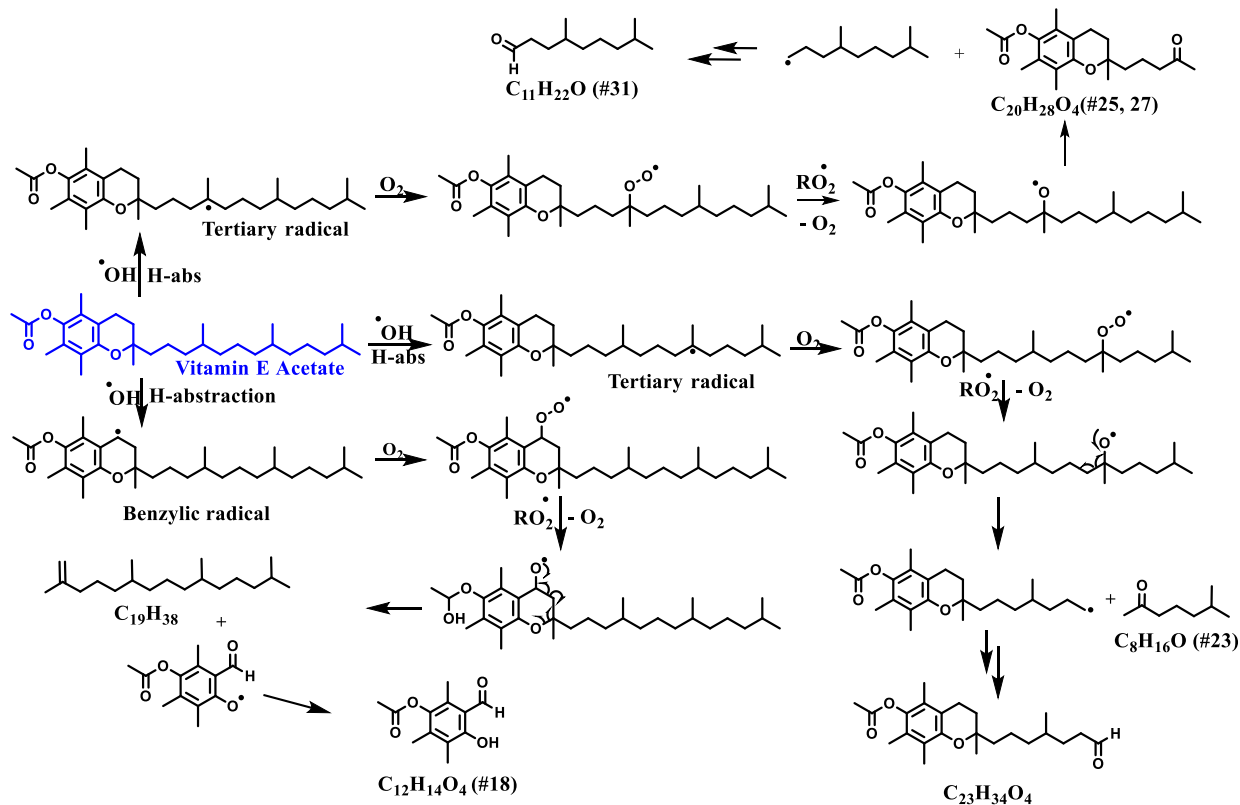


More thermal degradation products identified in Table 1



Scheme 4.1 Proposed oxidation and thermal degradation pathway of VEA. The corresponding peaks in Table 1 was labeled after the chemical formulas. The thermal degradation products C₁₇H₂₂O₄, C₂₂H₃₂O₄, C₂₃H₃₄O₄, C₂₅H₃₈O₄ was identified but not labeled in Figure 4.2 due to the relative small peak intensity.

Many smaller thermal degradation carbonyls and acids appear to be formed by oxidation and bond cleavage of the aliphatic side-chain of VEA. The bond cleavage pathways for VEA degradation is proposed in **Scheme 4.1**. A proposed radical reaction mechanism is shown in **Scheme 4.2**. The thermal degradation reaction is initiated by H-abstraction by radicals such as OH, followed by the rapid reaction with O₂ to form peroxy radicals (RO₂).^{310,311} The peroxy radical can react with other RO₂ (or reducing agents) to form carbonyls or alkoxy (RO) radicals.^{312,313} Alkoxy radicals may further react to form carbonyls (by β-scission), alcohols (by H-abstraction), and possibly alkenes (by H₂O elimination/radicals reaction).³¹³⁻³¹⁵ The primary thermal



Scheme 4.2 Proposed radical reaction mechanism for the thermal degradation of VEA. The corresponding peaks in Table 1 was labeled after the chemical formulas. The formation of most abundant peaks (peak 18 - $\text{C}_{12}\text{H}_{14}\text{O}_4$, 23 - $\text{C}_8\text{H}_{16}\text{O}$, 31 - $\text{C}_{11}\text{H}_{22}\text{O}$) from benzylic radical and tertiary radical were shown (cleavage bonds f, i, l in Scheme 4.1)

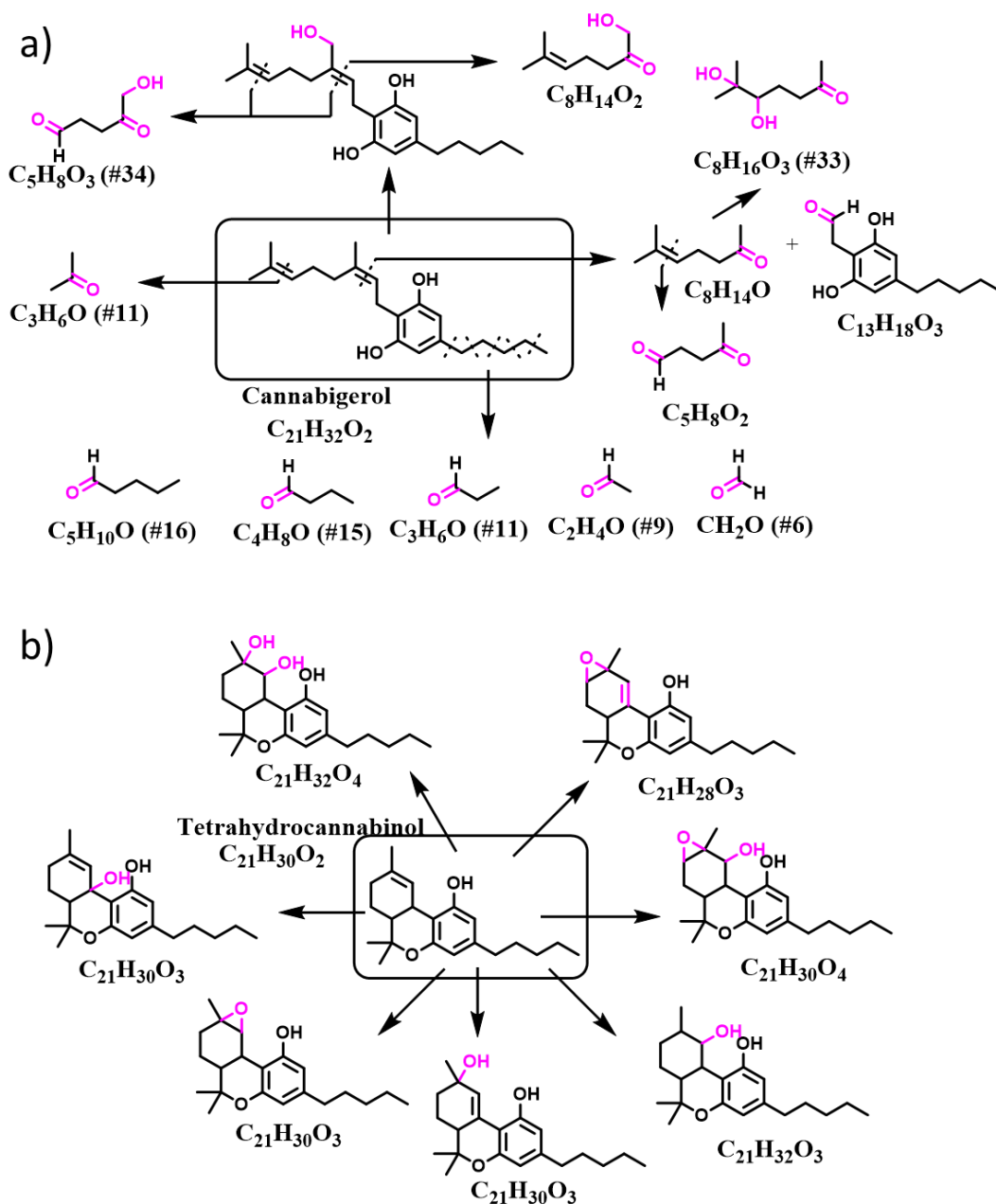
degradation products may go through further oxidation steps and form more thermal degradation products (e.g., dicarbonyl).³¹³ These RO_2 -based mechanisms have been well studied and shown to be important in various chemical systems, like the atmosphere, biological redox, or fuel combustion.³¹⁶⁻³¹⁹ The relative peak intensity of carbonyls in **Figure 4.2a** support the proposed radical reaction mechanism in **Scheme 4.2**, since the most abundant peaks (peak 18 - $\text{C}_{12}\text{H}_{14}\text{O}_4$, 23 - $\text{C}_8\text{H}_{16}\text{O}$, 31 - $\text{C}_{11}\text{H}_{22}\text{O}$) represented the formation of benzylic radical and tertiary radical formed in the first H-abstraction step (cleavage bonds f, i, l in **Scheme 4.1**) which can be stabilized by the conjugation effect from benzene ring and positive hyper-conjugation effect from the adjacent C-H bonds.³²⁰⁻³²² The proposed thermal degradation pathway is also supported by the

detection of alkanes, including 2,6-dimethyl-1-heptene and 1-pristene, by Riordan-Short et al.⁹² and Mikheev et al.,³²³ since these alkanes are generated in the proposed mechanism. Thus, our observations suggest that the C-C single bonds on the side-chain of VEA is easily oxidized and cleaved during the vaping process, which will cause the formation of a series of carbonyls that has VEA-specific structure, and also alkenes and alcohols. These primary products may go through further thermal degradation process to generate secondary thermal degradation products like acids and dicarbonyls. Regarding products like duroquinone, durohydroquinone and ketene that have been identified previously by vaping or heating VEA,^{70,93,324} we could not identify ketene as it will form the same adduct molecular structure as acetic acid when reacting with 2,4-DNPH. We did not observe duroquinone for unknown reasons, possibly due to the difference in sample collection and methods of detection.

Figure 4.2c shows the stacked SIC of vaping aerosol of THC oil. Besides thermal degradation carbonyl compounds, a large variety of cannabinoids was also identified by HPLC-HRMS, since the phenolic hydroxyl group in cannabinoid structure is slightly acidic and can also be deprotonated in the negative mode of ESI. The thermal degradation products identified in the vaping aerosol of extracted THC oil may not only be generated by THC, but can also be from the thermal degradation of other cannabinoids, such as cannabinol (CBN), cannabidiol (CBD), cannabichromene (CBC), cannabigerol (CBG) and corresponding acid (e.g., THCA), which have also been identified in the unvaped extracted THC oil. The mechanism of the production of carbonyls (e.g., formaldehyde, acetaldehyde, butyraldehyde) identified in the vaping aerosol of extracted THC oil may also involve the oxidation of the aliphatic side-chain followed by bond cleavage, since the main cannabinoids also have the side-chains with 5 carbons.

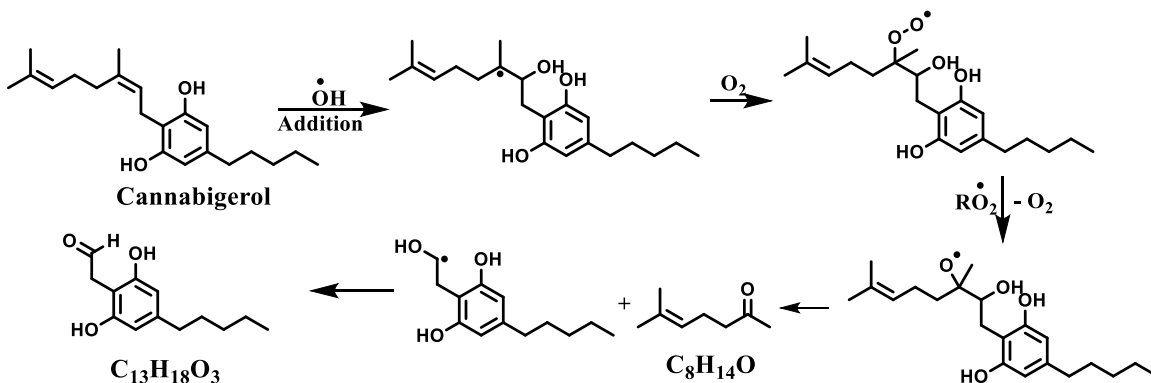
Moreover, CBG may be the source of certain carbonyl products (e.g., $C_5H_8O_3$, $C_8H_{14}O$) since it has a second side-chain with unsaturated bonds (**Scheme 4.3a**); the specific mechanism is shown in **Scheme 4.4**. In contrast to VEA, the oxidation of CBG by OH proceeds through addition to the double bonds in the side chain instead of H-abstraction, consistent with the oxidation of other alkenes.³²⁵⁻³²⁷ The mechanism for the following steps are similar to the H-abstraction route. The oxidation may also occur on the six member ring of cannabinoids such as THC can occur through pathways proposed in **Scheme 4.3b** and **Scheme 4.5**. For example, OH-initiated H-abstraction on THC can occur at the allylic site (forming a resonance-stabilized alkyl radical) and OH-addition can occur at the endocyclic C=C, preferentially forming the tertiary alkyl radical. Then peroxy radical (RO_2) chemistry occurs through similar pathways as VEA, finally generating alcohols and potentially epoxides. Multiple SIC peaks are found at the m/z representing oxidized products of cannabinoids, suggesting a lot of different isomers exist. Our identification results are similar to those of Carbone et al.,³⁰⁶ who utilized NMR for identification. Carbone et al. indicated peroxide products may also be formed during the oxidation process, a mechanism not shown in our schemes but would be consistent with RO_2 chemistry. The oxidation products shown in **Scheme 4.3b** have the same number of carbons as THC; however, some thermal degradation products with different carbon numbers (e.g., $C_{15}H_{16}O_3$, $C_{26}H_{40}O_3$) were also identified (**Table 4.1**) and are hard to trace back to precursor compounds. It is possible they may already exist in the original unvaped THC oil. Borille et al.³⁰⁹ found 123 cannabinoid compounds or metabolites and 8 non-cannabinoid constituents in the extracts of cannabis plants by ESI-MS, with carbon number of cannabinoids range from C_{15} to C_{55} . All molecular formulas of the THC oxidation products shown in **Scheme 4.3b** were also identified in cannabis extracts,³²⁸⁻³³³ suggesting that these components may already exist in the cannabis plant, and that oxidation from plant metabolism or during extraction could

have occurred in addition to vaping. Moreover, the $C_{19}H_{28}O_3$ has been identified as Cannabiglendol- C_3 (8-hydroxy-isohexahydrocannabivarinor);^{309,328} and there exist many possibilities for $C_{23}H_{34}O_4$ (e.g., cannabigerolic acid monomethyl ether or 10-ethoxy-9-



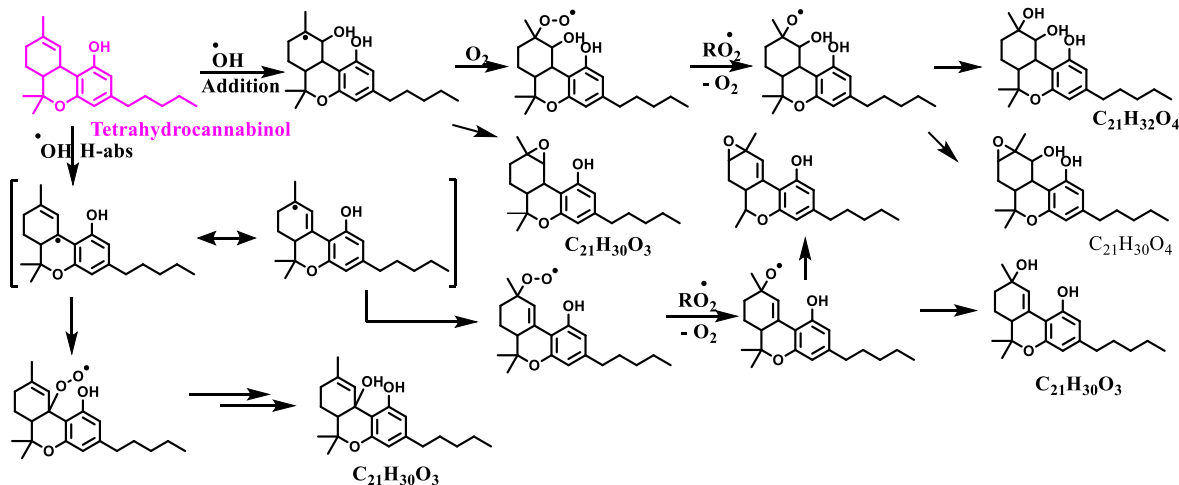
Scheme 4.3 Proposed oxidation and thermal degradation pathway of CBG and THC. The corresponding peaks of carbonyls in Table 1 was labeled after the chemical formulas. The thermal degradation carbonyl products $C_8H_{14}O$, $C_8H_{14}O_2$, $C_5H_8O_2$, $C_{13}H_{18}O_3$ were identified but not labeled in Figure 4.2 due to the relative small peak intensity. The peaks of cannabinoids cannot be labeled due to the existence of isomers.

hydroxytetrahydrocannabinol);^{309, 334} C₁₅H₁₆O₃/C₁₅H₁₈O₃ had been identified as cannabispirenone/cannabispiran.^{335,336} Some compounds in **Table 4.1** still remains unidentified (e.g., C₂₆H₄₀O₃).



Scheme 4.4 Proposed radical reaction mechanism for the thermal degradation of CBG.

Besides the oxidation products from vaping THC oil, for which the oxidation mechanism is described in **Scheme 4.3**, there remains unexplained formation pathway for the generation of some thermal degradation products (e.g., hexanal, diacetyl). Couch et al.^{337,338} found the risk of exposure to VOC including diacetyl and 2,3-pentanedione during the decarboxylation and grinding process of dried cannabis material, but there is no clear mechanism given for their formation. The generation of these compounds may due to the thermal degradation of terpenes and terpenoids



Scheme 4.5 Proposed radical reaction mechanism for the thermal degradation of THC.

(e.g., limonene, myrcene, linalool, alpha-pinene). Since there is still over 50% mass in the unvaped THC oil that remains uncharacterized, it is likely that a portion of that mass are terpenes.^{308, 339-341} Meehan-Atrash et al.⁹⁸ identified degradation products from myrcene, limonene and linalool, including methacrolein, hydroxyacetone, methyl vinyl ketone.⁹⁴ Tang et al.⁹⁷ found 11 thermal degradation products from mixture of terpenoids, 7 of them are carbonyls including formaldehyde, acetaldehyde, acetone, acrolein, methacrolein, valeraldehyde and hexanal. These findings are consistent with the identification results in this work, illustrating that the extracted THC oil is a complex mixture, the complexity of which increases with thermal degradation chemistry. Further research on individual components is still needed for a better understanding on the whole picture of thermal degradation.

For the mixture of THC oil and VEA, it is clear from the stacked SIC (**Fig. 4.2b**) that the peaks shown in the chromatograph are mainly from aerosolization products of vaped THC oil instead of VEA. It is clear that the total signal from aerosolization products of the mixture is between that of vaping pure VEA and THC oil. Moreover, the oxidation of THC may also be suppressed by adding of VEA. While the signal ratio of cannabinoids (THC, THCA, CBG, CBD, CBC) in vaping aerosol of the mixture (**Fig. 4.2b**) compared to unvaped THC oil (**Fig. 4.2c**) is 0.34, the same ratio for oxidated cannabinoids in **Scheme 4.3b** is 0.22 (**Scheme 4.5**). THC was shown to

Table 4.2. Particle mass collected on Cambridge Filter Pad by vaping VEA, VEA/extracted THC oil, and extracted THC oil. Low temperature range is 315 ± 10 °F (157 °C), medium temperature range is 455 ± 10 °F (235 °C), high temperature range is 545 ± 10 °F (285 °C). N.D. = not detected, the high temperature data for THC is unavailable.

	THC (mg/puff)	THC/VEA (mg/puff)	VEA (mg/puff)
Low temperature	1.2 ± 0.2	N.D	N.D
Medium temperature	10.8 ± 1	1.5 ± 0.2	0.8 ± 0.1
High temperature	-	5 ± 1	2.7 ± 0.3

have a stronger tendency to degrade compared to VEA, since the boiling point for THC is 157 °C, while VEA start to decay at 240 °C without boiling.³⁴²⁻³⁴⁴

Table 4.2 shows the particle mass collected on the glass fiber filter at three temperatures and various e-liquid composition. It is clear that increasing temperature will increase the particle mass on the filter, which is consistent with expectations.^{141,165} However, the particle mass production is non-linearly suppressed with the addition of VEA compared to THC oil at the same temperature. The reason might be the formation of non-ideal solution with significant intermolecular

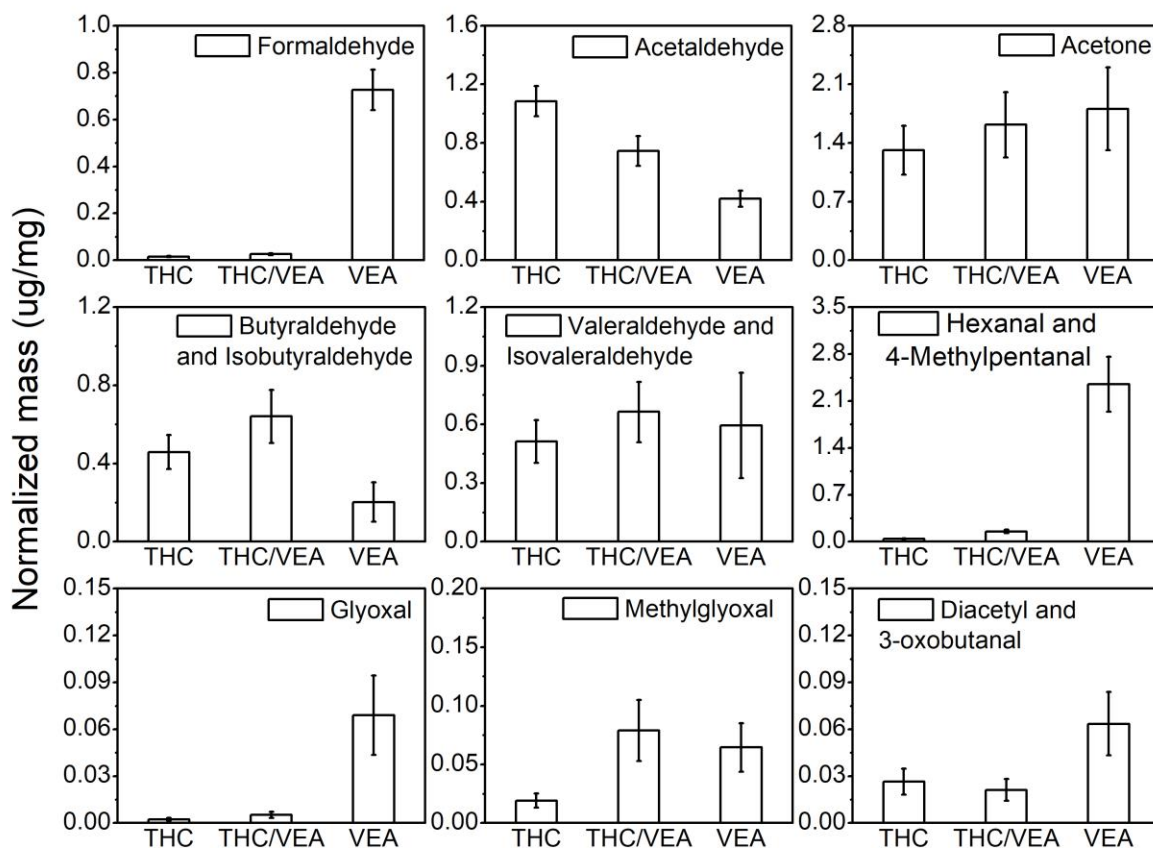


Figure 4.3 The normalized mass of thermal degradation carbonyl compounds by particle mass collected on Cambridge Filter Pad by vaping VEA, extracted THC oil and their mixture at 455 ± 10°F (235 °C).

interactions when VEA is added to the THC oil, as Lanzarotta et al.³⁰³ had found that hydrogen bonding exists between the molecules of VEA and THC. Given the fact that THC has a much higher aerosolization rate compared to VEA (10:1 at 455 °F), the cartridge may be enriched in VEA since vaping continues until it is 100% VEA.

In order to figure out the influence of VEA to the formation of carbonyls, it is informative to normalize the mass of carbonyls by the particle mass collected (**Table 4.2**) at the same temperature (455 °F). While e-cigarette users who used nicotine products will self-titrate nicotine intake in daily use,^{173,172} there is also evidence that people who use higher potency cannabis for recreational purpose can titrate their THC dose.³⁴⁵ **Figure 4.4** shows the normalized mass of 9 thermal degradation carbonyl compounds by particle mass produced from vaping VEA, THC oil and their mixture at 455 ± 10 °F (235 °C). Within the C₄ – C₆ carbonyls shown in **Figure 4.4**, butyraldehyde, valeraldehyde, hexanal are thought to be from the thermal degradation of cannabinoids and terpenes (**Scheme 4.3**), supported by Tang et al.,⁹⁷ while isobutyraldehyde, isovaleraldehyde and 4-methylpentanal are from the thermal degradation of VEA (**Scheme 4.1**), supported by Riordan-Short et al.⁹² Since some isomers (e.g., butyraldehyde vs. isobutyraldehyde) can't be separated in this work, we discuss the pair of isomers together.

From the normalized carbonyl concentration, it is clear that certain carbonyls such as formaldehyde, hexanal/4-methylpentanal, glyoxal, diacetyl/3-oxobutanal are produced in much higher abundance from VEA compared to extracted THC oil. Although some products like formaldehyde can be produced from both VEA and THC, the production of formaldehyde from VEA is more favorable since it involves a tertiary radical intermediate in the first step (**Scheme 4.2**), which is more stable than the secondary radicals formed from the side-chain of THC.^{346,245}

The proposed chemistry is, thus, consistent with higher formaldehyde formation by VEA. The same explanation can also apply to the generation of 4-methylpentanal, which only comes from VEA and thus likely dominates the distribution of the isomer pair over hexanal. The formation of glyoxal, diacetyl and 3-oxobutanal from VEA likewise may be enhanced compared to THC due to higher stability of radical intermediates. Diacetyl is thought to be byproducts of cannabis plants,⁶¹ and there is no clear indication of formation of diacetyl from VEA (**Scheme 4.3**). The formation of its isomer 3-oxobutanal can be expected from VEA, however. The corresponding SIC of diacetyl shows that multiple peaks (isomers) exists in the vaping aerosol of extracted THC oil, but only one peak shown in the vaping aerosol of pure VEA, suggesting that cannabinoids and terpenes may generate multiple isomers which have the same m/z as diacetyl, but VEA probably generates only 3-oxobutanal. Since the diacetyl/3-oxobutanal pair is slightly enhanced with VEA, this is in agreement with the fact that they are from different origins and both isomers are formed when VEA and THC are vaped together. In some cases, the mixture produced more carbonyl emissions compared to the pure compounds (e.g., Butyraldehyde/isobutyraldehyde, valeraldehyde/isovaleraldehyde, methylglyoxal). Although this trend is less clear within error, it may suggest some synergetic effects between THC and VEA. Moreover, the THC oil tend to produce higher acetaldehyde than VEA, which is also understandable, since the proposed thermal degradation pathway of VEA cannot explain the formation of acetaldehyde but there are reasonable pathways from cannabinoids such as CBG (**Scheme 4.3a**). More research is needed for further understanding of the thermal degradation chemistry of VEA and THC.

Chapter 5. Conclusion

In this dissertation, a series of studies were conducted to examine the aerosolization and thermal degradation chemistry of electronic cigarettes with the e-liquid with the composition of PG/VG/nicotine and VEA/THC oil. The most important method developed in this dissertation unambiguously identified and quantified carbonyl compounds, acids, and potentially cannabinoids in e-cigarettes aerosol using HPLC-HRMS. The method includes a theoretical chemistry model that is developed for the prediction of sensitivities of deprotonation-based electrospray ionization for carbonyls and acids for which analytical standards (corresponding DNPH hydrazones) are unavailable commercially. The initial investigation identified and quantified 19 carbonyl compounds and acids from the vaping aerosol of the 1st generation e-cigarettes, which includes thermal degradation products from PG and VG, as well as flavoring chemicals and acid additives. Hydroxycarbonyls such as hydroxyacetone, lactaldehyde, and dihydroxyacetone, not quantified in the majority of previous e-cigarette research, were found to be significant thermal degradation products in the e-cigarette aerosol. To date, the inhalation toxicology of these hydroxycarbonyls is still unknown, which emphasizes the need for more research on the toxicology of complex products formed in vaping. The characterization of flavoring chemicals in this work shows the potential application of the HRMS method to other flavored e-cigarettes, as a large variety of flavoring chemical are carbonyls and the specific flavoring additives are proprietary.

In addition to carbonyls and acids, the composition of e-cigarette aerosol (both particle and gas phase) as well as the relationship between the e-cigarette emissions and vaping parameters (e.g., coil temperature, e-liquid composition, puff duration) are also important for the systematic evaluation of health risks associated with e-cigarette use. A GC-MS method was developed for the

quantification of PG, VG and nicotine in the particle phase of e-cigarette aerosol, while the gas phase composition was quantified by CIMS. An exponential relationship was found between the generated particle mass and measured coil temperatures, which is different than the temperatures set by the vaping device. The mass loss of e-liquid was found mainly distributed in the gas phase, and the PG fraction in the gas phase is significantly higher than the particle phase which may due to the their volatility difference. The PG:VG fraction in the particle phase is close to that from the original e-liquid. Moreover, a general exponential trend was also found between the generated carbonyl mass and the measured temperatures, while some carbonyls (e.g., formaldehyde, hydroxyacetone, acetaldehyde, lactaldehyde/1-hydroxypropanal, acrolein and propionaldehyde) were shown to have a steeper exponential relationship than others (e.g., acetone, dihydroxyacetone and glyceraldehyde). Accordingly, two possible mechanism were proposed for the thermal degradation of PG and VG including a thermal dehydration pathway and radical reaction pathway. The thermal dehydration pathway was shown to be the main mechanism within the temperature range used for e-cigarettes. The total mass loss of e-liquid and the generated particle mass both decreased with increasing VG fraction. Some carbonyl compounds (e.g., hydroxyacetone, lactaldehyde/1-hydroxypropanal, acrolein, and dihydroxyacetone) are mainly or entirely generated from VG, while others (e.g. propionaldehyde, acetaldehyde) are mainly or entirely generated from PG. E-cigarette emissions (particle mass and representative carbonyls) have a linear-like relationship with the puff duration (when puff volume is not controlled) within the range of 2 – 4 s.

In addition, the e-liquid of THC oil with VEA added as diluent was also tested for aerosolization and thermal degradation chemistry under different vaping parameters. It was shown adding VEA

suppressed the generation of particle mass at a higher efficiency than its volume fraction would indicate, suggesting that the THC and VEA mixture forms a non-ideal solution with significant intermolecular interactions. Moreover, VEA and the ingredients in THC oil (e.g., cannabinoids and terpenes) can also degrade into different thermal degradation products including carbonyls, acids and oxidative cannabinoids. A radical reaction mechanism was proposed for the thermal degradation of VEA and THC. The stability of the alkyl radicals formed in the initial step of OH-initiated reaction is critical to the generation of final products. Multiple carbonyls were quantified and normalized by the generated particle mass in different e-liquid ratios of THC oil and VEA. The results show that some carbonyls (e.g., formaldehyde, 4-methylpentanal, and glyoxal) were mainly generated by thermal degradation of VEA, which also emphasize the need of further research to better understand the chemistry of cannabis vaping with different diluents as the cannabis vaping market size has been growing rapidly.

In conclusion, this dissertation utilized a systematic approach to research on the aerosolization and thermal degradation chemistry of different e-cigarettes and e-liquids. The findings suggest that, although e-cigarettes have been regarded as safe alternatives for traditional smoking worldwide, the health risk of e-cigarettes use should to be evaluated in further detail and more toxicology investigations are needed to enable exposure risk estimation of exposure to specific compounds as well as complex mixtures that can be formed during the vaping process.

Reference

1. Administration, T. U. S. F. a. D., Vaporizers, E-Cigarettes, and other Electronic Nicotine Delivery Systems (ENDS). **2020**.
2. Strongin, R. M., E-cigarette chemistry and analytical detection. *Annual Review of Analytical Chemistry* **2019**, *12*, 23-39.
3. Malas, M.; van der Tempel, J.; Schwartz, R.; Minichiello, A.; Lightfoot, C.; Noormohamed, A.; Andrews, J.; Zawertailo, L.; Ferrence, R., Electronic cigarettes for smoking cessation: a systematic review. *Nicotine and Tobacco Research* **2016**, *18* (10), 1926-1936.
4. Bozier, J.; Chivers, E. K.; Chapman, D. G.; Larcombe, A. N.; Bastian, N. A.; Masso-Silva, J. A.; Byun, M. K.; McDonald, C. F.; Alexander, L. E. C.; Ween, M. P., The evolving landscape of e-cigarettes: a systematic review of recent evidence. *Chest* **2020**, *157* (5), 1362-1390.
5. Williams, M.; Talbot, P., Design features in multiple generations of electronic cigarette atomizers. *International Journal of Environmental Research and Public Health* **2019**, *16* (16), 2904.
6. Williams, M.; Li, J.; Talbot, P., Effects of model, method of collection, and topography on chemical elements and metals in the aerosol of tank-style electronic cigarettes. *Scientific Reports* **2019**, *9* (1), 1-14.
7. Hoffmann, D. H., Ilse, The changing cigarette, 1950-1995. *Journal of Toxicology and Environmental Health Part A* **1997**, *50* (4), 307-364.
8. Cottrell, J. C.; Sohn, S. S.; Vogel, W. H., Toxic effects of marihuana tar on mouse skin. *Archives of Environmental Health: An International Journal* **1973**, *26* (5), 277-278.
9. Benowitz, N. L.; Jacob III, P.; Kozlowski, L. T.; Yu, L., Influence of smoking fewer cigarettes on exposure to tar, nicotine, and carbon monoxide. *New England Journal of Medicine* **1986**, *315* (21), 1310-1313.
10. Chen, C.; Zhuang, Y.-L.; Zhu, S.-H., E-cigarette design preference and smoking cessation: a US population study. *American Journal of Preventive Medicine* **2016**, *51* (3), 356-363.
11. Zhuang, Y.-L.; Cummins, S. E.; Sun, J. Y.; Zhu, S.-H., Long-term e-cigarette use and smoking cessation: a longitudinal study with US population. *Tobacco Control* **2016**, *25* (Suppl 1), i90-i95.
12. Wang, R. J.; Bhadriraju, S.; Glantz, S. A., E-cigarette use and adult cigarette smoking cessation: a meta-analysis. *American Journal of Public Health* **2021**, *111* (2), 230-246.
13. Tan, A. S.; Bigman, C. A., E-cigarette awareness and perceived harmfulness: prevalence and associations with smoking-cessation outcomes. *American Journal of Preventive Medicine* **2014**, *47* (2), 141-149.
14. Margham, J.; McAdam, K.; Forster, M.; Liu, C.; Wright, C.; Mariner, D.; Proctor, C., Chemical composition of aerosol from an e-cigarette: a quantitative comparison with cigarette smoke. *Chemical Research in Toxicology* **2016**, *29* (10), 1662-1678.
15. Dutra, L. M.; Grana, R.; Glantz, S. A., Philip Morris research on precursors to the modern e-cigarette since 1990. *Tobacco Control* **2017**, *26* (e2), e97-e105.
16. Dautzenberg, B.; Birkui, P.; Noël, M.; Dorsett, J.; Osman, M.; Dautzenberg, M.-D., E-cigarette: a new tobacco product for schoolchildren in Paris. *Open J Respir Dis* **2013**, *3* (1), 21-4.
17. Demick, B., A high-tech approach to getting a nicotine fix. *Los Angeles Times* **2009**, *25*.
18. Hiemstra, P. S.; Bals, R., Basic science of electronic cigarettes: assessment in cell culture and in vivo models. *Respiratory Research* **2016**, *17*{Hiemstra, 2016 #611} (1), 1-5.
19. Yingst, J. M.; Veldheer, S.; Hrabovsky, S.; Nichols, T. T.; Wilson, S. J.; Foulds, J., Factors associated with electronic cigarette users' device preferences and transition from first generation to advanced generation devices. *Nicotine & Tobacco Research* **2015**, *17* (10), 1242-1246.

20. Dawkins, L.; Kimber, C.; Puwanesarasa, Y.; Soar, K., First-versus second-generation electronic cigarettes: predictors of choice and effects on urge to smoke and withdrawal symptoms. *Addiction* **2015**, *110* (4), 669-677.
21. Chen, W.; Wang, P.; Ito, K.; Fowles, J.; Shusterman, D.; Jaques, P. A.; Kumagai, K., Measurement of heating coil temperature for e-cigarettes with a “top-coil” clearomizer. *PloS One* **2018**, *13* (4), e0195925.
22. Pearson, J. L.; Reed, D. M.; Villanti, A. C., Vapes, e-cigs, and mods: What do young adults call e-cigarettes? *Nicotine and Tobacco Research* **2020**, *22* (5), 848-852.
23. Galstyan, E.; Galimov, A.; Sussman, S., Commentary: the emergence of pod mods at vape shops. *Evaluation & the health professions* **2019**, *42* (1), 118-124.
24. Gieringer, D.; St. Laurent, J.; Goodrich, S., Cannabis vaporizer combines efficient delivery of THC with effective suppression of pyrolytic compounds. *Journal of Cannabis Therapeutics* **2004**, *4* (1), 7-27.
25. Raber, J. C.; Elzinga, S.; Kaplan, C., Understanding dabs: contamination concerns of cannabis concentrates and cannabinoid transfer during the act of dabbing. *The Journal of Toxicological Sciences* **2015**, *40* (6), 797-803.
26. Meehan-Atrash, J.; Luo, W.; McWhirter, K. J.; Strongin, R. M., Aerosol gas-phase components from cannabis e-cigarettes and Dabbing: mechanistic insight and quantitative risk analysis. *ACS Omega* **2019**, *4* (14), 16111-16120.
27. Securities, W. F., Nielsen: Tobacco All Channel Data Cig Pricing Remains Strong; E-Cig \$ Sales Growth Re-Accelerates. *Equity Research. San Francisco, CA: Wells Fargo Securities* **2015**.
28. Singh, T.; Arrazola, R. A.; Corey, C. G.; Husten, C. G.; Neff, L. J.; Homa, D. M.; King, B. A., Tobacco use among middle and high school students—United States, 2011–2015. *Morbidity and Mortality Weekly Report* **2016**, *65* (14), 361-367.
29. Wang, T. W.; Neff, L. J.; Park-Lee, E.; Ren, C.; Cullen, K. A.; King, B. A., E-cigarette use among middle and high school students—United States, 2020. *Morbidity and Mortality Weekly Report* **2020**, *69* (37), 1310.
30. DeVito, E. E.; Krishnan-Sarin, S., E-cigarettes: impact of e-liquid components and device characteristics on nicotine exposure. *Current Neuropharmacology* **2018**, *16* (4), 438-459.
31. Qu, Y.; Kim, K.-H.; Szulejko, J. E., The effect of flavor content in e-liquids on e-cigarette emissions of carbonyl compounds. *Environ. Res.* **2018**, *166*, 324-333.
32. Jacob, S. E.; Scheman, A.; McGowan, M. A., Propylene glycol. *Dermatitis* **2018**, *29* (1), 3-5.
33. Hasegawa, N.; Kamiya, A.; Matsunaga, T.; Kitano, N.; Harada, M., Analysis of crack formation during fuel cell catalyst ink drying process. Reduction of catalyst layer cracking by addition of high boiling point solvent. *Colloids and Surfaces A: Physicochemical and Engineering Aspects* **2021**, 127153.
34. Wilson, K. C.; Reardon, C.; Theodore, A. C.; Farber, H. W., Propylene glycol toxicity: a severe iatrogenic illness in ICU patients receiving IV benzodiazepines: a case series and prospective, observational pilot study. *Chest* **2005**, *128* (3), 1674-1681.
35. Zar, T.; Graeber, C.; Perazella, M. A. In *Reviews: recognition, treatment, and prevention of propylene glycol toxicity*, Seminars in Dialysis, Wiley Online Library: 2007; pp 217-219.
36. Lim, T. Y.; Poole, R. L.; Pageler, N. M., Propylene glycol toxicity in children. *The Journal of Pediatric Pharmacology and Therapeutics* **2014**, *19* (4), 277-282.
37. Christoph, R.; Schmidt, B.; Steinberner, U.; Dilla, W.; Karinen, R., Glycerol. *Ullmann's Encyclopedia of Industrial Chemistry* **2000**.
38. Lide, D. R.; Milne, G. W. A., *CRC handbook of data on organic compounds*. CRC Press: 1993.
39. Crupi, V.; Longo, F.; Majolino, D.; Venuti, V., The hydrogen-bond network in propylene-glycol studied by Raman spectroscopy. *J. Mol. Struct.* **2006**, *790* (1-3), 141-146.
40. Li, Y.; Burns, A. E.; Burke, G. J.; Poindexter, M. E.; Madl, A. K.; Pinkerton, K. E.; Nguyen, T. B., Application of High-Resolution Mass Spectrometry and a Theoretical Model to the Quantification of

Multifunctional Carbonyls and Organic Acids in e-Cigarette Aerosol. *Environ. Sci. Technol.* **2020**, *54* (9), 5640-5650.

41. Li, Y.; Burns, A. E.; Tran, L. N.; Abellar, K. A.; Poindexter, M.; Li, X.; Madl, A. K.; Pinkerton, K. E.; Nguyen, T. B., Impact of e-Liquid Composition, Coil Temperature, and Puff Topography on the Aerosol Chemistry of Electronic Cigarettes. *Chemical Research in Toxicology* **2021**.

42. Spindle, T. R.; Talih, S.; Hiler, M. M.; Karaoghlanian, N.; Halquist, M. S.; Breland, A. B.; Shihadeh, A.; Eissenberg, T., Effects of electronic cigarette liquid solvents propylene glycol and vegetable glycerin on user nicotine delivery, heart rate, subjective effects, and puff topography. *Drug and Alcohol Dependence* **2018**, *188*, 193-199.

43. Fagerström, K., Nicotine: pharmacology, toxicity and therapeutic use. *Journal of Smoking Cessation* **2014**, *9* (2), 53-59.

44. Millar, N.; Gotti, C.; Marks, M.; Wonnacott, S., Nicotinic acetylcholine receptors, introduction. *IUPHAR/BPS Guide to PHARMACOLOGY, guidetopharmacology.org/GRAC/FamilyIntroductionForward* **2014**.

45. Kishioka, S.; Kiguchi, N.; Kobayashi, Y.; Saika, F., Nicotine effects and the endogenous opioid system. *Journal of Pharmacological Sciences* **2014**, *125* (2), 117-124.

46. Cameron, J. M.; Howell, D. N.; White, J. R.; Andrenyak, D. M.; Layton, M. E.; Roll, J. M., Variable and potentially fatal amounts of nicotine in e-cigarette nicotine solutions. *Tobacco Control* **2014**, *23* (1), 77-78.

47. Cheng, T., Chemical evaluation of electronic cigarettes. *Tobacco Control* **2014**, *23* (suppl 2), ii11-ii17.

48. Etter, J. F.; Zäther, E.; Svensson, S., Analysis of refill liquids for electronic cigarettes. *Addiction* **2013**, *108* (9), 1671-1679.

49. Goniewicz, M. L.; Kuma, T.; Gawron, M.; Knysak, J.; Kosmider, L., Nicotine levels in electronic cigarettes. *Nicotine & Tobacco Research* **2013**, *15* (1), 158-166.

50. Wölkart, G.; Kollau, A.; Stessel, H.; Russwurm, M.; Koesling, D.; Schrammel, A.; Schmidt, K.; Mayer, B., Effects of flavoring compounds used in electronic cigarette refill liquids on endothelial and vascular function. *PLoS One* **2019**, *14* (9), e0222152.

51. Gillman, I. G.; Pennington, A. S.; Humphries, K. E.; Oldham, M. J., Determining the impact of flavored e-liquids on aldehyde production during Vaping. *Regulatory Toxicology and Pharmacology* **2020**, *112*, 104588.

52. Clapp, P. W.; Pawlak, E. A.; Lackey, J. T.; Keating, J. E.; Reeber, S. L.; Glish, G. L.; Jaspers, I., Flavored e-cigarette liquids and cinnamaldehyde impair respiratory innate immune cell function. *American Journal of Physiology-Lung Cellular and Molecular Physiology* **2017**, *313* (2), L278-L292.

53. Allen, J. G.; Flanigan, S. S.; LeBlanc, M.; Vallarino, J.; MacNaughton, P.; Stewart, J. H.; Christiani, D. C., Flavoring chemicals in e-cigarettes: diacetyl, 2, 3-pentanedione, and acetoin in a sample of 51 products, including fruit-, candy-, and cocktail-flavored e-cigarettes. *Environmental health perspectives* **2016**, *124* (6), 733-739.

54. Rosbrook, K.; Green, B. G., Sensory effects of menthol and nicotine in an e-cigarette. *Nicotine & Tobacco Research* **2016**, *18* (7), 1588-1595.

55. Pankow, J. F., Calculating compound dependent gas-droplet distributions in aerosols of propylene glycol and glycerol from electronic cigarettes. *J. Aerosol Sci* **2017**, *107*, 9-13.

56. Krüsemann, E. J.; Pennings, J. L.; Cremers, J. W.; Bakker, F.; Boesveldt, S.; Talhout, R., GC-MS analysis of e-cigarette refill solutions: A comparison of flavoring composition between flavor categories. *J. Pharm. Biomed. Anal.* **2020**, *188*, 113364.

57. Tierney, P. A.; Karpinski, C. D.; Brown, J. E.; Luo, W.; Pankow, J. F., Flavour chemicals in electronic cigarette fluids. *Tobacco Control* **2016**, *25* (e1), e10-e15.

58. Behar, R. Z.; Luo, W.; McWhirter, K. J.; Pankow, J. F.; Talbot, P., Analytical and toxicological evaluation of flavor chemicals in electronic cigarette refill fluids. *Scientific Reports* **2018**, *8* (1), 1-11.
59. Rose, C. S., Early detection, clinical diagnosis, and management of lung disease from exposure to diacetyl. *Toxicology* **2017**, *388*, 9-14.
60. Khlystov, A.; Samburova, V., Flavoring compounds dominate toxic aldehyde production during e-cigarette vaping. *Environ. Sci. Technol.* **2016**, *50* (23), 13080-13085.
61. Seeman, J. I.; Fournier, J. A.; Paine, J. B.; Waymack, B. E., The form of nicotine in tobacco. Thermal transfer of nicotine and nicotine acid salts to nicotine in the gas phase. *J. Agric. Food. Chem.* **1999**, *47* (12), 5133-5145.
62. Jenssen, B. P.; Wilson, K. M., What is new in electronic-cigarettes research? *Current Opinion in Pediatrics* **2019**, *31* (2), 262.
63. Voos, N.; Goniewicz, M. L.; Eissenberg, T., What is the nicotine delivery profile of electronic cigarettes? *Expert Opinion on Drug Delivery* **2019**, *16* (11), 1193-1203.
64. Marks, M. D.; Tian, L.; Wenger, J. P.; Omburo, S. N.; Soto-Fuentes, W.; He, J.; Gang, D. R.; Weiblen, G. D.; Dixon, R. A., Identification of candidate genes affecting Δ^9 -tetrahydrocannabinol biosynthesis in *Cannabis sativa*. *J. Exp. Bot.* **2009**, *60* (13), 3715-3726.
65. Meier, M. H.; Docherty, M.; Leischow, S. J.; Grimm, K. J.; Pardini, D., Cannabis concentrate use in adolescents. *Pediatrics* **2019**, *144* (3).
66. Bidwell, L. C.; YorkWilliams, S. L.; Mueller, R. L.; Bryan, A. D.; Hutchison, K. E., Exploring cannabis concentrates on the legal market: User profiles, product strength, and health-related outcomes. *Addictive Behaviors Reports* **2018**, *8*, 102-106.
67. Czégény, Z.; Nagy, G.; Babinszki, B.; Bajtel, Á.; Sebestyén, Z.; Kiss, T.; Csupor-Löffler, B.; Tóth, B.; Csupor, D., CBD, a precursor of THC in e-cigarettes. *Scientific Reports* **2021**, *11* (1), 1-6.
68. Cooray, R.; Gupta, V.; Suphioglu, C., Current aspects of the endocannabinoid system and targeted THC and CBD phytocannabinoids as potential therapeutics for Parkinson's and Alzheimer's diseases: a review. *Molecular Neurobiology* **2020**, *57* (11), 4878-4890.
69. Chan, G. C.; Hall, W.; Freeman, T. P.; Ferris, J.; Kelly, A. B.; Winstock, A., User characteristics and effect profile of Butane Hash Oil: An extremely high-potency cannabis concentrate. *Drug and alcohol dependence* **2017**, *178*, 32-38.
70. Jiang, H.; Ahmed, C. S.; Martin, T. J.; Canchola, A.; Oswald, I. W.; Garcia, J. A.; Chen, J. Y.; Koby, K. A.; Buchanan, A. J.; Zhao, Z., Chemical and toxicological characterization of vaping emission products from commonly used vape juice diluents. *Chemical Research in Toxicology* **2020**, *33* (8), 2157-2163.
71. Redtenbacher, J., Ueber die zerlegungsprodukte des glyceryloxydes durch trockene destillation. *Justus Liebigs Annalen der Chemie* **1843**, *47* (2), 113-148.
72. Nef, J., Dissociation processes in the glycol-glycerine sequence. *Justus Liebigs Ann. Chem* **1904**, *335*, 191-245.
73. Hafner, K.; Schulz, U.; Wagner, K., *Justus Liebigs Ann. Chem. Ann. Chem* **1964**, *678*, 39-53.
74. Jensen, R. P.; Strongin, R. M.; Peyton, D. H., Solvent chemistry in the electronic cigarette reaction vessel. *Scientific reports* **2017**, *7* (1), 1-11.
75. Laino, T.; Tuma, C.; Curioni, A.; Jochowitz, E.; Stolz, S., A revisited picture of the mechanism of glycerol dehydration. *The Journal of Physical Chemistry A* **2011**, *115* (15), 3592-3595.
76. Laino, T.; Tuma, C.; Moor, P.; Martin, E.; Stolz, S.; Curioni, A., Mechanisms of propylene glycol and triacetin pyrolysis. *The Journal of Physical Chemistry A* **2012**, *116* (18), 4602-4609.
77. Díaz, E.; Sad, M. E.; Iglesia, E., Homogeneous oxidation reactions of propanediols at low temperatures. *ChemSusChem* **2010**, *3* (9), 1063-1070.
78. Stein, Y. S.; Antal Jr, M. J.; Jones jr, M., A study of the gas-phase pyrolysis of glycerol. *Journal of Analytical and Applied Pyrolysis* **1983**, *4* (4), 283-296.

79. Antal Jr, M.; Mok, W.; Roy, J.; Anderson, D., Pyrolytic sources of hydrocarbons from biomass. *Journal of Analytical and Applied Pyrolysis* **1985**, *8*, 291-303.
80. Jensen, R. P.; Strongin, R. M.; Peyton, D. H., Solvent chemistry in the electronic cigarette reaction vessel. *Scientific Reports* **2017**, *7*, 42549.
81. Magneron, I.; Mellouki, A.; Le Bras, G.; Moortgat, G.; Horowitz, A.; Wirtz, K., Photolysis and OH-initiated oxidation of glycolaldehyde under atmospheric conditions. *The Journal of Physical Chemistry A* **2005**, *109* (20), 4552-4561.
82. Lee, C.; Park, C., Bacterial responses to glyoxal and methylglyoxal: reactive electrophilic species. *International Journal of Molecular Sciences* **2017**, *18* (1), 169.
83. Jensen, R. P.; Luo, W.; Pankow, J. F.; Strongin, R. M.; Peyton, D. H., Hidden formaldehyde in e-cigarette aerosols. *New England Journal of Medicine* **2015**, *372* (4), 392-394.
84. Salamanca, J. C.; Meehan-Atrash, J.; Vreeke, S.; Escobedo, J. O.; Peyton, D. H.; Strongin, R. M., E-cigarettes can emit formaldehyde at high levels under conditions that have been reported to be non-averse to users. *Scientific Reports* **2018**, *8* (1), 1-6.
85. Uchiyama, S.; Ohta, K.; Inaba, Y.; Kunugita, N., Determination of carbonyl compounds generated from the E-cigarette using coupled silica cartridges impregnated with hydroquinone and 2, 4-dinitrophenylhydrazine, followed by high-performance liquid chromatography. *Analytical Sciences* **2013**, *29* (12), 1219-1222.
86. Kosmider, L.; Sobczak, A.; Fik, M.; Knysak, J.; Zaciera, M.; Kurek, J.; Goniewicz, M. L., Carbonyl compounds in electronic cigarette vapors: effects of nicotine solvent and battery output voltage. *Nicotine & Tobacco Research* **2014**, *16* (10), 1319-1326.
87. Lee, Y.-S.; Kim, K.-H.; Lee, S. S.; Brown, R. J.; Jo, S.-H., Analytical method for measurement of tobacco-specific nitrosamines in E-cigarette liquid and aerosol. *Applied Sciences* **2018**, *8* (12), 2699.
88. Bustamante, G.; Ma, B.; Yakovlev, G.; Yershova, K.; Le, C.; Jensen, J.; Hatsukami, D. K.; Stepanov, I., Presence of the Carcinogen N'-Nitrosornicotine in Saliva of E-cigarette Users. *Chemical Research in Toxicology* **2018**, *31* (8), 731-738.
89. Farsalinos, K. E.; Gillman, G.; Poulas, K.; Voudris, V., Tobacco-specific nitrosamines in electronic cigarettes: comparison between liquid and aerosol levels. *International journal of environmental research and public health* **2015**, *12* (8), 9046-9053.
90. Grana, R.; Benowitz, N.; Glantz, S. A., E-cigarettes: a scientific review. *Circulation* **2014**, *129* (19), 1972-1986.
91. Kim, H.-J.; Shin, H.-S., Determination of tobacco-specific nitrosamines in replacement liquids of electronic cigarettes by liquid chromatography–tandem mass spectrometry. *Journal of Chromatography A* **2013**, *1291*, 48-55.
92. Seamus Riordan-Short, T. D. N., Nahanni Sagar, Matthew Noestheden, Rob O'Brien, Thermal decomposition of vitamin E acetate in a surrogate vaping environment. *Thermoscientific Customer Application Note* **2020**, 73327.
93. Wu, D.; O'Shea, D. F., Potential for release of pulmonary toxic ketene from vaping pyrolysis of vitamin E acetate. *Proceedings of the National Academy of Sciences* **2020**, *117* (12), 6349-6355.
94. Meehan-Atrash, J.; Luo, W.; McWhirter, K. J.; Dennis, D. G.; Sarlah, D.; Jensen, R. P.; Afreh, I.; Jiang, J.; Barsanti, K. C.; Ortiz, A., The influence of terpenes on the release of volatile organic compounds and active ingredients to cannabis vaping aerosols. *RSC Advances* **2021**, *11* (19), 11714-11723.
95. Küppers, F.; Bercht, C.; Salemink, C.; Lousberg, R., Cannabis. XIV. Pyrolysis of cannabidiol—analysis of the volatile constituents. *Journal of Chromatography A* **1975**, *108* (2), 375-379.
96. Ross, S. A.; ElSohly, M. A., The volatile oil composition of fresh and air-dried buds of Cannabis sativa. *J. Nat. Prod.* **1996**, *59* (1), 49-51.

97. Tang, X.; Cancelada, L.; Rapp, V. H.; Russell, M. L.; Maddalena, R. L.; Litter, M. I.; Gundel, L. A.; Destailats, H., Emissions from Heated Terpenoids Present in Vaporizable Cannabis Concentrates. *Environ. Sci. Technol.* **2021**, *55* (9), 6160-6170.
98. Meehan-Atrash, J.; Luo, W.; Strongin, R. M., Toxicant formation in dabbing: the terpene story. *ACS Omega* **2017**, *2* (9), 6112-6117.
99. Lee, M.-S.; LeBouf, R. F.; Son, Y.-S.; Koutrakis, P.; Christiani, D. C., Nicotine, aerosol particles, carbonyls and volatile organic compounds in tobacco-and menthol-flavored e-cigarettes. *Environmental Health* **2017**, *16* (1), 1-10.
100. LeBouf, R. F.; Stefaniak, A. B.; Virji, M. A., Validation of evacuated canisters for sampling volatile organic compounds in healthcare settings. *J. Environ. Monit.* **2012**, *14* (3), 977-983.
101. Eddingsaas, N.; Pagano, T.; Cummings, C.; Rahman, I.; Robinson, R.; Hensel, E., Qualitative analysis of e-liquid emissions as a function of flavor additives using two aerosol capture methods. *International Journal of Environmental Research and Public Health* **2018**, *15* (2), 323.
102. Regan, A. K.; Promoff, G.; Dube, S. R.; Arrazola, R., Electronic nicotine delivery systems: adult use and awareness of the 'e-cigarette' in the USA. *Tobacco Control* **2013**, *22* (1), 19-23.
103. Dai, H.; Leventhal, A. M., Prevalence of e-cigarette use among adults in the United States, 2014-2018. *Jama* **2019**, *322* (18), 1824-1827.
104. Murthy, V. H., E-cigarette use among youth and young adults: a major public health concern. *JAMA Pediatrics* **2017**, *171* (3), 209-210.
105. Cullen, K. A.; Gentzke, A. S.; Sawdey, M. D.; Chang, J. T.; Anic, G. M.; Wang, T. W.; Creamer, M. R.; Jamal, A.; Ambrose, B. K.; King, B. A., E-cigarette use among youth in the United States, 2019. *Jama* **2019**, *322* (21), 2095-2103.
106. Olfson, M.; Wall, M. M.; Liu, S.-M.; Sultan, R. S.; Blanco, C., E-cigarette use among young adults in the US. *American Journal of Preventive Medicine* **2019**, *56* (5), 655-663.
107. Hughes, K.; Bellis, M. A.; Hardcastle, K. A.; McHale, P.; Bennett, A.; Ireland, R.; Pike, K., Associations between e-cigarette access and smoking and drinking behaviours in teenagers. *BMC Public Health* **2015**, *15* (1), 244.
108. Wasowicz, A.; Feleszko, W.; Goniewicz, M. L., E-Cigarette use among children and young people: the need for regulation. Taylor & Francis: 2015.
109. Wackowski, O. A.; Delnevo, C. D., Smokers' attitudes and support for e-cigarette policies and regulation in the USA. *Tobacco Control* **2015**, *24* (6), 543-546.
110. Goniewicz, M. L.; Gawron, M.; Nadolska, J.; Balwicki, L.; Sobczak, A., Rise in electronic cigarette use among adolescents in Poland. *Journal of Adolescent Health* **2014**, *55* (5), 713-715.
111. Abbara, S.; Kay, F. U., Electronic Cigarette or Vaping-associated Lung Injury (EVALI): The Tip of the Iceberg. *Radiology: Cardiothoracic Imaging* **2019**, *1* (4), e190212.
112. Navon, L.; Jones, C. M.; Ghinai, I.; King, B. A.; Briss, P. A.; Hacker, K. A.; Layden, J. E., Risk Factors for E-Cigarette, or Vaping, Product Use—Associated Lung Injury (EVALI) Among Adults Who Use E-Cigarette, or Vaping, Products—Illinois, July–October 2019. *Morbidity and Mortality Weekly Report* **2019**, *68* (45), 1034.
113. Kalininskiy, A.; Bach, C. T.; Nacca, N. E.; Ginsberg, G.; Marraffa, J.; Navarette, K. A.; McGraw, M. D.; Croft, D. P., E-cigarette, or vaping, product use associated lung injury (EVALI): case series and diagnostic approach. *The Lancet Respiratory Medicine* **2019**.
114. Pisinger, C.; Døssing, M., A systematic review of health effects of electronic cigarettes. *Preventive Medicine* **2014**, *69*, 248-260.
115. Callahan-Lyon, P., Electronic cigarettes: human health effects. *Tobacco Control* **2014**, *23* (suppl 2), ii36-ii40.

116. Logue, J. M.; Sleiman, M.; Montesinos, V. N.; Russell, M. L.; Litter, M. I.; Benowitz, N. L.; Gundel, L. A.; Destailats, H., Emissions from electronic cigarettes: assessing vapers' intake of toxic compounds, secondhand exposures, and the associated health impacts. *Environ. Sci. Technol.* **2017**, *51* (16), 9271-9279.
117. Mallock, N.; Pieper, E.; Hutzler, C.; Henkler-Stephani, F.; Luch, A., Heated Tobacco Products: A review of current knowledge and initial assessments. *Frontiers in Public Health* **2019**, *7*.
118. Li, L.; Lin, Y.; Xia, T.; Zhu, Y., Effects of Electronic Cigarettes on Indoor Air Quality and Health. *Annual Review of Public Health* **2020**, *41*.
119. Cancelada, L.; Sleiman, M.; Tang, X.; Russell, M. L.; Montesinos, V. N.; Litter, M. I.; Gundel, L. A.; Destailats, H., Heated tobacco products: volatile emissions and their predicted impact on indoor air quality. *Environ. Sci. Technol.* **2019**, *53* (13), 7866-7876.
120. DeCarlo, P. F.; Avery, A. M.; Waring, M. S., Thirdhand smoke uptake to aerosol particles in the indoor environment. *Science Advances* **2018**, *4* (5), eaap8368.
121. Nguyen, C.; Li, L.; Sen, C. A.; Ronquillo, E.; Zhu, Y., Fine and ultrafine particles concentrations in vape shops. *Atmospheric Environment* **2019**, *211*, 159-169.
122. Baassiri, M.; Talih, S.; Salman, R.; Karaoghlanian, N.; Saleh, R.; El Hage, R.; Saliba, N.; Shihadeh, A., Clouds and "throat hit": Effects of liquid composition on nicotine emissions and physical characteristics of electronic cigarette aerosols. *Aerosol Science and Technology* **2017**, *51* (11), 1231-1239.
123. Bekö, G.; Morrison, G.; Weschler, C. J.; Koch, H. M.; Palmke, C.; Salthammer, T.; Schripp, T.; Toftum, J.; Clausen, G., Measurements of dermal uptake of nicotine directly from air and clothing. *Indoor Air* **2017**, *27* (2), 427-433.
124. Zhu, S.-H.; Sun, J. Y.; Bonnevie, E.; Cummins, S. E.; Gamst, A.; Yin, L.; Lee, M., Four hundred and sixty brands of e-cigarettes and counting: implications for product regulation. *Tobacco Control* **2014**, *23* (suppl 3), iii3-iii9.
125. Han, S.; Chen, H.; Zhang, X.; Liu, T.; Fu, Y. n., Levels of selected groups of compounds in refill solutions for electronic cigarettes. *Nicotine & Tobacco Research* **2015**, *18* (5), 708-714.
126. Hajek, P.; Etter, J. F.; Benowitz, N.; Eissenberg, T.; McRobbie, H., Electronic cigarettes: review of use, content, safety, effects on smokers and potential for harm and benefit. *Addiction* **2014**, *109* (11), 1801-1810.
127. Bullen, C.; McRobbie, H.; Thornley, S.; Glover, M.; Lin, R.; Laugesen, M., Effect of an electronic nicotine delivery device (e cigarette) on desire to smoke and withdrawal, user preferences and nicotine delivery: randomised cross-over trial. *Tobacco Control* **2010**, *19* (2), 98-103.
128. Casteel, S.; Vernon, R.; Bailey, J. E., Formaldehyde: toxicology and hazards. *Veterinary and Human Toxicology* **1987**, *29* (1), 31-33.
129. Jones, A., Measuring and reporting the concentration of acetaldehyde in human breath. *Alcohol and Alcoholism* **1995**, *30* (3), 271-285.
130. Moghe, A.; Ghare, S.; Lamoreau, B.; Mohammad, M.; Barve, S.; McClain, C.; Joshi-Barve, S., Molecular mechanisms of acrolein toxicity: relevance to human disease. *Toxicological Sciences* **2015**, *143* (2), 242-255.
131. Behar, R. Z.; Luo, W.; McWhirter, K. J.; Pankow, J. F.; Talbot, P., Analytical and toxicological evaluation of flavor chemicals in electronic cigarette refill fluids. *Scientific Reports* **2018**, *8* (1), 8288.
132. Petersen, A. B.; Wulf, H. C.; Gniadecki, R.; Gajkowska, B., Dihydroxyacetone, the active tanning ingredient in sunless tanning lotions, induces DNA damage, cell-cycle block and apoptosis in cultured HaCaT keratinocytes. *Mutation Research/Genetic Toxicology and Environmental Mutagenesis* **2004**, *560* (2), 173-186.
133. Liesivuori, J.; Savolainen; Heikki, Methanol and formic acid toxicity: biochemical mechanisms. *Pharmacology & Toxicology* **1991**, *69* (3), 157-163.

134. Sakuragawa, A.; Yoneno, T.; Inoue, K.; Okutani, T., Trace analysis of carbonyl compounds by liquid chromatography–mass spectrometry after collection as 2, 4-dinitrophenylhydrazine derivatives. *Journal of Chromatography A* **1999**, *844* (1-2), 403-408.
135. Jones, R. G., Reactions of hydrazine with heterocyclic 1, 2-dicarboxylic acid esters. *Journal of the American Chemical Society* **1956**, *78* (1), 159-163.
136. Godtfredsen, W.; Vangedal, S., The reaction of hydrazine with cinnamic acid derivatives. *Acta Chem. Scand* **1955**, *9* (9), 1498-1509.
137. Klager, S.; Vallarino, J.; MacNaughton, P.; Christiani, D. C.; Lu, Q.; Allen, J. G., Flavoring chemicals and aldehydes in e-cigarette emissions. *Environ. Sci. Technol.* **2017**, *51* (18), 10806-10813.
138. Flora, J. W.; Meruva, N.; Huang, C. B.; Wilkinson, C. T.; Ballentine, R.; Smith, D. C.; Werley, M. S.; McKinney, W. J., Characterization of potential impurities and degradation products in electronic cigarette formulations and aerosols. *Regulatory Toxicology and Pharmacology* **2016**, *74*, 1-11.
139. Cho, Y.-H.; Shin, H.-S., Use of a gas-tight syringe sampling method for the determination of tobacco-specific nitrosamines in E-cigarette aerosols by liquid chromatography-tandem mass spectrometry. *Analytical Methods* **2015**, *7* (11), 4472-4480.
140. Hadwiger, M. E.; Trehy, M. L.; Ye, W.; Moore, T.; Allgire, J.; Westenberger, B., Identification of amino-tadalafil and rimonabant in electronic cigarette products using high pressure liquid chromatography with diode array and tandem mass spectrometric detection. *Journal of Chromatography A* **2010**, *1217* (48), 7547-7555.
141. Sleiman, M.; Logue, J. M.; Montesinos, V. N.; Russell, M. L.; Litter, M. I.; Gundel, L. A.; Destailats, H., Emissions from electronic cigarettes: key parameters affecting the release of harmful chemicals. *Environ. Sci. Technol.* **2016**, *50* (17), 9644-9651.
142. Druzik, C. M.; Grosjean, D.; Van Neste, A.; Parmar, S. S., Sampling of atmospheric carbonyls with small DNPH-coated C18 cartridges and liquid chromatography analysis with diode array detection. *International Journal of Environmental Analytical Chemistry* **1990**, *38* (4), 495-512.
143. Hogenboom, A.; Van Leerdam, J.; De Voogt, P., Accurate mass screening and identification of emerging contaminants in environmental samples by liquid chromatography–hybrid linear ion trap Orbitrap mass spectrometry. *Journal of Chromatography A* **2009**, *1216* (3), 510-519.
144. Giovenco, D. P.; Hammond, D.; Corey, C. G.; Ambrose, B. K.; Delnevo, C. D., E-cigarette market trends in traditional US retail channels, 2012–2013. *Nicotine & Tobacco Research* **2014**, *17* (10), 1279-1283.
145. Oss, M.; Krueve, A.; Herodes, K.; Leito, I., Electrospray ionization efficiency scale of organic compounds. *Analytical Chemistry* **2010**, *82* (7), 2865-2872.
146. Wang, W.; He, Z.; Feng, N.; Cai, Y., Electronic cigarette use in China: Awareness, prevalence and regulation. *Tobacco Induced Diseases* **2019**, *17*.
147. Ribeiro, R. F.; Marenich, A. V.; Cramer, C. J.; Truhlar, D. G., Use of solution-phase vibrational frequencies in continuum models for the free energy of solvation. *The Journal of Physical Chemistry B* **2011**, *115* (49), 14556-14562.
148. Levsen, K.; Schiebel, H. M.; Terlouw, J. K.; Jobst, K. J.; Elend, M.; Preiß, A.; Thiele, H.; Ingendoh, A., Even-electron ions: a systematic study of the neutral species lost in the dissociation of quasi-molecular ions. *Journal of Mass Spectrometry* **2007**, *42* (8), 1024-1044.
149. De Vijlder, T.; Valkenburg, D.; Lemièrre, F.; Romijn, E. P.; Laukens, K.; Cuyckens, F., A tutorial in small molecule identification via electrospray ionization-mass spectrometry: The practical art of structural elucidation. *Mass Spectrometry Reviews* **2018**, *37* (5), 607-629.
150. Demarque, D. P.; Crotti, A. E.; Vessicchi, R.; Lopes, J. L.; Lopes, N. P., Fragmentation reactions using electrospray ionization mass spectrometry: an important tool for the structural elucidation and characterization of synthetic and natural products. *Natural Product Reports* **2016**, *33* (3), 432-455.

151. Schmidt, A. C.; Herzsuh, R.; Matysik, F. M.; Engewald, W., Investigation of the ionisation and fragmentation behaviour of different nitroaromatic compounds occurring as polar metabolites of explosives using electrospray ionisation tandem mass spectrometry. *Rapid Communications in Mass Spectrometry* **2006**, *20* (15), 2293-2302.
152. Zwiener, C.; Glauner, T.; Frimmel, F., Method optimization for the determination of carbonyl compounds in disinfected water by DNPH derivatization and LC-ESI-MS-MS. *Analytical and Bioanalytical Chemistry* **2002**, *372* (5-6), 615-621.
153. Wennberg, P. O.; Bates, K. H.; Crouse, J. D.; Dodson, L. G.; McVay, R. C.; Mertens, L. A.; Nguyen, T. B.; Praske, E.; Schwantes, R. H.; Smarte, M. D., Gas-phase reactions of isoprene and its major oxidation products. *Chemical Reviews* **2018**, *118* (7), 3337-3390.
154. Ehrmann, B. M.; Henriksen, T.; Cech, N. B., Relative importance of basicity in the gas phase and in solution for determining selectivity in electrospray ionization mass spectrometry. *Journal of the American Society for Mass Spectrometry* **2008**, *19* (5), 719-728.
155. Chalcraft, K. R.; Lee, R.; Mills, C.; Britz-McKibbin, P., Virtual quantification of metabolites by capillary electrophoresis-electrospray ionization-mass spectrometry: predicting ionization efficiency without chemical standards. *Analytical Chemistry* **2009**, *81* (7), 2506-2515.
156. Amad, M. a. H.; Cech, N. B.; Jackson, G. S.; Enke, C. G., Importance of gas-phase proton affinities in determining the electrospray ionization response for analytes and solvents. *Journal of Mass Spectrometry* **2000**, *35* (7), 784-789.
157. Krueve, A.; Kaupmees, K.; Liigand, J.; Leito, I., Negative electrospray ionization via deprotonation: predicting the ionization efficiency. *Analytical Chemistry* **2014**, *86* (10), 4822-4830.
158. Henriksen, T.; Juhler, R. K.; Svensmark, B.; Cech, N. B., The relative influences of acidity and polarity on responsiveness of small organic molecules to analysis with negative ion electrospray ionization mass spectrometry (ESI-MS). *Journal of the American Society for Mass Spectrometry* **2005**, *16* (4), 446-455.
159. Huang, Y.; Liu, L.; Liu, S., Towards understanding proton affinity and gas-phase basicity with density functional reactivity theory. *Chemical Physics Letters* **2012**, *527*, 73-78.
160. Marchese, R.; Grandori, R.; Carloni, P.; Raugei, S., A computational model for protein ionization by electrospray based on gas-phase basicity. *Journal of the American Society for Mass Spectrometry* **2012**, *23* (11), 1903-1910.
161. Stevens, J. P., Outliers and influential data points in regression analysis. *Psychological Bulletin* **1984**, *95* (2), 334.
162. Wheeler, S. E.; Houk, K., Integration grid errors for meta-GGA-predicted reaction energies: Origin of grid errors for the M06 suite of functionals. *Journal of Chemical Theory and Computation* **2010**, *6* (2), 395-404.
163. Mo, Y.; Peyerimhoff, S. D., Theoretical analysis of electronic delocalization. *The Journal of Chemical Physics* **1998**, *109* (5), 1687-1697.
164. De Proft, F.; Langenaeker, W.; Geerlings, P., Acidity of alkyl substituted alcohols: Are alkyl groups electron-donating or electron-withdrawing? *Tetrahedron* **1995**, *51* (14), 4021-4032.
165. Uchiyama, S.; Noguchi, M.; Sato, A.; Ishitsuka, M.; Inaba, Y.; Kunugita, N., Determination of Thermal Decomposition Products Generated from E-cigarettes. *Chemical Research in Toxicology* **2020**.
166. Ogunwale, M. A.; Li, M.; Ramakrishnam Raju, M. V.; Chen, Y.; Nantz, M. H.; Conklin, D. J.; Fu, X.-A., Aldehyde detection in electronic cigarette aerosols. *ACS Omega* **2017**, *2* (3), 1207-1214.
167. Bitzer, Z. T.; Goel, R.; Reilly, S. M.; Bhangu, G.; Trushin, N.; Foulds, J.; Muscat, J.; Richie Jr, J. P., Emissions of free radicals, carbonyls, and nicotine from the NIDA Standardized Research Electronic Cigarette and comparison to similar commercial devices. *Chemical Research in Toxicology* **2018**, *32* (1), 130-138.

168. Appelman, L.; Woutersen, R.; Fcron, V.; Hoofman, R. N.; Notten, W., Effect of variable versus fixed exposure levels on the toxicity of acetaldehyde in rats. *Journal of Applied Toxicology* **1986**, *6* (5), 331-336.
169. Kim, K.-H.; Jahan, S. A.; Lee, J.-T., Exposure to formaldehyde and its potential human health hazards. *Journal of Environmental Science and Health, Part C* **2011**, *29* (4), 277-299.
170. Nascimento Saldiva, P. H.; do Rio Caldeira, M. P.; Massad, E.; Calheiros, D. F.; Cardoso, L. M. N.; Miklós Böhm, G.; Saldiva, C. D., Effects of formaldehyde and acetaldehyde inhalation on rat pulmonary mechanics. *Journal of Applied Toxicology* **1985**, *5* (5), 288-292.
171. Etter, J.-F., A longitudinal study of cotinine in long-term daily users of e-cigarettes. *Drug and Alcohol Dependence* **2016**, *160*, 218-221.
172. Smets, J.; Baeyens, F.; Chaumont, M.; Adriaens, K.; Van Gucht, D., When less is more: vaping low-nicotine vs. high-nicotine e-liquid is compensated by increased wattage and higher liquid consumption. *International Journal of Environmental Research and Public Health* **2019**, *16* (5), 723.
173. Dawkins, L. E.; Kimber, C. F.; Doig, M.; Feyerabend, C.; Corcoran, O., Self-titration by experienced e-cigarette users: blood nicotine delivery and subjective effects. *Psychopharmacology* **2016**, *233* (15-16), 2933-2941.
174. Kosno, K.; Janik, I.; Celuch, M.; Mirkowski, J.; Kisała, J.; Pogocki, D., The role of pH in the mechanism of OH radical induced oxidation of nicotine. *Isr. J. Chem.* **2014**, *54* (3), 302-315.
175. Farsalinos, K. E.; Yannovits, N.; Sarri, T.; Voudris, V.; Poulas, K.; Leischow, S. J., Carbonyl emissions from a novel heated tobacco product (IQOS): comparison with an e-cigarette and a tobacco cigarette. *Addiction* **2018**, *113* (11), 2099-2106.
176. Counts, M.; Morton, M.; Laffoon, S.; Cox, R.; Lipowicz, P., Smoke composition and predicting relationships for international commercial cigarettes smoked with three machine-smoking conditions. *Regulatory Toxicology and Pharmacology* **2005**, *41* (3), 185-227.
177. Smith, K. R.; Hayat, F.; Andrews, J. F.; Migaud, M. E.; Gassman, N. R., Dihydroxyacetone Exposure Alters NAD (P) H and Induces Mitochondrial Stress and Autophagy in HEK293T Cells. *Chemical Research in Toxicology* **2019**, *32* (8), 1722-1731.
178. Bove, K. E., Ethylene glycol toxicity. *American Journal of Clinical Pathology* **1966**, *45* (1), 46-50.
179. Farsalinos, K. E.; Voudris, V.; Poulas, K., E-cigarettes generate high levels of aldehydes only in 'dry puff' conditions. *Addiction* **2015**, *110* (8), 1352-1356.
180. Li, S.; Karles, G.; Kobal, G.; Li, W.; Secrist, R.; Jarquin, M. D. C.; Di Novi, C.; Pithawalla, Y.; Kane, D., Pre-vaporization formulation for controlling acidity in an e-vaping device. Google Patents: 2019.
181. Morgan, D. L.; Jokinen, M. P.; Johnson, C. L.; Price, H. C.; Gwinn, W. M.; Bousquet, R. W.; Flake, G. P., Chemical reactivity and respiratory toxicity of the α -diketone flavoring agents: 2, 3-butanedione, 2, 3-pentanedione, and 2, 3-hexanedione. *Toxicologic Pathology* **2016**, *44* (5), 763-783.
182. Kanwal, R.; Kullman, G.; Piacitelli, C.; Boylstein, R.; Sahakian, N.; Martin, S.; Fedan, K.; Kreiss, K., Evaluation of flavorings-related lung disease risk at six microwave popcorn plants. *Journal of Occupational and Environmental Medicine* **2006**, *48* (2), 149-157.
183. Hickman, E.; Herrera, C. A.; Jaspers, I., Common e-cigarette flavoring chemicals impair neutrophil phagocytosis and oxidative burst. *Chemical Research in Toxicology* **2019**, *32* (6), 982-985.
184. Brown, J.; West, R.; Beard, E.; Michie, S.; Shahab, L.; McNeill, A., Prevalence and characteristics of e-cigarette users in Great Britain: findings from a general population survey of smokers. *Addictive Behaviors* **2014**, *39* (6), 1120-1125.
185. Huang, J.; Duan, Z.; Kwok, J.; Binns, S.; Vera, L. E.; Kim, Y.; Szczypka, G.; Emery, S. L., Vaping versus JUULing: how the extraordinary growth and marketing of JUUL transformed the US retail e-cigarette market. *Tobacco Control* **2019**, *28* (2), 146-151.
186. Kong, G.; Krishnan-Sarin, S., A call to end the epidemic of adolescent E-cigarette use. *Drug and Alcohol Dependence* **2017**, *174*, 215.

187. Arrazola, R. A.; Singh, T.; Corey, C. G.; Husten, C. G.; Neff, L. J.; Apelberg, B. J.; Bunnell, R. E.; Choiniere, C. J.; King, B. A.; Cox, S., Tobacco use among middle and high school students—United States, 2011–2014. *MMWR. Morbidity and Mortality Weekly Report* **2015**, *64* (14), 381.
188. Perikleous, E. P.; Steiropoulos, P.; Paraskakis, E.; Constantinidis, T. C.; Nena, E., E-cigarette use among adolescents: an overview of the literature and future perspectives. *Frontiers in Public Health* **2018**, *6*, 86.
189. Kong, G.; Morean, M. E.; Cavallo, D. A.; Camenga, D. R.; Krishnan-Sarin, S., Reasons for electronic cigarette experimentation and discontinuation among adolescents and young adults. *Nicotine & Tobacco Research* **2015**, *17* (7), 847-854.
190. Talih, S.; Salman, R.; Karaoghlanian, N.; El-Hellani, A.; Saliba, N.; Eissenberg, T.; Shihadeh, A., “Juice Monsters”: sub-ohm vaping and toxic volatile aldehyde emissions. *Chemical Research in Toxicology* **2017**, *30* (10), 1791-1793.
191. Protano, C.; Avino, P.; Manigrasso, M.; Vivaldi, V.; Perna, F.; Valeriani, F.; Vitali, M., Environmental electronic vape exposure from four different generations of electronic cigarettes: airborne particulate matter levels. *International Journal of Environmental Research and Public Health* **2018**, *15* (10), 2172.
192. Wagener, T. L.; Floyd, E. L.; Stepanov, I.; Driskill, L. M.; Frank, S. G.; Meier, E.; Leavens, E. L.; Tackett, A. P.; Molina, N.; Queimado, L., Have combustible cigarettes met their match? The nicotine delivery profiles and harmful constituent exposures of second-generation and third-generation electronic cigarette users. *Tobacco Control* **2017**, *26* (e1), e23-e28.
193. Barrington-Trimis, J. L.; Gibson, L. A.; Halpern-Felsher, B.; Harrell, M. B.; Kong, G.; Krishnan-Sarin, S.; Leventhal, A. M.; Loukas, A.; McConnell, R.; Weaver, S. R., Type of E-Cigarette device used among adolescents and young adults: findings from a pooled analysis of eight studies of 2166 vapers. *Nicotine and Tobacco Research* **2018**, *20* (2), 271-274.
194. Bitzer, Z. T.; Goel, R.; Reilly, S. M.; Elias, R. J.; Silakov, A.; Foulds, J.; Muscat, J.; Richie Jr, J. P., Effect of flavoring chemicals on free radical formation in electronic cigarette aerosols. *Free Radical Biology and Medicine* **2018**, *120*, 72-79.
195. Hasan, F.; Khachatryan, L.; Lomnicki, S., Comparative Studies of Environmentally Persistent Free Radicals on Total Particulate Matter Collected from Electronic and Tobacco Cigarettes. *Environ. Sci. Technol.* **2020**, *54* (9), 5710-5718.
196. Son, Y.; Mishin, V.; Laskin, J. D.; Mainelis, G.; Wackowski, O. A.; Delnevo, C.; Schwander, S.; Khlystov, A.; Samburova, V.; Meng, Q., Hydroxyl Radicals in E-Cigarette Vapor and E-Vapor Oxidative Potentials under Different Vaping Patterns. *Chemical Research in Toxicology* **2019**, *32* (6), 1087-1095.
197. Ooi, B. G.; Dutta, D.; Kazipeta, K.; Chong, N. S., Influence of the E-Cigarette Emission Profile by the Ratio of Glycerol to Propylene Glycol in E-Liquid Composition. *ACS Omega* **2019**, *4* (8), 13338-13348.
198. Son, Y.; Wackowski, O.; Weisel, C.; Schwander, S.; Mainelis, G.; Delnevo, C.; Meng, Q., Evaluation of e-vapor nicotine and nicotine concentrations under various e-liquid compositions, device settings, and vaping topographies. *Chemical Research in Toxicology* **2018**, *31* (9), 861-868.
199. Duell, A. K.; McWhirter, K. J.; Korzun, T.; Strongin, R. M.; Peyton, D. H., Sucralose-enhanced degradation of electronic cigarette liquids during Vaping. *Chemical Research in Toxicology* **2019**, *32* (6), 1241-1249.
200. Vreeke, S.; Peyton, D. H.; Strongin, R. M., Triacetin enhances levels of acrolein, formaldehyde hemiacetals, and acetaldehyde in electronic cigarette aerosols. *ACS Omega* **2018**, *3* (7), 7165-7170.
201. Pankow, J. F.; Duell, A. K.; Peyton, D. H., Free-Base Nicotine Fraction α fb in Non-Aqueous versus Aqueous Solutions: Electronic Cigarette Fluids Without versus With Dilution with Water. *Chemical Research in Toxicology* **2020**.
202. Melvin, M. S.; Avery, K. C.; Ballentine, R. M.; Flora, J. W.; Gardner, W.; Karles, G. D.; Pithawalla, Y. B.; Smith, D. C.; Ehman, K. D.; Wagner, K. A., Formation of Diacetyl and Other α -Dicarbonyl Compounds during the Generation of E-Vapor Product Aerosols. *ACS Omega* **2020**, *5* (28), 17565-17575.

203. Heyder, J.; Gebhart, J.; Rudolf, G.; Schiller, C. F.; Stahlhofen, W., Deposition of particles in the human respiratory tract in the size range 0.005–15 µm. *J. Aerosol Sci* **1986**, *17* (5), 811-825.
204. Deng, Q.; Ou, C.; Shen, Y.-M.; Xiang, Y.; Miao, Y.; Li, Y., Health effects of physical activity as predicted by particle deposition in the human respiratory tract. *Sci. Total Environ.* **2019**, *657*, 819-826.
205. Meng, Q.; Son, Y.; Kipen, H.; Laskin, D.; Schwander, S.; Delnevo, C., Particles released from primary e-cigarette vaping: particle size distribution and particle deposition in the human respiratory tract. In *A16. WHY SHOULD WE BE CONCERNED ABOUT E-CIGARETTES?*, American Thoracic Society: 2017; pp A1023-A1023.
206. Morris, J. B., Deposition of Inhaled Gases and Vapors. In *Comparative Biology of the Normal Lung*, Elsevier: 2015; pp 537-560.
207. Lechasseur, A.; Altmejd, S.; Turgeon, N.; Buonanno, G.; Morawska, L.; Brunet, D.; Duchaine, C.; Morissette, M. C., Variations in coil temperature/power and e-liquid constituents change size and lung deposition of particles emitted by an electronic cigarette. *Physiological Reports* **2019**, *7* (10), e14093.
208. Korzun, T.; Lazurko, M.; Munhenzva, I.; Barsanti, K. C.; Huang, Y.; Jensen, R. P.; Escobedo, J. O.; Luo, W.; Peyton, D. H.; Strongin, R. M., E-cigarette airflow rate modulates toxicant profiles and can lead to concerning levels of solvent consumption. *ACS Omega* **2018**, *3* (1), 30-36.
209. Gillman, I.; Kistler, K.; Stewart, E.; Paolantonio, A., Effect of variable power levels on the yield of total aerosol mass and formation of aldehydes in e-cigarette aerosols. *Regulatory Toxicology and Pharmacology* **2016**, *75*, 58-65.
210. Prévôt, N.; De Oliveira, F.; Perinel-Ragey, S.; Basset, T.; Vergnon, J.-M.; Pourchez, J., Nicotine delivery from the refill liquid to the aerosol via high-power e-cigarette device. *Scientific Reports* **2017**, *7* (1), 1-7.
211. Son, Y.; Mainelis, G.; Delnevo, C.; Wackowski, O. A.; Schwander, S.; Meng, Q., Investigating E-cigarette Particle Emissions and Human Airway Depositions under Various E-cigarette Use Conditions. *Chemical Research in Toxicology* **2019**.
212. Zhao, D.; Navas-Acien, A.; Ilievski, V.; Slavkovich, V.; Olmedo, P.; Adria-Mora, B.; Domingo-Relloso, A.; Aherrera, A.; Kleiman, N. J.; Rule, A. M., Metal concentrations in electronic cigarette aerosol: effect of open-system and closed-system devices and power settings. *Environ. Res.* **2019**, *174*, 125-134.
213. Saleh, Q. M.; Hensel, E. C.; Robinson, R. J., Method for Quantifying Variation in the Resistance of Electronic Cigarette Coils. *International Journal of Environmental Research and Public Health* **2020**, *17* (21), 7779.
214. Zhao, T.; Shu, S.; Guo, Q.; Zhu, Y., Effects of design parameters and puff topography on heating coil temperature and mainstream aerosols in electronic cigarettes. *Atmospheric Environment* **2016**, *134*, 61-69.
215. Dibaji, S. A. R.; Guha, S.; Arab, A.; Murray, B. T.; Myers, M. R., Accuracy of commercial electronic nicotine delivery systems (ENDS) temperature control technology. *PLoS One* **2018**, *13* (11).
216. Lopez, A. A.; Hiler, M. M.; Soule, E. K.; Ramôa, C. P.; Karaoghlanian, N. V.; Lipato, T.; Breland, A. B.; Shihadeh, A. L.; Eissenberg, T., Effects of electronic cigarette liquid nicotine concentration on plasma nicotine and puff topography in tobacco cigarette smokers: a preliminary report. *Nicotine & Tobacco Research* **2016**, *18* (5), 720-723.
217. Cunningham, A.; Slayford, S.; Vas, C.; Gee, J.; Costigan, S.; Prasad, K., Development, validation and application of a device to measure e-cigarette users' puffing topography. *Scientific Reports* **2016**, *6* (1), 1-7.
218. Talih, S.; Balhas, Z.; Eissenberg, T.; Salman, R.; Karaoghlanian, N.; El Hellani, A.; Baalbaki, R.; Saliba, N.; Shihadeh, A., Effects of user puff topography, device voltage, and liquid nicotine concentration on electronic cigarette nicotine yield: measurements and model predictions. *Nicotine & Tobacco Research* **2015**, *17* (2), 150-157.

219. Beauval, N.; Verrielle, M.; Garat, A.; Fronval, I.; Dusautoir, R.; Antherieu, S.; Garcon, G.; Lo-Guidice, J.-M.; Allorge, D.; Locoge, N., Influence of puffing conditions on the carbonyl composition of e-cigarette aerosols. *International Journal of Hygiene and Environmental Health* **2019**, *222* (1), 136-146.
220. Tayyarah, R.; Long, G. A., Comparison of select analytes in aerosol from e-cigarettes with smoke from conventional cigarettes and with ambient air. *Regulatory Toxicology and Pharmacology* **2014**, *70* (3), 704-710.
221. David, G.; Parmentier, E. A.; Taurino, I.; Signorell, R., tracing the composition of single e-cigarette aerosol droplets in situ by laser-trapping and Raman scattering. *Scientific Reports* **2020**, *10* (1), 1-8.
222. CORESTA, E.; Force, C. T., Routine analytical machine for e-cigarette aerosol generation and collection—definitions and standard conditions. *Paris, CORESTA* **2015**.
223. Farsalinos, K. E.; Romagna, G.; Tsiapras, D.; Kyzropoulos, S.; Voudris, V., Evaluation of electronic cigarette use (vaping) topography and estimation of liquid consumption: implications for research protocol standards definition and for public health authorities' regulation. *International Journal of Environmental Research and Public Health* **2013**, *10* (6), 2500-2514.
224. Robinson, R.; Hensel, E.; Roundtree, K.; Difrancesco, A.; Nonnemaker, J.; Lee, Y., Week long topography study of young adults using electronic cigarettes in their natural environment. *PloS One* **2016**, *11* (10), e0164038.
225. Robinson, R.; Hensel, E.; Morabito, P.; Roundtree, K., Electronic cigarette topography in the natural environment. *PloS One* **2015**, *10* (6), e0129296.
226. Gallart-Mateu, D.; Elbal, L.; Armenta, S.; De la Guardia, M., Passive exposure to nicotine from e-cigarettes. *Talanta* **2016**, *152*, 329-334.
227. Putzhammer, R.; Doppler, C.; Jakschitz, T.; Heinz, K.; Förste, J.; Danzl, K.; Messner, B.; Bernhard, D., Vapours of US and EU market leader electronic cigarette brands and liquids are cytotoxic for human vascular endothelial cells. *PloS One* **2016**, *11* (6), e0157337.
228. Hilpert, M.; Ilievski, V.; Coady, M.; Andrade-Gutierrez, M.; Yan, B.; Chillrud, S. N.; Navas-Acien, A.; Kleiman, N. J., A custom-built low-cost chamber for exposing rodents to e-cigarette aerosol: practical considerations. *Inhalation Toxicology* **2019**, *31* (11-12), 399-408.
229. Sosnowski, T. R.; Odziomek, M., Particle size dynamics: toward a better understanding of electronic cigarette aerosol interactions with the respiratory system. *Frontiers in Physiology* **2018**, *9*, 853.
230. Asgharian, B.; Price, O. T.; Rostami, A. A.; Pithawalla, Y. B., Deposition of inhaled electronic cigarette aerosol in the human oral cavity. *J. Aerosol Sci* **2018**, *116*, 34-47.
231. Zhang, Y.; Sumner, W.; Chen, D.-R., In vitro particle size distributions in electronic and conventional cigarette aerosols suggest comparable deposition patterns. *Nicotine & Tobacco Research* **2013**, *15* (2), 501-508.
232. Williams, R. H.; Shah, S. M.; Maggiore, J. A.; Erickson, T. B., Simultaneous detection and quantitation of diethylene glycol, ethylene glycol, and the toxic alcohols in serum using capillary column gas chromatography. *Journal of Analytical Toxicology* **2000**, *24* (7), 621-626.
233. Crouse, J. D.; McKinney, K. A.; Kwan, A. J.; Wennberg, P. O., Measurement of gas-phase hydroperoxides by chemical ionization mass spectrometry. *Analytical Chemistry* **2006**, *78* (19), 6726-6732.
234. St. Clair, J. M.; McCabe, D. C.; Crouse, J. D.; Steiner, U.; Wennberg, P. O., Chemical ionization tandem mass spectrometer for the in situ measurement of methyl hydrogen peroxide. *Review of Scientific Instruments* **2010**, *81* (9), 094102.
235. Paulot, F.; Crouse, J.; Kjaergaard, H.; Kroll, J.; Seinfeld, J.; Wennberg, P., Isoprene photooxidation: new insights into the production of acids and organic nitrates. *Atmospheric Chemistry and Physics* **2009**, *9* (4), 1479-1501.
236. Nguyen, T.; Coggon, M.; Flagan, R.; Seinfeld, J., Reactive uptake and photo-fenton oxidation of glycolaldehyde in aerosol liquid water. *Environ. Sci. Technol.* **2013**, *47* (9), 4307-4316.

237. Floyd, E. L.; Queimado, L.; Wang, J.; Regens, J. L.; Johnson, D. L., Electronic cigarette power affects count concentration and particle size distribution of vaping aerosol. *PLoS One* **2018**, *13* (12), e0210147.
238. Laidler, K. J., The development of the Arrhenius equation. *J. Chem. Educ.* **1984**, *61* (6), 494.
239. Peleg, M.; Normand, M. D.; Corradini, M. G., The Arrhenius equation revisited. *Critical Reviews in Food Science and Nutrition* **2012**, *52* (9), 830-851.
240. Sierra, C. A., Temperature sensitivity of organic matter decomposition in the Arrhenius equation: some theoretical considerations. *Biogeochemistry* **2012**, *108* (1-3), 1-15.
241. Bitzer, Z. T.; Goel, R.; Reilly, S. M.; Foulds, J.; Muscat, J.; Elias, R. J.; Richie Jr, J. P., Effects of solvent and temperature on free radical formation in electronic cigarette aerosols. *Chemical Research in Toxicology* **2018**, *31* (1), 4-12.
242. Bühler, W.; Dinjus, E.; Ederer, H.; Kruse, A.; Mas, C., Ionic reactions and pyrolysis of glycerol as competing reaction pathways in near-and supercritical water. *The Journal of Supercritical Fluids* **2002**, *22* (1), 37-53.
243. Herrmann, H.; Hoffmann, D.; Schaefer, T.; Bräuer, P.; Tilgner, A., Tropospheric aqueous-phase free-radical chemistry: Radical sources, spectra, reaction kinetics and prediction tools. *ChemPhysChem* **2010**, *11* (18), 3796-3822.
244. Zipse, H., Radical stability—a theoretical perspective. In *Radicals in Synthesis I*, Springer: 2006; pp 163-189.
245. Hioe, J.; Zipse, H., Radical stability and its role in synthesis and catalysis. *Organic & biomolecular chemistry* **2010**, *8* (16), 3609-3617.
246. Tsang, W., The stability of alkyl radicals. *Journal of the American Chemical Society* **1985**, *107* (10), 2872-2880.
247. Sharma, A.; Reva, I.; Fausto, R.; Hesse, S.; Xue, Z.; Suhm, M. A.; Nayak, S. K.; Sathishkumar, R.; Pal, R.; Guru Row, T. N., Conformation-changing aggregation in hydroxyacetone: a combined low-temperature FTIR, jet, and crystallographic study. *Journal of the American Chemical Society* **2011**, *133* (50), 20194-20207.
248. Lozynski, M.; Rusinska-Rozsak, D.; Mack, H.-G., MP2 and density functional studies of hydrogen bonding in model trioses: D-(+)-glyceraldehyde and dihydroxyacetone. *The Journal of Physical Chemistry A* **1997**, *101* (8), 1542-1548.
249. Sillrén, P.; Bielecki, J.; Mattsson, J.; Börjesson, L.; Matic, A., A statistical model of hydrogen bond networks in liquid alcohols. *The Journal of Chemical Physics* **2012**, *136* (9), 094514.
250. Root, L. J.; Berne, B., Effect of pressure on hydrogen bonding in glycerol: A molecular dynamics investigation. *The Journal of Chemical Physics* **1997**, *107* (11), 4350-4357.
251. John, E.; Coburn, S.; Liu, C.; McAughey, J.; Mariner, D.; McAdam, K. G.; Bakos, I.; Dóbbé, S., Gas-Particle Partitioning of Formaldehyde in Mainstream Cigarette Smoke. *Beiträge zur Tabakforschung International/Contributions to Tobacco Research* **2020**, *29* (1), 2-20.
252. Davis, D. L.; Nielsen, M. T., *Tobacco: production, chemistry and technology*. 1999.
253. Stabbert, R.; Dempsey, R.; Diekmann, J.; Euchenhofer, C.; Hagemeister, T.; Haussmann, H.-J.; Knorr, A.; Mueller, B. P.; Pospisil, P.; Reininghaus, W., Studies on the contributions of smoke constituents, individually and in mixtures, in a range of in vitro bioactivity assays. *Toxicology in Vitro* **2017**, *42*, 222-246.
254. Eschner, M. S.; Selmani, I.; Gröger, T. M.; Zimmermann, R., Online comprehensive two-dimensional characterization of puff-by-puff resolved cigarette smoke by hyphenation of fast gas chromatography to single-photon ionization time-of-flight mass spectrometry: quantification of hazardous volatile organic compounds. *Analytical Chemistry* **2011**, *83* (17), 6619-6627.
255. Gerberich, H. R.; Seaman, G. C.; Staff, U. b., Formaldehyde. *Kirk-Othmer Encyclopedia of Chemical Technology* **2000**, 1-22.

256. Pankow, J. F.; Kim, K.; Luo, W.; McWhirter, K. J., Gas/Particle partitioning constants of nicotine, selected toxicants, and flavor chemicals in solutions of 50/50 propylene glycol/glycerol as used in electronic cigarettes. *Chemical Research in Toxicology* **2018**, *31* (9), 985-990.
257. Geiss, O.; Bianchi, I.; Barrero-Moreno, J., Correlation of volatile carbonyl yields emitted by e-cigarettes with the temperature of the heating coil and the perceived sensorial quality of the generated vapours. *International Journal of Hygiene and Environmental Health* **2016**, *219* (3), 268-277.
258. Pankow, J. F.; Tavakoli, A. D.; Luo, W.; Isabelle, L. M., Percent free base nicotine in the tobacco smoke particulate matter of selected commercial and reference cigarettes. *Chemical Research in Toxicology* **2003**, *16* (8), 1014-1018.
259. Lipowicz, P.; Piade, J., Evaporation and subsequent deposition of nicotine from mainstream cigarette smoke in a denuder tube. *J. Aerosol Sci* **2004**, *35* (1), 33-45.
260. Lisko, J. G.; Tran, H.; Stanfill, S. B.; Blount, B. C.; Watson, C. H., Chemical composition and evaluation of nicotine, tobacco alkaloids, pH, and selected flavors in e-cigarette cartridges and refill solutions. *Nicotine & Tobacco Research* **2015**, *17* (10), 1270-1278.
261. El-Hellani, A.; El-Hage, R.; Baalbaki, R.; Salman, R.; Talih, S.; Shihadeh, A.; Saliba, N. A., Free-base and protonated nicotine in electronic cigarette liquids and aerosols. *Chemical Research in Toxicology* **2015**, *28* (8), 1532-1537.
262. Talih, S.; Salman, R.; El-Hage, R.; Karaoghlanian, N.; El-Hellani, A.; Saliba, N.; Shihadeh, A., Effect of free-base and protonated nicotine on nicotine yield from electronic cigarettes with varying power and liquid vehicle. *Scientific Reports* **2020**, *10* (1), 1-5.
263. Sun, T.; Teja, A. S., Density, viscosity and thermal conductivity of aqueous solutions of propylene glycol, dipropylene glycol, and tripropylene glycol between 290 K and 460 K. *Journal of Chemical & Engineering Data* **2004**, *49* (5), 1311-1317.
264. Segur, J. B.; Oberstar, H. E., Viscosity of glycerol and its aqueous solutions. *Industrial & Engineering Chemistry* **1951**, *43* (9), 2117-2120.
265. Fang, H.; Ni, K.; Wu, J.; Li, J.; Huang, L.; Reible, D., The effects of hydrogen bonding on the shear viscosity of liquid water. *International Journal of Sediment Research* **2019**, *34* (1), 8-13.
266. Duell, A. K.; Pankow, J. F.; Gillette, S. M.; Peyton, D. H., Boiling points of the propylene glycol+glycerol system at 1 atmosphere pressure: 188.6–292 C without and with added water or nicotine. *Chem. Eng. Commun.* **2018**, *205* (12), 1691-1700.
267. Corma, A.; Huber, G. W.; Sauvinaud, L.; O'Connor, P., Biomass to chemicals: catalytic conversion of glycerol/water mixtures into acrolein, reaction network. *J. Catal.* **2008**, *257* (1), 163-171.
268. Garner, C.; Stevens, R.; Tayyarah, R.; Morton, M., 2015 Collaborative Study for Determination of Glycerin, Propylene Glycol, Water and Nicotine in Collected Aerosol of E-Cigarettes. Tobacco, C. C. f. S. R. R. t., Ed. 2017.
269. Lee, Y. O.; Nonnemaker, J. M.; Bradfield, B.; Hensel, E. C.; Robinson, R. J., Examining daily electronic cigarette puff topography among established and nonestablished cigarette smokers in their natural environment. *Nicotine and Tobacco Research* **2018**, *20* (10), 1283-1288.
270. Casebolt, R.; Cook, S. J.; Islas, A.; Brown, A.; Castle, K.; Dutcher, D. D., Carbon monoxide concentration in mainstream E-cigarette emissions measured with diode laser spectroscopy. *Tobacco Control* **2020**, *29* (6), 652-655.
271. Chen, R.; Aherrera, A.; Isichei, C.; Olmedo, P.; Jarmul, S.; Cohen, J. E.; Navas-Acien, A.; Rule, A. M., Assessment of indoor air quality at an electronic cigarette (Vaping) convention. *Journal of Exposure Science & Environmental Epidemiology* **2018**, *28* (6), 522-529.
272. Herrington, J. S.; Myers, C., Electronic cigarette solutions and resultant aerosol profiles. *Journal of Chromatography A* **2015**, *1418*, 192-199.
273. Harvanko, A. M.; Havel, C. M.; Jacob, P.; Benowitz, N. L., Characterization of Nicotine Salts in 23 Electronic Cigarette Refill Liquids. *Nicotine and Tobacco Research* **2020**, *22* (7), 1239-1243.

274. Gaworski, C. L.; Oldham, M. J.; Coggins, C. R., Toxicological considerations on the use of propylene glycol as a humectant in cigarettes. *Toxicology* **2010**, *269* (1), 54-66.
275. Heck, J. D.; Gaworski, C. L.; Rajendran, N.; Morrissey, R. L., Toxicologic evaluation of humectants added to cigarette tobacco: 13-week smoke inhalation study of glycerin and propylene glycol in Fischer 344 rats. *Inhalation Toxicology* **2002**, *14* (11), 1135-1152.
276. Dalton, P.; Soreth, B.; Maute, C.; Novaleski, C.; Banton, M., Lack of respiratory and ocular effects following acute propylene glycol exposure in healthy humans. *Inhalation Toxicology* **2018**, *30* (3), 124-132.
277. Brochu, P.; Ducré-Robitaille, J.-F.; Brodeur, J., Physiological daily inhalation rates for free-living individuals aged 1 month to 96 years, using data from doubly labeled water measurements: a proposal for air quality criteria, standard calculations and health risk assessment. *Human and Ecological Risk Assessment* **2006**, *12* (4), 675-701.
278. Hartwig, A.; Commission, M., Glycerin [MAK Value Documentation, 2016]. *The MAK-Collection for Occupational Health and Safety: Annual Thresholds and Classifications for the Workplace* **2002**, *2* (2), 369-374.
279. Organization, W. H., International Agency for Research on Cancer. **2019**.
280. Ashton, H.; Stepney, R.; Thompson, J., Self-titration by cigarette smokers. *Br Med J* **1979**, *2* (6186), 357-360.
281. Heatherton, T. F.; Kozlowski, L. T.; Frecker, R. C.; Rickert, W.; Robinson, J., Measuring the heaviness of smoking: using self-reported time to the first cigarette of the day and number of cigarettes smoked per day. *British Journal of Addiction* **1989**, *84* (7), 791-800.
282. Siegel, M. B.; Tanwar, K. L.; Wood, K. S., Electronic cigarettes as a smoking-cessation tool: results from an online survey. *American Journal of Preventive Medicine* **2011**, *40* (4), 472-475.
283. Blagev, D. P.; Harris, D.; Dunn, A. C.; Guidry, D. W.; Grissom, C. K.; Lanspa, M. J., Clinical presentation, treatment, and short-term outcomes of lung injury associated with e-cigarettes or vaping: a prospective observational cohort study. *The Lancet* **2019**, *394* (10214), 2073-2083.
284. Chatham-Stephens, K.; Roguski, K.; Jang, Y.; Cho, P.; Jatlaoui, T. C.; Kabbani, S.; Glidden, E.; Ussery, E. N.; Trivers, K. F.; Evans, M. E., Characteristics of hospitalized and nonhospitalized patients in a nationwide outbreak of e-cigarette, or vaping, product use-associated lung injury—United States, November 2019. *Morbidity and Mortality Weekly Report* **2019**, *68* (46), 1076.
285. Taylor, J.; Wiens, T.; Peterson, J.; Saravia, S.; Lunda, M.; Hanson, K.; Wogen, M.; D’Heilly, P.; Margetta, J.; Bye, M., Characteristics of e-cigarette, or vaping, products used by patients with associated lung injury and products seized by law enforcement—Minnesota, 2018 and 2019. *Morbidity and Mortality Weekly Report* **2019**, *68* (47), 1096.
286. Moritz, E. D.; Zapata, L. B.; Lekichvili, A.; Glidden, E.; Annor, F. B.; Werner, A. K.; Ussery, E. N.; Hughes, M. M.; Kimball, A.; DeSisto, C. L., Update: characteristics of patients in a national outbreak of e-cigarette, or vaping, product use-associated lung injuries—United States, October 2019. *Morbidity and Mortality Weekly Report* **2019**, *68* (43), 985.
287. Kamal, M. A.; Raghunathan, V., Modulated phases of phospholipid bilayers induced by tocopherols. *Biochimica et Biophysica Acta (BBA)-Biomembranes* **2012**, *1818* (11), 2486-2493.
288. Fukuzawa, K.; Hayashi, K.; Suzuki, A., Effects of α -tocopherol analogs on lysosome membranes and fatty acid monolayers. *Chem. Phys. Lipids* **1977**, *18* (1), 39-48.
289. Steiner, M., Vitamin E changes the membrane fluidity of human platelets. *Biochimica et Biophysica Acta (BBA)-Biomembranes* **1981**, *640* (1), 100-105.
290. Sagalowicz, L.; Guillot, S.; Acquistapace, S.; Schmitt, B.; Maurer, M.; Yaghmur, A.; De Campo, L.; Rouvet, M.; Leser, M.; Glatter, O., Influence of vitamin E acetate and other lipids on the phase behavior of mesophases based on unsaturated monoglycerides. *Langmuir* **2013**, *29* (26), 8222-8232.

291. Kalininskiy, A.; Bach, C. T.; Nacca, N. E.; Ginsberg, G.; Marraffa, J.; Navarette, K. A.; McGraw, M. D.; Croft, D. P., E-cigarette, or vaping, product use associated lung injury (EVALI): case series and diagnostic approach. *The Lancet Respiratory Medicine* **2019**, *7* (12), 1017-1026.
292. Trivers, K. F.; Watson, C. V.; Neff, L. J.; Jones, C. M.; Hacker, K., Tetrahydrocannabinol (THC)-containing e-cigarette, or vaping, product use behaviors among adults after the onset of the 2019 outbreak of e-cigarette, or vaping, product use-associated lung injury (EVALI). *Addictive Behaviors* **2021**, *121*, 106990.
293. MacMurdo, M.; Lin, C.; Saeedan, M. B.; Doxtader, E. E.; Mukhopadhyay, S.; Arrossi, V.; Reynolds, J.; Ghosh, S.; Choi, H., e-Cigarette or vaping product use-associated lung injury: clinical, radiologic, and pathologic findings of 15 cases. *Chest* **2020**, *157* (6), e181-e187.
294. Fedt, A.; Bhattarai, S.; Oelstrom, M. J., Vaping-Associated Lung Injury: A New Cause of Acute Respiratory Failure. *Journal of Adolescent Health* **2020**, *66* (6), 754-757.
295. Thakrar, P. D.; Boyd, K. P.; Swanson, C. P.; Wideburg, E.; Kumbhar, S. S., E-cigarette, or vaping, product use-associated lung injury in adolescents: a review of imaging features. *Pediatric Radiology* **2020**, *50* (3), 338-344.
296. Lilly, C. M.; Khan, S.; Waksmundzki-Silva, K.; Irwin, R. S., Vaping-associated respiratory distress syndrome: case classification and clinical guidance. *Critical Care Explorations* **2020**, *2* (2).
297. Blount, B. C.; Karwowski, M. P.; Shields, P. G.; Morel-Espinosa, M.; Valentin-Blasini, L.; Gardner, M.; Braselton, M.; Brosius, C. R.; Caron, K. T.; Chambers, D., Vitamin E acetate in bronchoalveolar-lavage fluid associated with EVALI. *New England Journal of Medicine* **2020**, *382* (8), 697-705.
298. Krishnasamy, V. P., Update: Characteristics of a Nationwide Outbreak of E-cigarette, or Vaping, Product Use-Associated Lung Injury—United States, August 2019–January 2020. *MMWR. Morbidity and Mortality Weekly Report* **2020**, *69*.
299. Duffy, B.; Li, L.; Lu, S.; Durocher, L.; Dittmar, M.; Delaney-Baldwin, E.; Panawennage, D.; LeMaster, D.; Navarette, K.; Spink, D., Analysis of cannabinoid-containing fluids in illicit vaping cartridges recovered from pulmonary injury patients: identification of vitamin E acetate as a major diluent. *Toxics* **2020**, *8* (1), 8.
300. Information for the Public, F. A., and Recommendations, Lung Injuries Associated with Use of Vaping Products. *U.S. Food&Drug Administration* **2020**.
301. Food; Administration, D., Lung injuries associated with use of vaping products.
302. Espinosa, M. M.; Blount, B. C.; Valentin-Blasini, L., Liquid chromatography-tandem mass spectrometry method for measuring vitamin E acetate in bronchoalveolar lavage fluid. *J. Chromatogr. B* **2021**, *1171*, 122607.
303. Lanzarotta, A.; Falconer, T. M.; Flurer, R.; Wilson, R. A., Hydrogen Bonding between Tetrahydrocannabinol and Vitamin E Acetate in Unvaped, Aerosolized, and Condensed Aerosol e-Liquids. *Analytical Chemistry* **2020**, *92* (3), 2374-2378.
304. DiPasquale, M.; Gbadamosi, O.; Nguyen, M. H.; Castillo, S. R.; Rickeard, B. W.; Kelley, E. G.; Nagao, M.; Marquardt, D., A mechanical mechanism for vitamin e acetate in E-cigarette/Vaping-Associated lung injury. *Chemical Research in Toxicology* **2020**, *33* (9), 2432-2440.
305. Renaud-Young, M.; Mayall, R. M.; Salehi, V.; Goledzinowski, M.; Comeau, F. J.; MacCallum, J. L.; Birss, V. I., Development of an ultra-sensitive electrochemical sensor for Δ^9 -tetrahydrocannabinol (THC) and its metabolites using carbon paper electrodes. *Electrochim. Acta* **2019**, *307*, 351-359.
306. Carbone, M.; Castelluccio, F.; Daniele, A.; Sutton, A.; Ligresti, A.; Di Marzo, V.; Gavagnin, M., Chemical characterisation of oxidative degradation products of Δ^9 -THC. *Tetrahedron* **2010**, *66* (49), 9497-9501.
307. Berman, P.; Futoran, K.; Lewitus, G. M.; Mukha, D.; Benami, M.; Shlomi, T.; Meiri, D., A new ESI-LC/MS approach for comprehensive metabolic profiling of phytocannabinoids in Cannabis. *Scientific reports* **2018**, *8* (1), 1-15.

308. Aizpurua-Olaizola, O.; Soydaner, U.; Öztürk, E.; Schibano, D.; Simsir, Y.; Navarro, P.; Etxebarria, N.; Usobiaga, A., Evolution of the cannabinoid and terpene content during the growth of *Cannabis sativa* plants from different chemotypes. *J. Nat. Prod.* **2016**, *79* (2), 324-331.
309. Borille, B. T.; Ortiz, R. S.; Mariotti, K. C.; Vanini, G.; Tose, L. V.; Filgueiras, P. R.; Marcelo, M. C.; Ferrão, M. F.; Anzanello, M. J.; Limberger, R. P., Chemical profiling and classification of cannabis through electrospray ionization coupled to Fourier transform ion cyclotron resonance mass spectrometry and chemometrics. *Analytical Methods* **2017**, *9* (27), 4070-4081.
310. Davidson, D.; Herbon, J.; Horning, D.; Hanson, R., OH concentration time histories in n-alkane oxidation. *Int. J. Chem. Kinet.* **2001**, *33* (12), 775-783.
311. Houle, F.; Hinsberg, W.; Wilson, K., Oxidation of a model alkane aerosol by OH radical: the emergent nature of reactive uptake. *PCCP* **2015**, *17* (6), 4412-4423.
312. Bennett, J. E.; Summers, R., Product studies of the mutual termination reactions of sec-alkylperoxy radicals: Evidence for non-cyclic termination. *Can. J. Chem.* **1974**, *52* (8), 1377-1379.
313. Ruehl, C. R.; Nah, T.; Isaacman, G.; Worton, D. R.; Chan, A. W.; Kolesar, K. R.; Cappa, C. D.; Goldstein, A. H.; Wilson, K. R., The influence of molecular structure and aerosol phase on the heterogeneous oxidation of normal and branched alkanes by OH. *The Journal of Physical Chemistry A* **2013**, *117* (19), 3990-4000.
314. Atkinson, R., Atmospheric reactions of alkoxy and β -hydroxyalkoxy radicals. *Int. J. Chem. Kinet.* **1997**, *29* (2), 99-111.
315. Baldwin, R.; Walker, R. In *Elementary reactions in the oxidation of alkenes*, Symposium (International) on Combustion, Elsevier: 1981; pp 819-829.
316. Wang, Z.; Ehn, M.; Rissanen, M. P.; Garmash, O.; Quéléver, L.; Xing, L.; Monge-Palacios, M.; Rantala, P.; Donahue, N. M.; Berndt, T., Efficient alkane oxidation under combustion engine and atmospheric conditions. *Communications chemistry* **2021**, *4* (1), 1-8.
317. Calvert, J. G.; Derwent, R. G.; Orlando, J. J.; Wallington, T. J.; Tyndall, G. S., Mechanisms of atmospheric oxidation of the alkanes. **2008**.
318. Carter, W. P.; Darnall, K. R.; Lloyd, A. C.; Winer, A. M.; Pitts Jr, J. N., Evidence for alkoxy radical isomerization in photooxidations of C4–C6 alkanes under simulated atmospheric conditions. *Chemical Physics Letters* **1976**, *42* (1), 22-27.
319. George, I.; Abbatt, J., Heterogeneous oxidation of atmospheric aerosol particles by gas-phase radicals. *Nature Chemistry* **2010**, *2* (9), 713.
320. Chatgillaloglu, C.; Ingold, K.; Scaiano, J., Rate constants and Arrhenius parameters for the reactions of primary, secondary, and tertiary alkyl radicals with tri-n-butyltin hydride. *Journal of the American Chemical Society* **1981**, *103* (26), 7739-7742.
321. Zipse, H., Radical stability—a theoretical perspective. *Radicals in Synthesis I* **2006**, 163-189.
322. Gryn'ova, G.; Marshall, D. L.; Blanksby, S. J.; Coote, M. L., Switching radical stability by pH-induced orbital conversion. *Nature chemistry* **2013**, *5* (6), 474-481.
323. Mikheev, V. B.; Klupinski, T. P.; Ivanov, A.; Lucas, E. A.; Strozier, E. D.; Fix, C., Particle size distribution and chemical composition of aerosolized vitamin E acetate. *Aerosol Science and Technology* **2020**, *54* (9), 993-998.
324. Tang, C.; Tao, G.; Wang, Y.; Liu, Y.; Li, J., Identification of α -Tocopherol and Its Oxidation Products by Ultra-Performance Liquid Chromatography Coupled with Quadrupole Time-of-Flight Mass Spectrometry. *J. Agric. Food. Chem.* **2019**, *68* (2), 669-677.
325. Teng, A.; Crouse, J.; Lee, L.; St Clair, J.; Cohen, R.; Wennberg, P., Hydroxy nitrate production in the OH-initiated oxidation of alkenes. *Atmospheric Chemistry and Physics* **2015**, *15* (8), 4297-4316.
326. Sprengnether, M.; Demerjian, K. L.; Donahue, N. M.; Anderson, J. G., Product analysis of the OH oxidation of isoprene and 1, 3-butadiene in the presence of NO. *Journal of Geophysical Research: Atmospheres* **2002**, *107* (D15), ACH 8-1-ACH 8-13.

327. La, Y.; Camredon, M.; Ziemann, P.; Valorso, R.; Matsunaga, A.; Lannuque, V.; Lee-Taylor, J.; Hodzic, A.; Madronich, S.; Aumont, B., Impact of chamber wall loss of gaseous organic compounds on secondary organic aerosol formation: explicit modeling of SOA formation from alkane and alkene oxidation. *Atmospheric Chemistry and Physics* **2016**, *16* (3), 1417-1431.
328. ElSohly, M. A.; Slade, D., Chemical constituents of marijuana: the complex mixture of natural cannabinoids. *Life Sci.* **2005**, *78* (5), 539-548.
329. Fishedick, J. T.; Hazekamp, A.; Erkelens, T.; Choi, Y. H.; Verpoorte, R., Metabolic fingerprinting of *Cannabis sativa* L., cannabinoids and terpenoids for chemotaxonomic and drug standardization purposes. *Phytochemistry* **2010**, *71* (17-18), 2058-2073.
330. Tettey, J. N.; Crean, C.; Rodrigues, J.; Yap, T. W. A.; Lim, J. L. W.; Lee, H. Z. S.; Ching, M., United Nations Office on Drugs and Crime: recommended methods for the identification and analysis of synthetic cannabinoid receptor agonists in seized materials. *Forensic science international: Synergy* **2021**, *3*.
331. Radwan, M. M.; Ross, S. A.; Slade, D.; Ahmed, S. A.; Zulfiqar, F.; ElSohly, M. A., Isolation and characterization of new cannabis constituents from a high potency variety. *Planta Med.* **2008**, *74* (3), 267.
332. Radwan, M. M.; ElSohly, M. A.; El-Alfy, A. T.; Ahmed, S. A.; Slade, D.; Husni, A. S.; Manly, S. P.; Wilson, L.; Seale, S.; Cutler, S. J., Isolation and pharmacological evaluation of minor cannabinoids from high-potency *Cannabis sativa*. *J. Nat. Prod.* **2015**, *78* (6), 1271-1276.
333. Radwan, M. M.; ElSohly, M. A.; Slade, D.; Ahmed, S. A.; Khan, I. A.; Ross, S. A., Biologically active cannabinoids from high-potency *Cannabis sativa*. *J. Nat. Prod.* **2009**, *72* (5), 906-911.
334. Eiras, M.; De Oliveira, D.; Ferreira, M.; Benassi, M.; Cazenave, S.; Catharino, R., Fast fingerprinting of cannabinoid markers by laser desorption ionization using silica plate extraction. *Analytical methods* **2014**, *6* (5), 1350-1352.
335. Vásquez-Ocmín, P.; Marti, G.; Bonhomme, M.; Mathis, F.; Fournier, S.; Bertani, S.; Maciuk, A., Cannabinoids vs. whole metabolome: relevance of cannabinomics in analyzing *Cannabis* varieties. *bioRxiv* **2021**.
336. Pavlovic, R.; Panseri, S.; Giupponi, L.; Leoni, V.; Citti, C.; Cattaneo, C.; Cavaletto, M.; Giorgi, A., Phytochemical and ecological analysis of two varieties of hemp (*Cannabis sativa* L.) grown in a mountain environment of Italian Alps. *Frontiers in Plant Science* **2019**, *10*, 1265.
337. Couch, J. R.; Grimes, G. R.; Green, B. J.; Wiegand, D. M.; King, B.; Methner, M. M., Review of NIOSH cannabis-related health hazard evaluations and research. *Annals of work exposures and health* **2020**, *64* (7), 693-704.
338. Couch, J. R.; Grimes, G. R.; Wiegand, D. M.; Green, B. J.; Glassford, E. K.; Zwack, L. M.; Lemons, A. R.; Jackson, S. R.; Beezhold, D. H., Potential occupational and respiratory hazards in a Minnesota cannabis cultivation and processing facility. *American journal of industrial medicine* **2019**, *62* (10), 874-882.
339. Booth, J. K.; Page, J. E.; Bohlmann, J., Terpene synthases from *Cannabis sativa*. *Plos one* **2017**, *12* (3), e0173911.
340. Booth, J. K.; Bohlmann, J., Terpenes in *Cannabis sativa*—From plant genome to humans. *Plant Science* **2019**, *284*, 67-72.
341. Romano, L. L.; Hazekamp, A., Cannabis oil: chemical evaluation of an upcoming cannabis-based medicine. *Cannabinoids* **2013**, *1* (1), 1-11.
342. Gaoni, Y.; Mechoulam, R., Isolation, structure, and partial synthesis of an active constituent of hashish. *Journal of the American chemical society* **1964**, *86* (8), 1646-1647.
343. Adams, R.; Cain, C.; McPhee, W.; Wearn, R., Structure of Cannabidiol. XII. Isomerization to Tetrahydrocannabinols¹. *Journal of the American Chemical Society* **1941**, *63* (8), 2209-2213.
344. Bolognesi, C.; Castle, L.; Cravedi, J.-P.; Engel, K.-H.; Fowler, P.; Franz, R.; Grob, K.; Gurtler, R.; Husoy, T.; Karenlampi, S., Safety assessment of the substance diethyl [[3, 5-bis (1, 1-dimethylethyl)-4-hydroxyphenyl] methyl] phosphonate, for use in food contact materials. *EFSA JOURNAL* **2016**, *14* (7).

345. Leung, J.; Stjepanović, D.; Dawson, D.; Hall, W. D., Do Cannabis Users Reduce Their THC Dosages When Using More Potent Cannabis Products? A Review. *Frontiers in psychiatry* **2021**, *12*, 163.
346. Kossiakoff, A.; Rice, F. O., Thermal decomposition of hydrocarbons, resonance stabilization and isomerization of free radicals¹. *Journal of the American Chemical Society* **1943**, *65* (4), 590-595.